

Fall 12-1-2018

A Computational Analysis of the Gradient Concentration Profile of DEET and the Mosquito Behavioral Response

Brandon Carver
University of Southern Mississippi

Follow this and additional works at: https://aquila.usm.edu/masters_theses



Part of the [Computational Engineering Commons](#), and the [Electrical and Electronics Commons](#)

Recommended Citation

Carver, Brandon, "A Computational Analysis of the Gradient Concentration Profile of DEET and the Mosquito Behavioral Response" (2018). *Master's Theses*. 600.
https://aquila.usm.edu/masters_theses/600

This Masters Thesis is brought to you for free and open access by The Aquila Digital Community. It has been accepted for inclusion in Master's Theses by an authorized administrator of The Aquila Digital Community. For more information, please contact Joshua.Cromwell@usm.edu.

A COMPUTATIONAL ANALYSIS OF THE GRADIENT CONCENTRATION
PROFILE OF DEET AND THE MOSQUITO BEHAVIORAL RESPONSE

by

Brandon J Carver

A Thesis
Submitted to the Graduate School,
the College of Arts and Sciences
and the School of Computing Sciences and Computer Engineering
at The University of Southern Mississippi
in Partial Fulfillment of the Requirements
for the Degree of Master of Science

Approved by:

Dr. Amer Dawoud, Committee Chair,
Dr. Anton Netchaev,
Dr. Wonyrull Koh

Dr. Amer Dawoud
Committee Chair

Dr. Andrew Sung
Director of School

Dr. Karen S. Coats
Dean of the Graduate School

December 2018

COPYRIGHT BY

Brandon J Carver

2018

Published by the Graduate School



ABSTRACT

DEET is a common active ingredient in most spatial repellents. DEET is also a volatile organic compound. DEET prevents mosquitoes from detecting and coming into contact with an human individual. Gas sensing technologies such as metal oxide semiconductor sensors can detect VOCs. The World Health Organization provides the majority of efficacy testing methods. This research adapts methods from the WHO and use of MOS sensors to further understand how and why DEET affects mosquitos. A custom developed system is used to measure DEET dissipation and observe mosquito behavioral response to the DEET. DEET dissipations and mosquito behavior is measured within a holding chamber. When DEET is present within the holding chamber mosquito activity decreases due to their exposure to the spatial repellent. This research provides an alternate method of measuring DEET's efficacy.

ACKNOWLEDGMENTS

I would like to thank a few people that helped me along the way for this project including Dr. Randy Buchanan and Dr. Anton Netchaev for providing the precursor projects that lead to getting this project, Earl Henson for helping out whenever I needed, Stephen Adams for answering numerous electrical and design questions and providing support, Dr. Amer Dawoud for providing software for mosquito tracking, and Dr. Donald Yee and Dr. Amer Dawoud for becoming PIs for the project to allow continued system development.

TABLE OF CONTENTS

ABSTRACT	ii
ACKNOWLEDGMENTS	iii
LIST OF TABLES	viii
LIST OF ILLUSTRATIONS	xi
LIST OF ABBREVIATIONS	xvi
CHAPTER I – INTRODUCTION	1
CHAPTER II – BACKGROUND	2
2.1 Mosquito: Common disease vector	2
2.2 Vector control methods	2
2.3 Spatial repellents	3
2.4 DEET	4
2.5 Metal Oxide Semiconductor sensors	5
CHAPTER III - LITERATURE REVIEW	7
3.1 DEET	7
3.2 Metal Oxide sensors	11
CHAPTER IV – EXPERIMENTAL APPARATUS	14
4.1 Overview of system	14
4.2 Chamber	14
4.2.1 Chamber material	15

4.2.2 Chamber end and bracket design	15
4.2.3 Chamber ports	15
4.2.4 Chamber measurements	16
4.2.5 CAD of Chamber	16
4.2.6 Chamber notches.....	16
4.2.7 Standard Chamber set up	17
4.3 Sensor Array	17
4.3.1 Array Sensors.....	17
4.3.2 MOS Sensors	18
4.3.3 MOS Sensor Circuitry.....	18
4.4 Sensor Tree	20
4.5 Dynamic environment control	21
4.6 Camera	23
4.7 Circuitry	24
4.7.1 Sensor Wires	24
4.7.2 MOS sensor board.....	25
4.7.3 DAQ Connection board	28
4.7.4 Temperature Amplifying board	28
4.7.5 Servo and Relay Control board.....	31
4.7.6 Complete circuit view	34

4.8 Software	34
4.8.1 DAQ Sensor Data Collection software	35
4.8.2 LabVIEW Data Collection.....	35
4.8.3 LabVIEW Humidity Control	36
4.8.4 Mosquito Image Acquisition.....	37
4.8.5 Mosquito Image Conversion.....	38
4.8.6 Mosquito Image Tracking.....	39
CHAPTER V – METHODOLOGY	42
5.1 Overview of Experiments	42
5.2 Experiment Methodology	42
5.2.1 MOS Sensor Voltage Methodology	42
5.2.2 Mosquito Data Methodology	43
5.2.3 Testing Methodology Differences	45
5.2.4 DEET Concentrations	46
5.3 Data Processing.....	46
5.3.1 MOS Sensor Voltage Data Processing	46
5.3.2 Mosquito Image Data Processing	48
5.4 Results.....	49
5.4.1 MOS Sensor Test Results	49
5.4.2 Mosquito Activity Results	52

CHAPTER VI – DISCUSSION AND CONCLUSION	87
6.1 Discussion	87
6.1.1 MOS Sensor Data	87
6.1.2 Mosquito Activity Data.....	88
6.1.3 Combined Data	90
6.2 Conclusion	91
APPENDIX A – Tables and Figures.....	92
REFERENCES	137

LIST OF TABLES

Table 5.1 Compiled top 10% quadrants for sensor with greatest voltage response	49
Table 5.2 Compiled top 25% quadrants for sensor with greatest voltage response	49
Table 5.3 Compiled top 50% quadrants for sensor with greatest voltage response	50
Table 5.4 Compiled top 10% quadrants for sensor with greatest voltage response plot ..	50
Table 5.5 Compiled top 25% quadrants for sensor with greatest voltage response plot ..	51
Table 5.6 Compiled top 25% quadrants for sensor with greatest voltage response plot ..	51
Table 5.7 7-18-2017-1 test Bait trial mosquito activity during test.....	52
Table 5.8 7-18-2017-1 test Bait + 1ml trial mosquito activity during test	53
Table 5.9 7-18-2017-1 test Bait + 2ml trial mosquito activity during test	54
Table 5.10 7-18-2017-1 test Bait + 3ml trial mosquito activity during test	55
Table 5.11 7-18-2017-1 test quadrant mosquito count	56
Table 5.12 7-18-2017-1 test quadrant mosquito counts plotted	56
Table 5.13 7-18-2017-2 test Bait trial mosquito activity during test.....	57
Table 5.14 7-18-2017-2 test Bait +1ml trial mosquito activity during test	58
Table 5.15 7-18-2017-2 test Bait + 2ml trial mosquito activity during test	59
Table 5.16 7-18-2017-2 test Bait + 3ml trial mosquito activity during test	60
Table 5.17 7-18-2017-2 test quadrant mosquito counts.....	61
Table 5.18 7-18-2017-2 test quadrant mosquito counts plotted	61
Table 5.19 7-20-2017 test Bait trial mosquito activity during test	62
Table 5.20 7-20-2017 test Bait + 1ml trial mosquito activity during test.....	63
Table 5.21 7-20-2017 test Bait + 2ml trial mosquito activity during test.....	64
Table 5.22 7-20-2017 test Bait + 3ml trial mosquito activity during test.....	65

Table 5.23 7-20-2017 test quadrant mosquito counts	66
Table 5.24 7-20-2017 test quadrant mosquito counts plotted	66
Table 5.25 7-21-2017-1 test Bait trial mosquito activity during test	67
Table 5.26 7-21-2017-1 test Bait + 1ml trial mosquito activity during test	68
Table 5.27 7-21-2017-1 test Bait + 2ml trial mosquito activity during test	69
Table 5.28 7-21-2017-1 test Bait + 3ml trial mosquito activity during test	70
Table 5.29 7-21-2017-1 test quadrant mosquito counts.....	71
Table 5.30 7-21-2017-1 test quadrant mosquito counts plotted	71
Table 5.31 7-21-2017-2 test Bait trial mosquito activity during test.....	72
Table 5.32 7-21-2017-2 test Bait + 1ml trial mosquito activity during test	73
Table 5.33 7-21-2017-2 test Bait + 2ml trial mosquito activity during test	74
Table 5.34 7-21-2017-2 test Bait + 3ml trial mosquito activity during test	75
Table 5.35 7-21-2017-1 test quadrant mosquito counts.....	76
Table 5.36 7-21-2017-1 test quadrant mosquito counts plotted	76
Table 5.37 7-22-2017-1 test Bait trial mosquito activity during test.....	77
Table 5.38 7-22-2017-1 test Bait + 1ml trial mosquito activity during test	78
Table 5.39 7-22-2017-1 test Bait + 2ml trial mosquito activity during test	79
Table 5.40 7-22-2017-1 test Bait + 3ml trial mosquito activity during test	80
Table 5.41 7-22-2017-1 test quadrant mosquito counts.....	81
Table 5.42 7-22-2017-1 test quadrant mosquito counts plotted	81
Table 5.43 7-22-2017-2 test Bait trial mosquito activity during test	82
Table 5.44 7-22-2017-2 test Bait + 1ml trial mosquito activity during test	83
Table 5.45 7-22-2017-2 test Bait + 2ml trial mosquito activity during test	84

Table 5.46 7-22-2017-2 test Bait + 3ml trial mosquito activity during test	85
Table 5.47 7-22-2017-2 test quadrant mosquito counts.....	86
Table 5.48 7-22-2017-2 test quadrant mosquito counts plotted	86
Table A.1 10-18-2017 MOS sensor and quadrants sorted by greatest voltage.....	92
Table A.2 10-19-2017 MOS sensor and quadrants sorted by greatest voltage.....	93
Table A.3 10-31-2017 MOS sensor and quadrants sorted by greatest voltage.....	94
Table A.4 11-1-2017-1 MOS sensor and quadrants sorted by greatest voltage	95
Table A.5 11-1-2017-2 MOS sensor and quadrants sorted by greatest voltage	96
Table A.6 12-8-2017-1 MOS sensor and quadrants sorted by greatest voltage	97
Table A.7 12-8-2017-2 MOS sensor and quadrants sorted by greatest voltage	98
Table A.8 12-9-2017 MOS sensor and quadrants sorted by greatest voltage.....	99
Table A.9 Top 50% of MOS sensors with greatest voltage response.....	100
Table A.10 Top 25% of MOS sensors with greatest voltage response.....	101
Table A.11 Top 10% of MOS sensors with greatest voltage response.....	102
Table A.12 Compiled top 10% of MOS sensors with greatest voltage change.....	103
Table A.13 Compiled top 25% of MOS sensors with greatest voltage change.....	103
Table A.14 Compiled top 50% of MOS sensors with greatest voltage change.....	104

LIST OF ILLUSTRATIONS

Figure 4.1 MOS sensor circuit	26
Figure 4.2 MOS sensor board diagram.	27
Figure 4.3 Temperature amplifier circuit.....	29
Figure 4.4 Temperature amplifier board diagram.....	30
Figure 4.5 Servo and relay control circuit	32
Figure 4.6 Servo and relay control board diagram	33
Figure 4.7 LabVIEW data collection flow chart.....	35
Figure 4.8 LabVIEW Humidity Control flow chart.....	36
Figure 4.9 Image Acquisition flow chart	37
Figure 4.10 Image Conversion flow chart	38
Figure 4.11 Mosquito Image Tracking flow chart	39
Figure 5.1 7-18-2017-1 test Bait trial mosquito heat map	52
Figure 5.2 7-18-2017-1 test Bait + 1ml trial mosquito heat map	53
Figure 5.3 7-18-2017-1 test Bait + 2ml trial mosquito heat map	54
Figure 5.4 7-18-2017-1 test Bait + 3ml trial mosquito heat map	55
Figure 5.5 7-18-2017-2 test Bait trial mosquito heat map	57
Figure 5.6 7-18-2017-2 test Bait + 1ml trial mosquito heat map	58
Figure 5.7 7-18-2017-2 test Bait + 2ml trial mosquito heat map	59
Figure 5.8 7-18-2017-2 test Bait + 3ml trial mosquito heat map	60
Figure 5.9 7-20-2017 test Bait trial mosquito heat map	62
Figure 5.10 7-20-2017 test Bait + 1ml trial mosquito heat map.....	63
Figure 5.11 7-20-2017 test Bait + 2ml trial mosquito heat map.....	64

Figure 5.12 7-20-2017 test Bait + 3ml trial mosquito heat map	65
Figure 5.13 7-21-2017-1 test Bait trial mosquito heat map	67
Figure 5.14 7-21-2017-1 test Bait + 1ml trial mosquito heat map.....	68
Figure 5.15 7-21-2017-1 test Bait + 2ml trial mosquito heat map.....	69
Figure 5.16 7-21-2017-1 test Bait + 3ml trial mosquito heat map.....	70
Figure 5.17 7-21-2017-2 test Bait trial mosquito heat map	72
Figure 5.18 7-21-2017-2 test Bait + 1ml trial mosquito heat map.....	73
Figure 5.19 7-21-2017-2 test Bait + 2ml trial mosquito heat map.....	74
Figure 5.20 7-21-2017-2 test Bait + 3ml trial mosquito heat map.....	75
Figure 5.21 7-22-2017-1 test Bait trial mosquito heat map	77
Figure 5.22 7-22-2017-1 test Bait + 1ml trial mosquito heat map.....	78
Figure 5.23 7-22-2017-1 test Bait + 2ml trial mosquito heat map.....	79
Figure 5.24 7-22-2017-1 test Bait + 3ml trial mosquito heat map.....	80
Figure 5.25 7-22-2017-2 test Bait trial mosquito heat map	82
Figure 5.26 7-22-2017-2 test Bait + 1ml trial mosquito heat map.....	83
Figure 5.27 7-22-2017-2 test Bait + 2ml trial mosquito heat map.....	84
Figure 5.28 7-22-2017-2 test Bait + 3ml trial mosquito heat map.....	85
Figure A.1 Cylinder apparatus from Guidelines for Efficacy Testing of Spatial Repellents	104
Figure A.2 Y-tube olfactometer Guidelines for Efficacy Testing of Spatial Repellents	105
Figure A.3 Chamber with chamber ends removed with three tier sensor arm inside	105
Figure A.4 Image of chamber with chamber end show together	106
Figure A.5 Image of chamber with chamber end held together with bracket.....	106

Figure A.6 Image of chamber end with septa sealing 29/42 ground glass joint	107
Figure A.7 Image of four 29/42 ground glass joint at top of chamber	107
Figure A.8 Image of mosquito introduction ports	108
Figure A.9 CAD of the prototype chamber provided to TUDOR scientific.....	108
Figure A.10 CAD of the prototype chamber that TUDOR Scientific produced	109
Figure A.11 Notch place at the top of the chamber for expanding rod	109
Figure A.12 Notch placed at the bottom of the chamber for the expandable rod.....	110
Figure A.13 Standard chamber setup.....	110
Figure A.14 TGS 2602 metal oxide semiconductor sensor	111
Figure A.15 LM35DZ temperature sensor.....	111
Figure A.16 HIH-4030 humidity sensor	111
Figure A.17 Metal oxide substrate.....	112
Figure A.18 TGS 2602 sensor circuit	112
Figure A.19 First iteration sensor tree arms.....	113
Figure A.20 Second iteration sensor tree arms	113
Figure A.21 3d printed center rings	113
Figure A.22 3d Printed ring locations.....	114
Figure A.23 Sensor locations on top tier of sensor tree.....	114
Figure A.24 Sensor locations on center tier of sensor tree	115
Figure A.25 Sensor locations on bottom tier of sensor tree.....	115
Figure A.26 Top sensor arm configuration with sensor arm measurements	116
Figure A.27 Center sensor arm configuration with sensor arm measurements	116
Figure A.28 Bottom sensor arm configuration with sensor arm measurements.....	117

Figure A.29 Servo-controlled valves	117
Figure A.30 Environment control setup.....	118
Figure A.31 LXG-120M camera.....	118
Figure A.32 Mosquito image recording setup	119
Figure A.33 MOS sensor board connection.....	119
Figure A.34 MOS sensor wire four pin connector.....	120
Figure A.35 MOS sensor chamber socket diagram	120
Figure A.36 MOS sensor circuit chamber socket wire	120
Figure A.37 Sensor board A and B front and back side.	121
Figure A.38 Sensor board bottom view with sensor connections made	121
Figure A.39 Sensor board with sensor connections made	122
Figure A.40 TBX-68 DAQ connection terminal block	122
Figure A.41 National Instruments USB-6255 DAQ.....	123
Figure A.42 SH68-68-EPM shielded data cable.....	123
Figure A.43 Temperature amplifying board	124
Figure A.44 Servo and relay control board.....	124
Figure A.45 Complete system circuitry diagram.....	125
Figure A.46 LabVIEW program GUI interface	125
Figure A.47 LabVIEW program back end.....	126
Figure A.48 MOS sensor testing injection setup	127
Figure A.49 Mosquito bait.....	127
Figure A.50 Mosquito testing injection setup.....	128
Figure A.51 Sensor arm top configuration with quadrants and sensor locations	128

Figure A.52 Sensor arm middle configuration with quadrants and sensor locations	129
Figure A.53 Sensor arm bottom configuration with quadrants and sensor locations	129
Figure A.54 Mosquito tracking software quadrant count diagram	130

LIST OF ABBREVIATIONS

<i>DEET</i>	<i>N,N</i> -Diethyl- <i>meta</i> -toluamide
<i>VOC</i>	Volatile Organic Compound
<i>WHO</i>	World Health Organization
<i>LLIN</i>	Long-lasting insecticidal nets
<i>CAD</i>	Computer Assisted Drawing
<i>DAQ</i>	Data Acquisition
<i>NIC</i>	Network interface card
<i>LIFA</i>	LabVIEW interface for Arduino
<i>PWM</i>	Pulse width modulation
<i>LabVIEW</i>	Lab Virtual Instrument Eng Workbench
<i>GUI</i>	Graphical User Interface
<i>CSV</i>	Comma-separated values
<i>C++</i>	General purpose programming language
<i>USB</i>	Universal Serial Bus
<i>COM</i>	Communication
<i>PNG</i>	Portable Network Graphics
<i>BMP</i>	Bitmap image file
<i>OpenCV</i>	Open source computer vision
<i>SDK</i>	Software development kit

CHAPTER I – INTRODUCTION

DEET (*N,N*-Diethyl-*meta*-toluamide) is among the most used active ingredient in spatial repellents. DEET is a volatile organic compound (VOC). A VOC is a carbon-based chemical that evaporates into the air at room temperature. DEET creates a vapor barrier to avert insects from coming into contact with human skin (Katz 2008). Gas sensing technologies that target the dissipation of VOCs exist. Metal oxide semiconductor (MOS) sensors can detect VOCs. MOS sensors are inexpensive and sensitive to target gases (Liu 2012). The World Health Organization's (WHO) methods that measure the efficacy of DEET are host focused. The methods rely on the use humans or animals as a measurement point (WHO 2009). No computational measurement technique exists to determine the dissipation of DEET within open air. MOS sensors can measure the dissipation of DEET in a controlled environment. Observing the dissipation of DEET and the behavioral response of mosquitoes could present a method of testing the efficacy of DEET.

CHAPTER II – BACKGROUND

2.1 Mosquito: Common disease vector

Mosquitoes are a common vector for diseases such as malaria, West Nile fever, and Yellow fever (Rentokill 2015). The WHO reported 214 million cases of malaria in the year 2015 with 438,000 deaths on record (Ronca 2008). Zika is also mosquito-borne, making the mosquito the deadliest means of spreading diseases in the world. Countries that have temperate climates and seasonal mosquito activity have maintained mosquito populations. The United States and other countries enjoy reduced mosquito activity. Countries without temperate climates and seasonal activity have not eliminated mosquitoes as a transmission vector. In areas with lack of funding, resistance to insecticides, and low awareness, malaria has a higher infection rate. Elimination of malaria in these areas is difficult due to these factors (Ronca 2008). 3.2 billion people live in locations that are at risk for Yellow fever, dengue fever, West Nile virus, and Zika. Locations include sub-Saharan Africa, the Mediterranean, Asia, and northern South America (Mal 2016). Elimination of these diseases in these areas is also difficult. Due to this, the use of methods for limiting the interaction between common vectors and humans have become popular.

2.2 Vector control methods

Vector control include methods that eliminates animals that transmits disease. Mosquito vector control measures vary by location and severity of mosquito population. Different species of mosquitoes carry various diseases dependent on location. Mosquito vector control in the United States focuses on reducing habitats that breed mosquitoes. Elimination of standing water in any form can reduce mosquito larval population. If

larval control methods are not executed, various methods for adult control exist. Methods include the use of electronic insect killers, mosquito traps, and space sprays of insecticide (AMCA 2016). Vector control methods in locations with deadly vectors differ from the methods in the United States. Methods vary due to poor implementation of mosquito control strategies, lack of entomologists, and lack of understanding of social norms in response to vector control (Impoinvil 2007). The severity of the mosquito population in these areas requires aggressive methods. Core and supplementary control methods provide separate guidelines one should follow. Core methods use indoor spraying and long-lasting insecticidal nets (LLIN). Indoor residual spraying uses an insecticide with a long-lasting residual activity once or twice a year. Spraying in suspected mosquito landing locations can prevent mosquitoes from interacting with humans. LLIN are nets treated with insecticide with a limited lifespan. LLIN can reduce the contact between humans and mosquitoes by creating a physical barrier. The limited lifespan of the nets requires reapplication of insecticide to the LLIN. Sub-Saharan Africa has received over a billion LLIN and facilitated the largest drop in malaria incident (Core 2016). Supplementary control methods include the use of larval control and personal protection (Supp 2016). Larval control replicates methods used in the United States. Personal protection is the use of physical barriers to prevent interaction between an individual and vector.

2.3 Spatial repellents

Vector control methods also take advantage of spatial repellents. Spatial repellents differ from insecticides, as they are not lethal to mosquitoes or disease vectors. Spatial repellents work in vapor phase to disrupt a mosquito's host seeking behavior. This

creates a barrier between humans and mosquitoes (Katz 2008). Insecticides' main use is to reduce the number of mosquitoes and in the process prevent the spread of vector-borne diseases. Spatial repellents have become an alternate solution by preventing contact between humans and mosquitoes. Spatial repellents used as vector control prevent constant exposure of mosquitoes to pesticides. Due to a limited selection of available insecticides, insecticide resistant mosquitoes have become an issue (Resist 2016). The use of spatial repellents reduces insecticide resistant mosquitoes from vector populations.

2.4 DEET

DEET is the active ingredient in most store purchased insect repellents. DEET was developed as an effective spatial repellent by the U.S. army in 1946. This has made it a popular choice as a spatial repellent (EPA 2016). DEET is a yellowish oil before its dispersal as a vapor. DEET's spatial repellent qualities are only available in the vapor phase. During this vapor phase, DEET blocks the olfactory receptors of a mosquito for CO₂ and 1-octen-3-ol. These attractants are present in human sweat and breath. This sensory inhibition eliminates the instinctual trigger to bite and feed upon humans (Ditzen 2008). During its vapor phase environmental conditions can have effects on DEET's efficacy. Temperature, relative humidity, convection and atmospheric pressure are among these environmental conditions. Several studies observe the effects the vapor phase dissipation of DEET has on mosquitoes.

The WHO has researched the efficacy of DEET. WHO has guidelines that define methods to test the efficacy of DEET. One such method requires the use of a human volunteer's limb. The volunteer's limb coated with a spatial repellent enters a mosquito cage with a fixed number of unfed mosquitoes. An individual records events such as

mosquito landings or bites on the volunteer's limb. An individual using a writing utensil marks landing and bite locations. The number of events over the course of a set time provides a measure of effectiveness of tested repellent. The process repeats for each spatial repellent. WHO studies have shown that DEET is very effective at preventing mosquitoes from landing (WHO 2009).

2.5 Metal Oxide Semiconductor sensors

Most methods that currently exist to measure the efficacy of DEET follow WHO guidelines. Many of the tests have shown how effective DEET is. Few have considered the dissipation of the DEET within air surrounding an application site. The location of mosquitoes within testing environments is also variable in many studies. The combination of the dissipation of DEET and the location of mosquitoes within an environment could present new data. This could display a behavioral reaction to areas of high DEET dissipation from mosquitoes. The use of metal oxide sensors (MOS) to develop a data driven computational profile of DEET and its effects on mosquitoes could produce data to further fight the spread of diseases popular with mosquito vectors.

Methods described above allow for an understanding of the efficacy of DEET and other spatial repellents. There are many questions unanswered. This research will answer three questions.

1. Can an accurate representation of the dissipation of DEET in the chamber be represented by the data that can be collected?
2. Will a change in mosquito behavior to the dissipation of DEET be directly observable?

3. Recent research has shown that mosquitoes can temporarily overcome or adapt to the repellency of DEET after an initial exposure. Is this observable?

CHAPTER III - LITERATURE REVIEW

3.1 DEET

DEET is an effective spatial repellent and its effectiveness has been the topic of many studies. Methods used to collect this data have been consistent and tend to reinforce competing study results. The studies conducted follow the WHO Guidelines for Efficacy Testing of Spatial Repellents and Guidelines for Efficacy Testing of Mosquito Repellents for Human Skin (WHO 2009). The development of alternate testing methods may expand the knowledge and understanding of the efficacy of DEET. A literature review of current testing methods provide a starting point for this research.

The WHO's guidelines provide several experiments to test the efficacy of DEET. These studies involve the measurement of movement away from chemical stimulus, interference with host detection, duration of protection, and interaction with human skin. The WHO's guidelines also provide testing apparatuses to complete specific studies. These testing methods use three species of mosquitoes: *Aedes aegypti*, *Culex quinquefasciatus* and *Anopheles stephensi*. The mosquitoes reside in enclosures at temperatures of $27\pm 2^{\circ}\text{C}$ with a relative humidity of $80\pm 10\%$. The screen enclosures maintain a day night schedule of 12 hours light and 12 hours dark (WHO 2016). The following sections will explore testing procedures put forth by the WHO.

Movement away from chemical stimulus is the measure of a mosquito's movement away from spatial repellent. A clear cylinder apparatus (Figure A.1) measures mosquito movement away from a chemical stimulus. The apparatus has three cylinders. Two metal cylinders reside at each end of a center clear cylinder. One of the metal cylinders contains a control substrate without spatial repellent treatment. The other metal

cylinder contains a treated substrate with 1.5ml of repellent. The metal cylinders have valves to prevent any repellent from entering the center cylinder until the start of the experiment. The clear cylinder has 20 female mosquitoes introduced under a static airflow. The mosquitoes acclimate to the environment for 30 seconds. Opening the valves on each metal cylinder allows control and spatial repellent fill into the entire cylinder. The mosquitoes are also allowed to move throughout the entire cylinder for ten minutes. An individual notes the number of mosquitoes prevented from entering the treated space within the cylinder. The number of prevented mosquitoes are compared to the total number of mosquitoes moving within the entire system. This ratio displays a spatial repellent's ability to prevent mosquitoes from entering the treated area.

Host attraction-inhibition is the measure of the ability of a spatial repellent to prevent the attraction to a host. A Y-tube olfactometer (Figure A.2) measures host attraction-inhibition. The Y-tube olfactometer has central cylinder with a holding port as well as two branches. Each branch has a trapping port. The holding port contains 10 female mosquitoes. The two trapping ports hold a control and a treatment sample. Mesh screens at these ports prevent mosquitoes from having direct contact with the samples. The treatment sample is spatial repellent with a host odor to attract mosquitoes. A circular door remains closed when placing the sample within the trapping ports. This allows the treatment and control samples to pass out of the ports via screen when a test starts. Mosquitoes added to the holding port remain there for 15 minutes to allow them to acclimate to the environment. With the control and treatment samples in place, the doors are open for 30 seconds. An individual notes the number of mosquitoes within treated and control trapping ports. The individual calculates the percentage of trapped

mosquitoes in treated trapping ports to all mosquitoes in the Y-tube olfactometer. Lower percentages of mosquitoes attracted to the host odors with treatment than the percentages of mosquitoes attracted to host odors with control give effective repellency. This percentage displays a spatial repellent's ability to prevent mosquitoes from detecting a host odor.

Duration of protection of a spatial repellent is the length of time a repellent prevents interaction between human and mosquito. The method measures the difference in the inhibition of landing or feeding, between treated and control groups. This method used over time produces the protective efficacy. The experiment uses products that use spatial repellent as their active ingredient. Free flight test rooms provide locations to expose humans to mosquitoes during this test. A volunteer remains within this free flight room during the entirety of the test. Products applied to the human test subjects use instructions according to the product label. The treated area of the free flight room is the person in the room. The control area is the area surrounding the person. A testing individual records the amount of mosquito landings and feedings. They also record the landing locations of mosquitoes. An individual records the duration of the test, duration of protective efficacy and the number of feedings and landings. The longer the spatial repellent prevents mosquitoes from landing and feeding on the individual the higher duration of protective efficacy it has.

Another measure that is currently used by the WHO to measure the efficacy of spatial repellents makes use of human volunteer's limbs. Some studies use laboratory animals or artificial membranes to simulate blood feeding for mosquitoes. To simulate an accurate testing environment the WHO has chosen to use human volunteers. The

parameters for the previous test hold true as both experiments are in the WHO guidelines. Spatial repellent dosages applied to a volunteer's left forearm vary from 10% to 90% over five successive applications. At the beginning of the test, the volunteer's left forearm has one ml of alcohol applied to the skin. The volunteer places his treated forearm within a cage with 50 to 100 mosquitoes. The forearm remains within the chamber for 30 seconds. The biting rate must be greater than 10 landings and or feedings during the 30-second period for the test to continue. The volunteer's left forearm has 1 ml of 10% spatial repellent applied to the skin and placed within the chamber for 30 seconds. This test repeats for five tests of varying spatial repellent dosages. As with previous test, the personnel record the landings and feedings that take place on the left forearm arm. The volunteer's right forearm must undergo a verification test to confirm mosquito activity. 1 mL of alcohol applied to the volunteer's right forearm. The volunteer's right forearm is exposed to the mosquitoes. If landing and feedings is less than 1 per 3 seconds for this test the experiment is valid. The reduction of mosquito landings and feedings as the amount of spatial repellent applied to the volunteer's forearm increases provides efficacy of tested spatial repellent.

Various research entities have used methods outlined in the WHO's documentation. Research involving the use of in-arm cages and human volunteers can be found in Fradin 2002, Beever 2004, Yoon 2014, and Abiy 2014. Methods involving the use of a Y-tube olfactometer can be found in Rodrigues 2015 and NMSU 15. The WHO guidelines have defined many studies and have found to be effective at measuring DEET efficacy.

3.2 Metal Oxide sensors

Gas-sensing technologies range from a wide variety in accuracy, price and uses (Liu 2012). Several different technologies with specific applications exist. The evaluation of each of these technologies was undertaken. The technologies proven to be the most relevant in this specific application were further explored for final consideration. Each of these technologies explored must be able to detect DEET above all else. Technologies evaluated were metal oxide semiconductor, polymers, moisture absorbing material, optical, calorimetric, gas chromatograph, and acoustic methods. Literature of recorded testing and actual testing of technologies provided information to eliminate non-viable technologies. System design required a location to observe mosquito behavior. Measuring within this space eliminated technologies too large or impractical to use. The technology chosen for this research includes metal oxide semiconductor sensors.

Metal oxide semiconductor type sensors have various characteristics. The characteristics can change across brands and types of MOS sensors. Sensitivity, selectivity, response time, repeatability, market availability are among these characteristics. These characteristics factor into selecting the sensor for the application. Sensitivity to a gas defines the sensor's response to a volume concentration of the target gas. Parts per million (ppm) defines the range of sensitivity a sensor will have. A VOC dispersed into a specific volume will have a concentration of VOC particles within the air. The higher this concentration is, a greater amount of detectable VOC particles at ppm are in the air. Selectivity to a target gas defines how well a sensor can detect a target gas alone and with other contaminants present and the sensor's sensitivity to them. Response time is the period of time required for a sensor output to adjust from the previous

measured value to the current value of the current input value. Repeatability of a sensor allows for repeated tests to occur with the same response recorded each time. Market availability defines how easy a sensor is to acquire. If it is a rare item that has specific applications its availability may be less than that of a sensor that is more popular-(Liu 2012).

MOS Sensors have a heated transition metal oxide as the sensing material. This material changes resistance when O^- of the target gas become distributed on the metal oxide surface. This reaction occurs due to the heated nature of the sensors. The energy applied to the target gas traps O^- on the material. The Redox reaction, which is described above, reduces the electrical resistance of the metal oxide semiconductor. MOS sensors that are sensitive to gas concentrations at higher temperatures are n-type semiconductors. Various metal oxides, such as SnO_2 , CuO , Cr_2O_3 , V_2O_5 , WO_3 and TiO_2 detect specific type of gases. The most popular semiconductors being tin dioxide (SnO_2) and tungsten trioxide (WO_3). Advantages of MOS sensors include low cost per unit and high sensitivity. Disadvantages stem from high operating temperatures, as temperatures of the metal oxide surface can change the target gases detected. Another disadvantage of MOS sensors is the recovery period between exposures of gas to the metal oxide substrate (Liu 2012).

The use of MOS sensors to detect DEET is not well documented. A literature review has shown they are not used despite being able to detect DEET. A metal oxide sensor targets specific gases known as Volatile Organic Compounds (VOC) (Liu 2012). A VOC is a carbon-based chemical that evaporates into the air at room temperature. DEET can be described as a VOC. DEET applied to an individual protects said individual

from mosquito bites and landings. This mechanism prevents mosquitoes from sensing carbon dioxide from the individual's skin. If DEET were not a VOC, DEET could not travel to the mosquito to prevent it from detecting carbon dioxide. Research has found that specific types of metal oxide sensors can detect DEET. (Coleman 2016) This research has found three individual MOS sensors are able to detect DEET.

CHAPTER IV – EXPERIMENTAL APPARATUS

4.1 Overview of system

The main goal of this research was to design a system to measure the dissipation of DEET and view mosquito behavior according to this dissipation. The system can measure the dissipation of DEET in a dynamic environment. The system maintains an environment where mosquitoes act normally during observation. The system has seven components: chamber, sensor array, sensor tree, environment control, camera, circuitry, and software. The chamber is a glass cylinder with two end caps held on by a custom bracket. The chamber provides a location to measure the dissipation of DEET and observe mosquito's behavior when exposed to DEET. The chamber has ports to feed wires for instrumentation, mosquito introduction, and airflow. The sensor array consists of humidity, temperature, and MOS sensors. MOS sensors measure the dissipation of DEET while temperature and humidity sensors measure and maintain the environment. The sensor tree holds the sensors in positions throughout the chamber. The sensor tree has three tiers with eight branches reaching into the chamber. This allows for measurement of DEET at these locations. Circuitry records sensor voltages via Data Acquisition (DAQ) and maintains control of environment. Environment control maintains the temperature, humidity, and airflow of the chamber. An ultra-high-definition camera observes mosquito behavior. Several pieces of software collect voltage data, capture and store mosquito images, and track mosquito movement.

4.2 Chamber

The system's chamber needed to fulfill two main requirements. The chamber must have enough space for the sensor array placed on the sensor tree. The chamber must also

not inhibit the mosquito's normal behavior. A cylindrical chamber design provided space for the sensor arm and allowed for consistent airflow. This consistent airflow helped provide a typical environment required for observing mosquito's behavior.

4.2.1 Chamber material

The chamber contains the mosquitoes while observing their behavior during exposure to DEET. This required chamber to be clear. Materials considered for the chamber were plexiglass and glass. Glass proved to be the better option, as it provided better visibility, higher thermal headway, and better construction versatility. Heating the glass chamber can assist in removing remaining DEET molecules after a test. Using glass as a material opened up customization of the chamber by taking advantage of a scientific glassblower.

4.2.2 Chamber end and bracket design

The chamber has three main components. The main cylinder is open on each end (Figure A.3). Two chamber ends attach to the main cylinder to create a closed environment. Each chamber end fits to each end of the main cylinder via glass flange (Figure A.4). A bracket holds each end onto the main cylinder at three points (Figure A.5). At the center of the chamber ends there is a 29/42 ground glass joint (Figure A.6). These joints provide air supply input and output at each end of the chamber.

4.2.3 Chamber ports

There are several locations on the chamber that provide access to inside the chamber. These locations allow for sensor wires, the introduction of mosquitoes and airflow. Four 29/42 ground glass joints are at the center of the top of the chamber (Figure A.7). The sensor wires feed through the back three 29/42 septa placed in the ground glass

joint. The sample injection needle feeds through the front 29/42 septa placed in the ground glass joint. Two separate ports placed 45 degrees from the top of the chamber introduce mosquitoes (Figure A.8).

4.2.4 Chamber measurements

The chamber is approximately 20.75 inches in length. The chamber has an outside diameter of 12 inches and inside diameter of 11.5 inches. The edges of the chamber have a glass flange. The chamber ends are approximately 7 inches in length and match the chamber's inside and outside diameters. The front and back 29/42 ground glass joints at the top of the chamber are approximately 10.25 inches from the left end and 9.375 inches from the right. The center 29/42 ground glass joints at the top of the chamber are approximately 8.125 inches from the left end and 6.175 inches from the right end. There is a gap between the two 29/42 ground glass joints at 4.150 inches.

4.2.5 CAD of Chamber

The chamber required several Computer Assisted Drawings (CAD) to complete its design. This assisted the scientific glassblower with a design to develop the physical chamber. The CAD drawing provided a guideline for TUDOR Scientific, a glass blowing company in South Carolina (Figure A.9) The CAD drawing displays the prototype chamber that TUDOR Scientific constructed (Figure A.10). TUDOR Scientific modified elements of the initial prototype chamber and produced the actual prototype chamber.

4.2.6 Chamber notches

The chamber required two glass notches built into the main cylinder. These notches were points where the sensor arm could attach to. TUDOR centered the top notch between the four 29/42 ground glass joints inside the chamber (Figure A.11). TUDOR

placed the bottom notch approximately 180° opposite of the top notch (Figure A.12). A rod placed over one of the notches expands to reach the opposite notch. This holds the expandable rod in place due to the tension created against the top and bottom of the chamber. This rod positions the sensor arm inside the chamber.

4.2.7 Standard Chamber set up

The chamber shown in Figure A.13 has the three-tier sensor tree. Wires fed through the septa seal the chamber and prevent any gas from escaping through the 29/42 ground glass joints at the top of the chamber. Forty wires fed through three septa provide connections to MOS temperature, and humidity sensors. Each tier of the sensor tree has twelve MOS sensors. Three temperature sensors reside at both chamber end joints and at the center of the center tier. A single humidity sensor resides at the center of the center tier. Zip ties secure any loose wires on the sensor arm.

4.3 Sensor Array

4.3.1 Array Sensors

MOS, humidity, and temperature sensors make up the sensor array. Each type of sensor measures different variables in the chamber during testing. The three sensors selected for the sensor array are the MOS sensor Figaro TGS2602 (Figure A.14), temperature sensor LM35DZ (Figure A.15), and humidity sensor HIH-4030 (Figure A.16). The TGS 2602 MOS sensor has shown to detect DEET (Coleman 2016). During the MOS sensor selection process, three sensors proved to be able to detect DEET. The TGS 2602 proved to have the greatest response to DEET. Guidelines used to select the MOS sensor were: strong response to DEET, testing under SOP, low level of noise when reading sensing voltage, market availability, and consistent response and baseline

between test. The TGS 2602 share the same pin configuration as other MOS sensors. Alternate MOS sensors are interchangeable with the TGS 2602 if necessary.

4.3.2 MOS Sensors

MOS sensors have a sensing element made of alumina substrate. A sensing voltage of five volts supplies voltage across the substrate. A heater voltage of five volts supplies voltage to an internal heater within the MOS casing. This internal heater heats the metal oxide substrate. When exposing the sensor to a target gas, O^- of the target gas become distributed on the metal oxide substrate (Figure A.17). This reduction-oxidation reaction increases the conductivity of the sensor substrate. Measuring the MOS sensor response requires a potentiometer placed in series with the MOS sensor. This increased conductivity across the substrate increases voltage flowing across the series potentiometer. The DAQ measures the voltage that flows across the potentiometer. Increased gas concentration detected by the MOS sensor increases the voltage measured by the DAQ across the potentiometer.

4.3.3 MOS Sensor Circuitry

Each MOS sensor requires a heater and sensor voltage supply. Figure A.18 shows the MOS sensor circuit. The heater voltage supply (V_H) applied voltage to the heater to maintain optimal sensing temperature on the substrate. The circuit voltage supply (V_C) applies voltage across the resistive sensing substrate of the sensor and the load potentiometer (R_L) connected in series. Both voltage supplies must maintain five volts with a two hundred millivolt tolerance.

Each of the MOS sensors used for detecting DEET uses the same circuitry displayed in Figure A.18. This figure displays the sensor as a box. This box displays R_H

and R_S as resistive elements of the sensor. The heater resistance (R_H) shows as a resistor attached to pins 1 and 4. The heater resistance for each sensor is approximately 59Ω at room temperature. The sensor resistance (R_S) shows as a variable resistor attached to pins 3 and 2. The sensor resistance (R_S) varies according to the response the sensor substrate has to the target gas. Heater voltage continues to stay the same over the course of a test.

A potentiometer is the load resistance (R_L) placed in series with the MOS sensor or sensor resistance (R_S). A total circuit voltage (V_C) of five volts applies across the MOS sensor and resistance load (R_L) in series. This voltage divider circuit has the sensor resistance (R_S) and load resistance (R_L) in series. If the resistance loads are not equal, the larger resistance load will have a larger voltage drop across its load. In Figure A.18 the DAQ sensor measurement shows as V_{RL} , this measures the voltage across the load resistance (R_L) to ground. The equation below calculates the voltage drop measured across the potentiometer or our load resistance (R_L).

$$V_{out} = \frac{R_L}{R_S + R_L} V_+ \quad (4.1)$$

The resistance (R_S) of the MOS sensor substrate is inversely proportional to the gas concentration. As the sensor substrate begins to detect gas the sensor resistance (R_S) reduces. The voltage divider relationship between the sensor resistance (R_S) and load potentiometer (R_L) change over the course of a test. Decreasing the sensor resistance (R_S) decreases the voltage drop across the sensor. This creates an increase in voltage dropped

across the potentiometer to ground. This voltage measured across the potentiometer provides an increasing value as the sensor detects a target gas.

4.4 Sensor Tree

Measuring DEET dissipation required placing MOS sensors inside the chamber. During the design process for the prototype chamber a design for a sensor tree was also developed. This sensor tree has multiple sensor locations to measure DEET throughout the chamber. The sensor tree went through several iterations as improvements to its design developed. The first sensor tree had two tiers with four sensor locations per tier (Figure A.19). A second design came later, a single tier with twelve sensor locations (Figure A.20). A three-tier design with thirty-six sensor locations became the final solution.

The sensor tree has several components. An expandable rod is the center point from which components attach to. This expandable rod fits vertically within the chamber when extended. Two glass notches in the chamber are anchor points for the expandable rod. Plasti-dip coats each end of the expandable rod. This coating prevents damage from occurring to chamber walls when the rod extends.

With the expandable rod in place, the next component added to the sensor tree is 3d printed rings (Figure A.21). Placed at vertical locations along the expandable rod, the 3d printed rings provide locations to add sensor arms. The sensor tree has three rings. Each ring has a specific position along the expandable rod (Figure A.22). Locking pins pass through the expandable rod and ring. This locking pin prevent the rings from moving. Eight horizontal locations on the ring provide locations to attach sensor arms.

With the 3d printed rings in place on the expandable rod the next component added is the sensor arms. The eight sensor arm locations on the 3d printed ring allow #8-32 threaded coupling nuts to fit inside them. #8-32 threaded rods cut at specific lengths make up the sensor arms for each tier. Each tier has sensor arms of different lengths. Screwing the threaded rods into the coupling nut creates a star pattern. Sensor locations selected along each sensor arm provide a data-point within the chamber (Figure A.23, A.24, A.25). Metal cradles placed at these locations allow for MOS sensors to rest in place on the sensor arm. #8-32 threaded nuts placed on both sides of the metal cradle maintain the cradles position. Each tier has twelve sensor locations.

As the chamber is cylindrical, the distance from the center of the chamber changes as you move vertically. The top and bottom tiers on the sensor tree have shorter rods to compensate for this. The center tier has the longest sensor arms due to its position. Sensor arms reaching towards the open ends of the chamber are the same length for each tier. Figure A.26, A.27, A.28 displays each tier with sensor arm measurements.

4.5 Dynamic environment control

Maintaining normal mosquito behavior is important to observing their behavioral response to DEET. To do this the environment inside the chamber must maintain a narrow window of humidity, temperature and airflow. This environment is comparable to a normal summer day with a small amount of wind. This air movement can affect how the mosquitoes move, how the MOS sensors detect VOCs, and maintaining humidity and temperature.

Mosquitoes are active within a small range of temperature and humidity. If this range is not maintained for temperature and humidity mosquitoes become inactive.

Mosquito inactivity can prevent mating, feeding behavior and movement. The temperature range required for normal mosquito behavior is 22 to 30 °C. The humidity range required for normal mosquito behavior is 65% to 80% relative humidity. During testing, the temperature of the chamber was approximately 25 °C. Humidity during testing was 65% relative humidity.

Several pieces of equipment make up the dynamic environment control. This includes an air pump, rubber tubing, servo-controlled valves, bubbler, hot plate, Drierite, and input flow meter. The air pump supplies airflow to the system. Rubber tubing connects each component throughout the system. The airflow from the air pump splits and connects to two servo-controlled valves (Figure A.29). The output of one valve connects to the input of the bubbler. This valve controls airflow to the bubbler. The bubbler increases the level of humidity inside the chamber. A hot plate heats the bubbler to 200°C to increase humidity output. The second valve connects to the input of the Drierite container. This valve controls airflow to the Drierite. Drierite decreases the level of humidity inside the chamber. Only one valve will be open at a time. The DAQ measures the current relative humidity inside the chamber. LabVIEW software decides which valve should be open to maintain chamber humidity at 65% relative humidity. The output of the bubbler and Drierite connects to a dual input flow meter. The flow meter's dual inputs reduce to one output. Each input has its airflow speed adjusted to ensure equal airflow from either bubbler or Drierite. The single output of the flow meter connects to the input of the chamber end. The environment control setup can be seen in Figure A.30.

A different method was used to control temperature during mosquito study trials. A water coil and water circulator were added to the existing environment control

system to achieve this. The water coil is a special glass apparatus. The water coil is a hollow glass coil placed within a glass tube. Hot water flowing through the apparatus's coils heats the air passed through the glass tube. A water circulator heats water pushed through the coil at approximately 85 °C. The heated air output connects to the input of the chamber end. This maintains the temperature in the chamber to approximately 25 °C. This allows the mosquitoes to act as they would in a normal environment.

4.6 Camera

A camera was added to the system during the course of development to record mosquito activity. Camera recordings provide visual data of how DEET affects mosquito's behavior and activity level. Custom written software tracks mosquitoes moving throughout the chamber. The camera used is a Baumer LXG 120M (Figure A.31). This digital monochrome camera has a recording resolution of 4096 x 3072 and a frame rate of 19 frames per second. The high recording resolution makes mosquitoes identifiable. The recording frame-rate captures the movement of the mosquitoes throughout the recording.

The camera required the use of support equipment. The supporting equipment includes two lamps, tripod, two Ethernet cables and a dual-network interface controller (NIC) card within a PC. Two lamps placed at each end of the chamber illuminate the test chamber during recordings. The two lamps must use LED bulbs. This prevents the camera from capturing 60 hertz noise from overhead lights. A tripod positions the camera in front of the chamber. The camera's resolution and frame-rate required a dual NIC card to handle bandwidth. Two Ethernet cables provided connection between the camera and

dual NIC enabled PC. This connection also provides power to the camera. The standard camera recording setup can be seen in Figure A.32.

4.7 Circuitry

The system's main circuitry includes several self-contained circuit boards that work together to power, record, amplify, and control parts of the system. There are five boards total, each with a purpose. The system's circuitry includes a MOS sensor board, DAQ connection board, temperature amplifying board, servo control board and an Arduino Mega. The system's main circuitry has wire connections used to connect sensors, and servos, and provide power to the systems components. A complete breakdown of the system's circuitry from sensor to computer is below.

4.7.1 Sensor Wires

All sensors attached to the system via system's sensor wires. Sensor wires reach specific positions within the chamber on the sensor arm. This includes thirty-six MOS sensors, three temperature sensors, and one humidity sensor. Each sensor connects to the sensor board with its own wire connection. This wire connections consist of three components: the board connection, sensor connection, and wire. Each sensor has all three components.

The board connection consists of a four-pin socket soldered to the sensor board (Figure A.33). The four conductors of the sensor wire have pins crimped and soldered to them. Shrink wrap placed over each crimped pin prevents the circuitry from shorting. These pins are then placed in a four-pin connector (Figure A.34). This four-pin connector connects in the socket of the sensor board.

The sensor connection describes a sensor socket placed on the sensor arm within the chamber. The sensor connection consists of a round keyed circuit board designed for the MOS T0-5 package (Figure A.35). The small circuit board is a four-pin socket. This makes swapping MOS sensors in and out of the chamber easy. The round circuit board has four conductors of the sensor wire soldered to them. These four conductors correspond to the four-pin connector that connects to the sensor board. Shrink wrap placed over each pin prevents the circuitry from shorting (Figure A.36). These four conductors provide heater and sensor voltages. A color code for each conductor ensures consistency

The wire connection between the four-pin connector to the four-pin round circuit board uses a shielded four conductor wire. Each individual conductor within the four-conductor wire is twenty-eight gauge. The total diameter of the wire is 2.72 mm. A smaller diameter wire saves space within the chamber. The smaller wire also allowed more sensor wires through the 29/42 septa.

4.7.2 MOS sensor board

The MOS sensor's support circuitry powers and measures the response of the sensors. Each sensor board connection has a four-pin socket. The four-pin socket has two pin connections that provide heater voltage and heater ground. This powers the heater within the MOS sensor casing. The remaining two pin connections provide sensor voltage and sensor ground. A five-volt supply provides power for the heater and sensor pins. Sensor wires connected to the four-pin socket complete the circuit. The sensor board provides power to the sensors via sensor wires. Figure A.37 shows the sensor board.

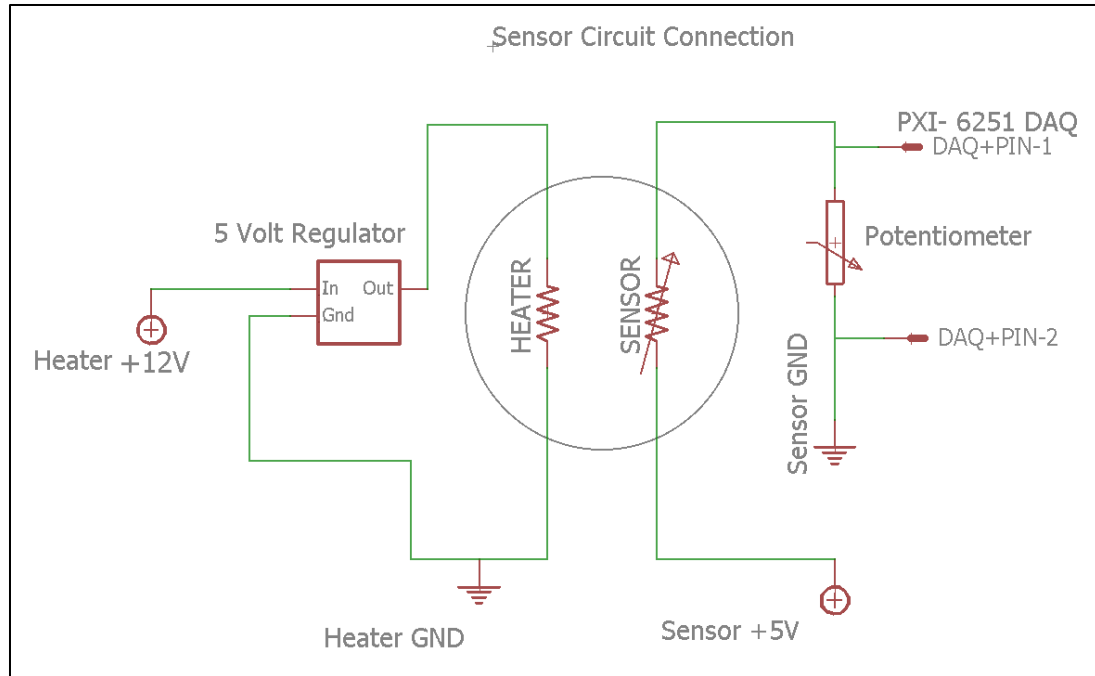


Figure 4.1 MOS sensor circuit

Figure 4.1 provides a schematic view of the sensor circuit. The heater within the MOS sensor package is a resistive heating element. The sensor within the MOS sensor package is a variable resistance element. The MOS sensor resistant element is in series with the potentiometer. Placing two DAQ measurement connections before and after the potentiometer provides a voltage reading across the potentiometer. This voltage corresponds to gas detected by the MOS sensors substrate. These DAQ measurement connections interface with the DAQ connection board. Two separate power supplies provide five volts to the sensor circuit and twelve volts to the heater circuit. The heater rail of the sensor board has a five-volt regulator to prevent higher voltage from being pushed across the circuit. This figure only provides a single MOS sensor connection.

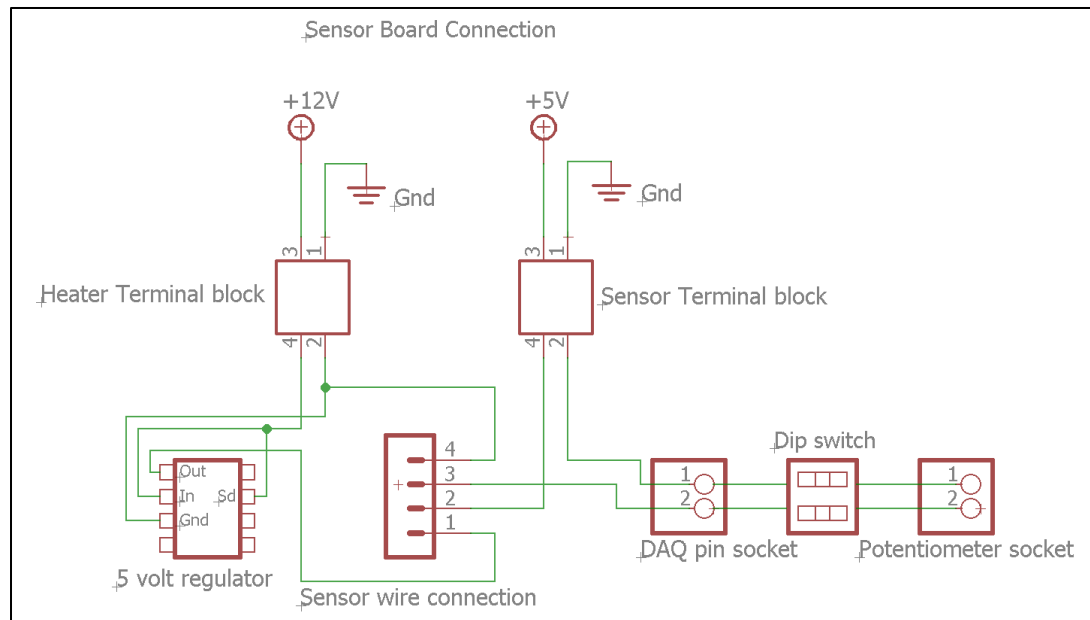


Figure 4.2 MOS sensor board diagram.

Figure 4.2 displays a single MOS sensor connection on the sensor board. The heater terminal block supplies twelve volts to the heater circuit. A twelve-volt supply provides voltage to the input pin of the five-volt regulator. The output of the regulator supplies five volts to the positive heater pin of the four-pin socket. The voltage regulator and ground side of the heater share a common ground. The sensor terminal block provides five volts to the sensor circuit. Five volts power supply provides the positive side of the sensing circuit and flows through DAQ pin socket, dip switch and potentiometer through the second DAQ pin socket to ground. The dip switch removes the potentiometer from the circuit to allow for resistance measurement during testing. This figure only provides a single MOS sensor connection.

4.7.3 DAQ Connection board

The DAQ collects voltage data from the sensor board through connections made to two 68-pin screw terminal boards (Figure A.40). Both TBX-68 connect to the DAQ (Figure A.41) via 68-pin shielded data cable (Figure A.42). The screw terminal boards provide forty differential analog channels for the DAQ. Thirty-six of the differential analog channels record voltages of each MOS sensor circuit. Each differential connection has a positive and negative terminal and measure the potential voltage difference between the two points. Each sensor board connection has two locations to connect the positive and negative differential connection. The four remaining differential analog channels record voltages of three temperature sensors and a humidity sensor.

4.7.4 Temperature Amplifying board

The temperature sensor used within the chamber is a LM35DZ. The temperature sensor provides a 10 milli-volt per degree change in Celsius. The DAQ is capable of measuring in the milli-volt range. Due to the prototype nature of the sensor board electrical noise can become an issue. Small levels of electrical noise can cause the DAQ to read erroneous values and display improper temperatures. Amplifying the milli-volt output of the LM35DZ prevents milli-volt noise. A five-volt supply provides power to the temperature sensors. The temperature sensor output voltage feeds into an amplifying circuit to increase its voltage output by ten.

This voltage increase allows the DAQ to measure volt changes compared to millivolt changes. The temperature amplifying board is shown in Figure A.43.

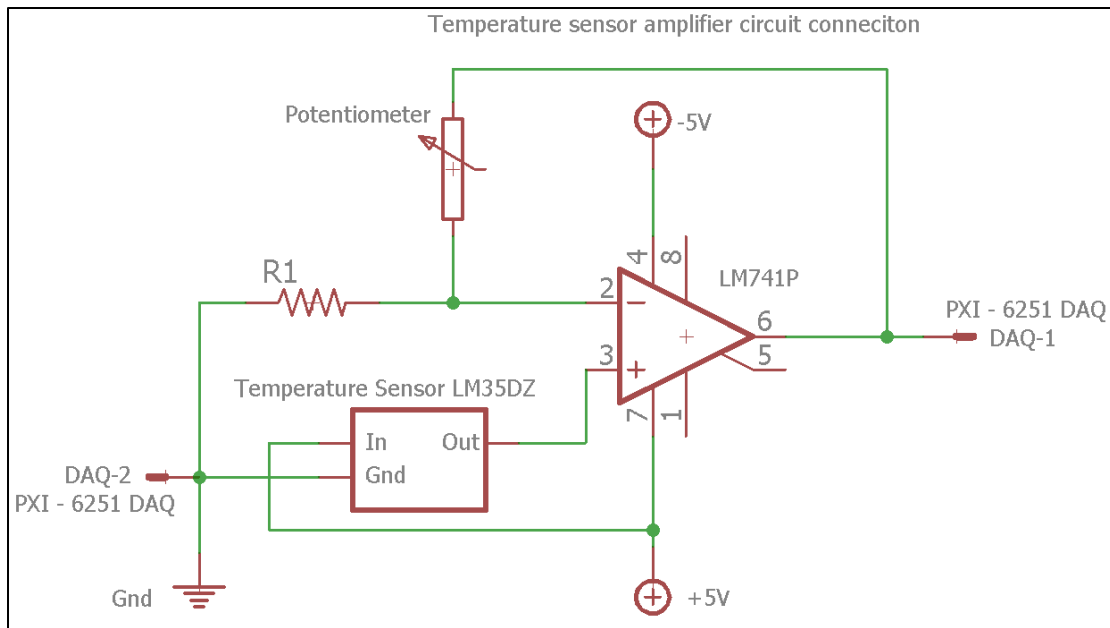


Figure 4.3 Temperature amplifier circuit

Figure 4.3 shows the schematic of the amplifying circuit. The amplifying circuit uses an LM741 operational amplifier with a resistance network adjusted to increase the temperature sensor voltage tenfold. The inverting input of the LM741 (2) connects to ground through resistor (R1) and through a potentiometer to the output side (6) of the LM741. Positive five volts supply V^+ (7) and negative five volts supply V^- (4). The non-inverting input of the LM741 (3) connects to the output of the temperature sensor. The positive DAQ pin connects to the output of the LM741 (6) providing the DAQ with an amplified signal. The negative DAQ pin attaches to ground. R1 has a value of 1k ohms and the potentiometer has an adjustable value up to 10k ohms. Adjusting the potentiometer modifies the characteristics of the resistance network until accomplishing tenfold amplification.

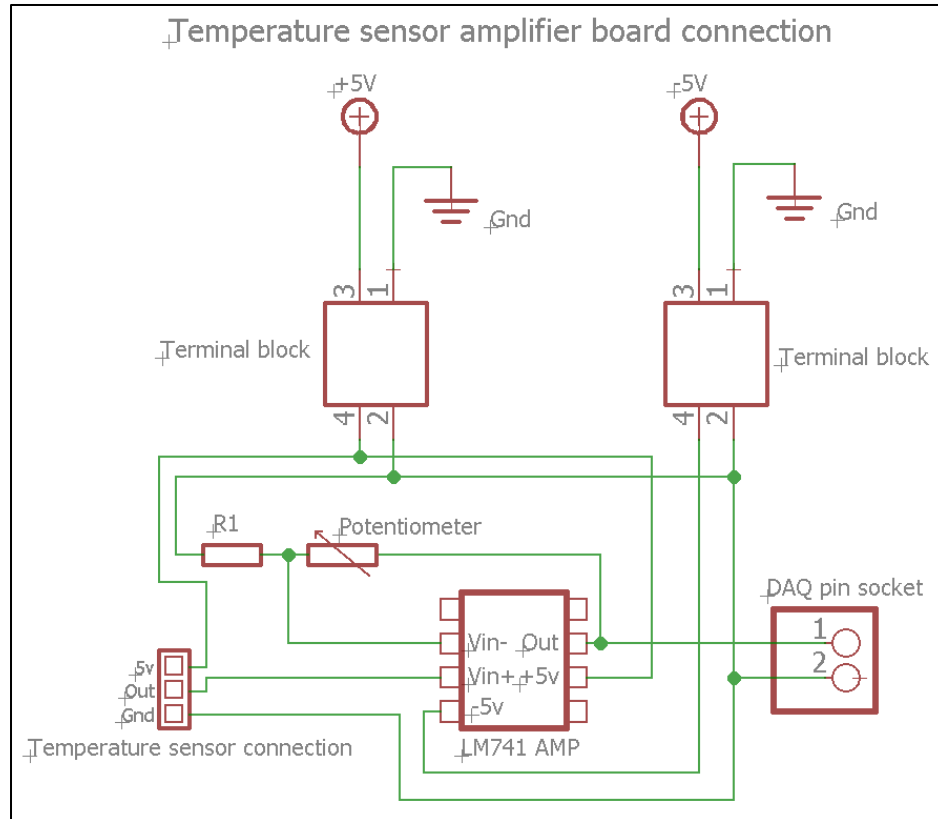


Figure 4.4 Temperature amplifier board diagram

Figure 4.4 displays a single temperature sensor connection on the amplifier board. Two power supplies connected to the two terminal blocks power inputs for negative five volts and positive five volts on the LM741. Op amps require two power supplies that provide positive and negative voltage. The inverting input (V_{in-}) of the LM741 attaches between R_1 and the Potentiometer. This resistance configuration determines the amplifying ratio of the circuit. The non-inverting input (V_{in+}) of the LM741 connects to the output of the temperature sensor socket. The output of the LM741 connects to the potentiometer to complete the feedback loop. The output of the LM741 is also connected to the DAQ socket for voltage measurement. The temperature sensor socket is also powered by the positive five volts power supply used for the LM741.

4.7.5 Servo and Relay Control board

The servo and relay control board (SRCB) connects several components of the system together. The board helps maintain the environment in the chamber. To do this the board provides power and signal to the servo-controlled valves. The board also controls power to the air pump and hot plate relays. Figure A.44 shows the SRCB.

A PC with the LabVIEW program connects to an Arduino Mega via USB cable. The Mega receives commands from the LabVIEW program using LabVIEW interface for Arduino (LIFA). The LabVIEW program measures the current humidity within the chamber via humidity sensor. When the sensor measures certain levels of humidity the LabVIEW program sends commands to the Arduino. These commands open and close valves controlling the flow of humidified or dehumidified air into the chamber. The LabVIEW program also sends commands to the Arduino to switch on relays that provide power to a hot plate and air pump.

Four pins from the Arduino Mega provide signal to the SRCB. Two pins provide pulse width modulation (PWM) signal to the two servo-controlled valves. This PWM signal opens and closes the valves. A power supply connected to the SRCB provides five volts to each servo-controlled valve. The second set of pins provides a digital output signal to the two relays. Both relays plug into a 120vac wall outlet and to the hot plate or air pump. The digital signal energizes the relay and provides power to the hot plate or air pump.

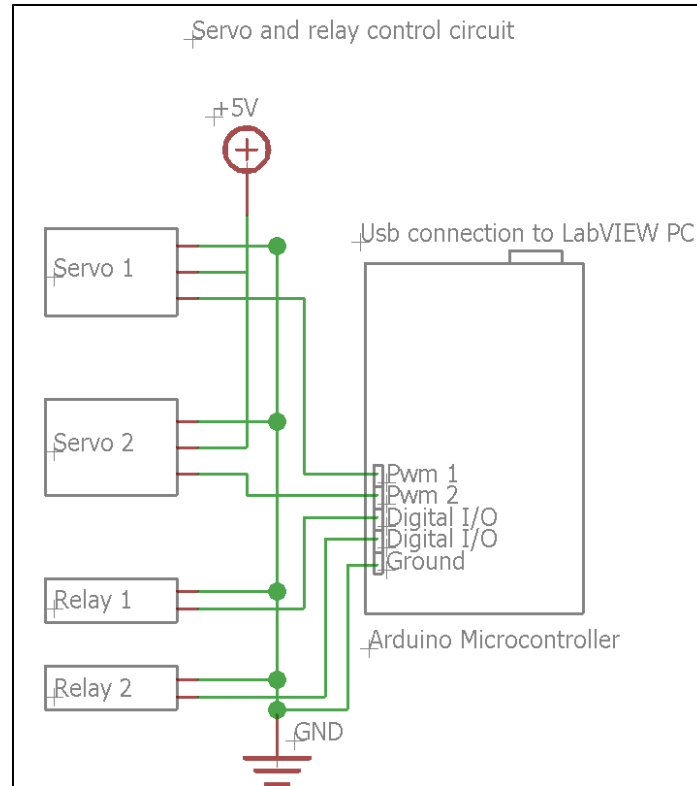


Figure 4.5 Servo and relay control circuit

Figure 4.5 displays the SRCB circuit. The LabVIEW PC connects to the Arduino Mega via USB. Two digital output pins on the Arduino Mega configured to provide PWM signal connect to servo one and two of the valve system. Each servo has 3 connections: Power, ground, and PWM signal. A power supply provides five volts to the power input of the two servos. The remaining two digital pins provide signal to relay one and two. Each relay has 2 connections: signal and ground. Each component shares a common ground.

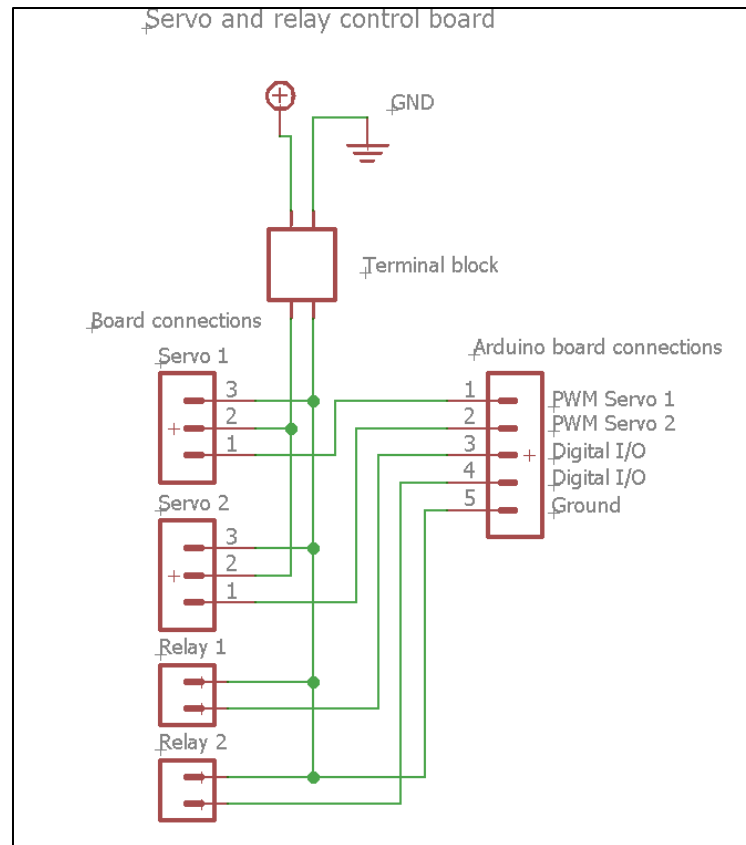


Figure 4.6 Servo and relay control board diagram

Figure 4.6 displays the servo and relay control board. The servo board connections use three-pin sockets for servos one and two. Two-pin sockets are used for the relay board connections. A five-pin socket provides board connections to the Arduino. A terminal block connected to a power supply provides five volts to the servos. The environment control system was not located near the circuitry of the main system. Wires connected the servos and relays to the SRCB.

4.7.6 Complete circuit view

Figure A.45 provides a complete view of the system. It shows simplified connections from each board to components. Thirty-seven sensors in the chamber connect to the sensor board via sensor wires. Two power supplies connect to the sensor board to provide heating and sensing voltages. Three temperature sensors in the chamber connect to the temperature amplifying board. This board connects to two power supplies that provide voltage to the op amp circuit. The DAQ connection board collects sensor voltage data from the sensor board and temperature amplifying board. The personal computer saves sensor voltage data sample by the DAQ. The personal computer collects MOS, temperature and humidity data. The humidity data determines the PWM signal sent to the servo and relay control board from the Arduino Mega. This board, powered by a single power supply, adjusts the servo-controlled valves to maintain humidity within the chamber.

4.8 Software

The system uses four pieces of developed software. This software provides several functions to the system. The sensor data software collects sensor voltage data via DAQ. The mosquito image capture software controls the LXG-120M camera to capture mosquito images. The image conversion software converts captured mosquito images to reduce image size and storage requirements. The mosquito tracking software uses the captured mosquito images to track mosquito movement. Each piece of software will be covered below.

4.8.1 DAQ Sensor Data Collection software

MOS, temperature and humidity sensors selected for use in the system are analog sensors. Analog sensors produce an analog signal proportional to phenomenon measured. The sensors chosen for the system produce a voltage analog signal. The USB-6255 provides forty differential analog channels to measure these voltage signals. The software utilizing this DAQ must be written in LabVIEW, a visual programming language. The DAQ sensor data collection software provides two functions to the system. One function collects sensor voltage data during a MOS sensor test and allows the user to view this data. The second function monitors the environment within the chamber and adjust humidity. This program's GUI interface can be seen in Figure A.46. The program's back end can be seen in Figure A.47.

4.8.2 LabVIEW Data Collection

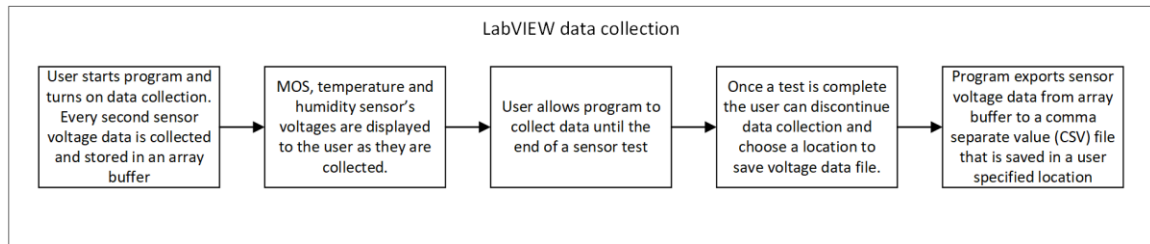


Figure 4.7 LabVIEW data collection flow chart

LabVIEW data collection is a component of the main DAQ program that collects sensor voltage data. The program records voltage data once a second from the sensor board via DAQ connections. The program collects voltage data of the MOS, temperature and humidity sensors. The program stores the voltage data in an array data structure. This occurs when a user begins collecting voltage data when testing. The program converts temperature and humidity voltage data into degrees Celsius and relative humidity. A user

can view the current MOS voltages, temperature and humidity during a test. When a user decides to stop collecting data, they can select a name and a location to save a comma separate value (CSV) file.

4.8.3 LabVIEW Humidity Control

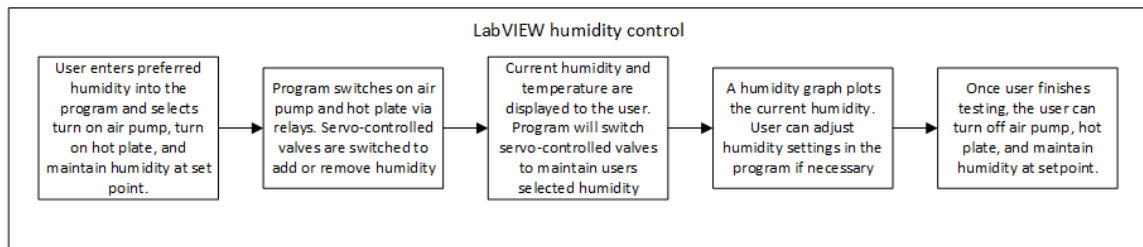


Figure 4.8 LabVIEW Humidity Control flow chart

LabVIEW humidity control is the second component of to the main DAQ program. The program offers several options to the user to maintain the environment within the chamber via DAQ and SRCB. This component combined with the data collection component provides controls to conduct a MOS sensor test. A user can turn on the system's air pump and hot plate by selecting specific controls. This control provides signals to the SRCB via Arduino micro controller. These signals switch on and off these components using relays. A user can also turn on maintain humidity at set point to allow LabVIEW to control humidity airflow. Users provides the program with a humidity set point they want the system to maintain. As the humidity in the chamber goes above or below the set point the LabVIEW program chooses which servo-controlled valve to open. The program selects the proper servo-controlled valve and adjusts it to the open position using the SRCB via Arduino micro controller. The software plots the current humidity for the user. The user can adjust the humidity controls if necessary. Once testing has been completed and sensor voltage data is saved a user can turn off environment controls.

4.8.4 Mosquito Image Acquisition

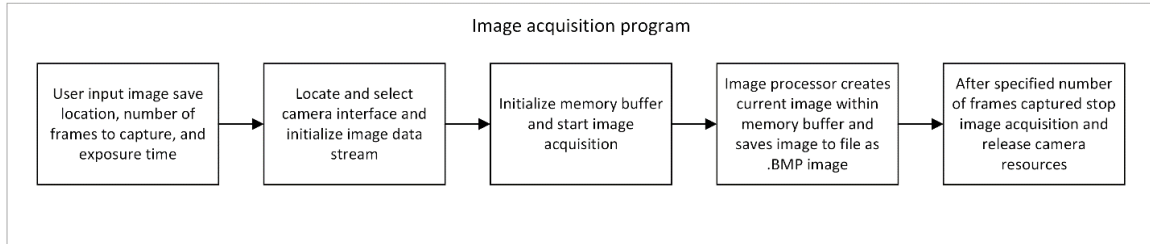


Figure 4.9 Image Acquisition flow chart

Understanding the mosquito behavioral response to DEET requires collecting image data of mosquito movement. This image data reveals behavioral changes in response to the dissipation of DEET. The Baumer Software development kit (SDK) provides programming tools required to develop C++ based programs to interface with Baumer cameras. This program based in C++ uses Baumer's SDK and OpenCV libraries to handle image processing.

The image acquisition software captures images from the data stream provided by the LXG-120M. A user selects the image save location, number of frames to capture, and exposure time. The SDK code used in the program searches for the Ethernet interface of the LXG-120M. Once the SDK finds the LXG-120M, a data stream initializes within the SDK code. A memory buffer initializes to temporarily store images before saving to file. The image processor of the SDK code creates an image of the camera's current view. The memory buffer contains this image. The current image within the memory buffer is converted into an OpenCV Mat format. The OpenCV imwrite function saves the image as a bitmap (BMP) file to the save location defined by the user. Each image saved is named "frame" with the current frame number after it. After image capture is complete the camera's data stream stops and memory buffer is released from resources.

4.8.5 Mosquito Image Conversion

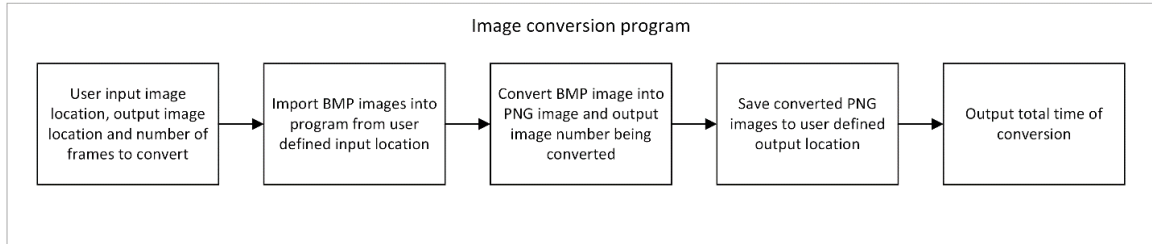


Figure 4.10 Image Conversion flow chart

The image conversion software reduces the amount of file space required to store the Bitmap (BMP) images. The BMP file-type provided fast saving of images but created very large files. BMP images are also lossless and uncompressed files. Converting the BMP images to the Portable Network Graphics (PNG) format could reduce file size and maintain image quality. This smaller image size reduced the amount of space required to store captured images. This software written in C++ use OpenCV libraries to handle image conversion and saving. A user selects the input image location, output image location, and the number of frames to convert. The program opens the image from the input image location as a BMP image. The BMP image is then converted to a PNG image and saved to the output image location. The time to convert the current image from BMP to PNG is output to screen.

4.8.6 Mosquito Image Tracking

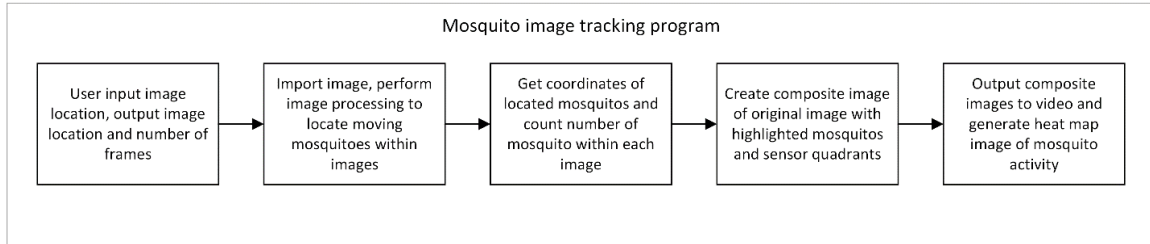


Figure 4.11 Mosquito Image Tracking flow chart

The mosquito image tracking software automates data processing of mosquito movement within the chamber. This program processes images collected by the LXG-120M. The program generates a video of tracked mosquitoes moving in the chamber. The program also generates a heatmap displaying the most active areas in the chamber. The program uses C++ and OpenCV libraries to handle image processing. Of the three programs used for mosquito images this one is the most complex.

The mosquito image tracking program provides a way to locate and track mosquitoes throughout the images captured by image acquisition program. A user selects the input image and output image location, and provides the number of frames to be processed. The program opens two images within the program using the OpenCV function `imread`. The images open within memory as a `Mat` OpenCV object. These images are the current image and the next image in the recorded sequence. The first image is subtracted from the second image. The resultant image shows changes in pixels that have occurred between each image. These changes are the mosquitoes that have moved between each image. Thresholding the resultant image removes any image noise from the image subtraction. Mosquitoes moving between each image appear as white pixels on a black background.

Locating the groups of white pixels within the resultant image provides the locations of the mosquitoes. Using the OpenCV function findContours provides a way to do this. FindContours draws a line around the white pixels representing the mosquito. Finding the center of each contour will provide the coordinates of each white pixel group. Before this can occur groups of white pixels require conditioning to contour the entire group of pixels. The Open CV erode function removes pixels from the outer parts of the pixel group. This also removes the mosquitoes shape. The pixel groups are then expanded using the OpenCV dilate function. This function adds pixels back to the pixel group. This causes the shape of the pixel groups to become circular. The findContours function locates each pixel group. The program calculates the center coordinates of each contour and stores them.

Measuring the mosquito's activity in the chamber requires dividing the chamber into quadrants. These quadrants correspond to the locations of the MOS sensors. Each quadrant has two separate counts associated with it. A current count and a total count for the quadrants update when mosquitoes coordinates are found within the quadrants. The current count displays the number of mosquitoes within a quadrant in a single frame of footage. The total count displays the total number of mosquitoes within a quadrant during the entire footage. After the finding the mosquito's coordinates a composite image is generated. This composite image has the original current image with the name of current test, date, frame number of the image sequence, and number of active mosquitoes within the current frame. The program draws circles around the mosquitoes to highlight their positions. The program draws rectangles on the composite image frame to display the boundaries of the quadrants. Current mosquito count and total mosquito count for each

quadrant are drawn above them. This visualizes what quadrants mosquitoes are currently in. Each frame goes through this process. The frames are then compiled into a video that can be reviewed after processing. A heatmap of all recorded mosquito movement of a test is compiled into one image.

CHAPTER V – METHODOLOGY

5.1 Overview of Experiments

Two data sets collected provide a view of mosquito's behavioral response to DEET. One set provides MOS sensor voltage data. Each MOS sensor provides a voltage response to the dissipation of DEET at specific locations inside the chamber. The higher the voltage recorded the higher the dissipation of DEET in an area. The second set of data provides mosquito movement within the chamber. A high definition camera records movement of mosquitoes exposed to DEET. After processing mosquito images highlighted areas of the chamber display areas of greatest mosquito activity. Each data set is collected with an increasing amount of DEET placed within the chamber over time. Data collection of the data sets occurred in two different instances. Two methodologies define how the system collects each data set. A standard operating procedure (SOP) outlining the process of data collection is in this document's appendix. A simplified SOP described below will outline essential testing procedures for both methodologies.

5.2 Experiment Methodology

5.2.1 MOS Sensor Voltage Methodology

The system uses all components except the camera to collect the MOS sensor voltage data. These trials use DEET with 95% purity. Each test involves three trials where 1 ml of DEET is introduced into the chamber. To begin testing, the MOS sensors within the chamber must be heated. Providing power to the system circuitry begins heating the MOS sensors and turns on the humidity and temperature sensors. Starting the LabVIEW program begins capturing voltage data via DAQ. Turning on the hot plate via LabVIEW program begins heating the bubbler. The chamber remains open for twenty

minutes to allow the MOS sensors to reach their voltage baseline in open air. Two 25ml Teflon dishes placed at the left end of the chamber provide locations for bait and DEET samples. An eighteen-inch injection needle feeds through the front 29/42 ground glass joint via septa. The needle is directed to the rightmost Teflon dish (Figure A.48). Both chamber ends placed on the chamber enclose the sensors within the controlled environment. An air connection from the flow meter placed into the 29/42 ground glass joint on the left chamber end provides airflow to the chamber. Turning on the air pump and selecting maintain humidity on the LabVIEW program maintains the chamber's environment at 65% relative humidity and 25°C. Allowing fifteen minutes to elapse provides time for MOS sensors to reach baseline within controlled environment. Once the environment establishes DEET testing can begin.

The MOS sensor response can scale from one to five volts depending on response. Adjusting the potentiometers on the sensor board changes the baseline of the MOS sensors. After the MOS sensors reach baseline adjusting them to one volt is the next step. A 1ml sample of DEET is pulled into a syringe. This syringe attaches to the needle directed to the Teflon dish. Before injecting the sample, a timer begins noting the time. At thirty seconds the 1ml sample is injected into the Teflon dish. Two more 1ml samples are added at 630 seconds and 1230 seconds. At 1800 seconds the test is completed. The LabVIEW program stops capturing the MOS voltage data and exports the captured voltage values to a CSV file.

5.2.2 Mosquito Data Methodology

The system uses all components to collect mosquito image data. This process is very similar to MOS sensor data collection methodology. These trials use DEET with

95% purity. Each test involves four trials. The first trial is bait only then 1 ml of DEET is introduced into the chamber for each subsequent trial. A total of twenty *Aedes aegypti* mosquitoes are placed into the chamber for each four-trial test. This number of mosquitoes is used for all mosquito testing. No MOS sensors are present within the chamber during this test. One humidity and one temperature sensor placed within the chamber ensure the environment of the mosquito test is identical to MOS sensor test. The LXG-120M camera is set up with all support equipment to record mosquitoes within the chamber. A sample of mosquito bait (Figure A.49) stimulates mosquito activity and encourages host seeking behavior. This sample of mosquito bait is placed in the leftmost 25ml Teflon dish (Figure A.50). An eighteen-inch injection needle feeds through the front 29/42 ground glass joint via septa. The needle is directed to the rightmost Teflon dish (Figure A.50). Both chamber ends placed on the chamber creates a controlled environment. A screen placed between chamber ends prevents mosquitoes from becoming trapped in each end. The air connection from the flow meter placed into the 29/42 ground glass joint on the left chamber end provides airflow to the chamber. Turning on the air pump and selecting maintain humidity on the LabVIEW program maintains the chamber's environment at 65% relative humidity and 25°C. Allowing fifteen minutes to elapse provides time for the controlled environment to reach correct humidity and temperature. Once the environment is established mosquito and DEET testing can begin.

The first trial observes mosquito activity with only bait. An individual introduces mosquitoes into the chamber 10 minutes before injecting DEET. The mosquitoes are introduced into the chamber via left mosquito hole (Figure A.50). A timer begins noting

the time as mosquitoes are introduced into the chamber. The LXG-120M camera begins recording at this time. This trial lasts for approximately 600 seconds. Preparing a syringe with 1ml of DEET before this trial completes ensures prompt injection of the sample. At the end of 600 seconds the camera stops recording. This is to allow the injection of the DEET to occur without interfering with mosquito recordings. The 1ml DEET sample is injected into the Teflon dish at approximately 630 seconds. The camera begins recording immediately after injecting the DEET sample. This process reoccurs at 1230 seconds and 1830 seconds. At 2400 seconds the test is complete. A total of four ten-minute recordings capture mosquito movement during these trials. The LXG-120M has a capture framerate of 19fps. A ten-minute recording captures 11400 frames.

5.2.3 Testing Methodology Differences

Each methodology uses different processes to collect data. MOS testing methodology uses all forty sensors during testing. The mosquito methodology only requires two sensors. These two sensors ensure proper humidity and temperature for a test. The MOS testing methodology has only a DEET sample introduced into the chamber. The mosquito methodology has both a bait and DEET sample introduced into the chamber. The methodologies have a different number of test trials, three trials for MOS testing methodology and four trials for mosquito methodology. The fourth trial of the mosquito methodology is the bait trial. The mosquito methodology requires camera and image capture equipment to be used.

5.2.4 DEET Concentrations

Each set of testing methodologies use 1 ml, 2 ml and 3 ml of DEET. The concentration of DEET molecules increases as the volume of DEET is increased. 1 ml of DEET within the chamber has a concentration of 24.24 ppm of DEET molecules. 2 ml of DEET within the chamber has 49 ppm of DEET molecules. 3 ml of DEET within the chamber has 73.37 ppm of DEET molecules. These concentrations are found within the chamber with a volume of 40.59 liters.

5.3 Data Processing

5.3.1 MOS Sensor Voltage Data Processing

MOS sensor voltage data provides a view of the DEET dissipation within the chamber. Thirty-six MOS sensors show a voltage response according to how much DEET is detected near each sensor location. Eight data sets collected have three separate trials conducted with 1ml of DEET to 3ml of DEET. These trials were conducted from 10-18-2017 to 12-9-2017. This produces a significant amount MOS voltage data. Microsoft Excel was used to process the MOS, temperature, and humidity data.

Processing the MOS sensor voltage data involved finding the total voltage change of each sensor for each trial. The total voltage change provides a measure of how much DEET a MOS sensor has detected at its position throughout a trial. Equation 5.1 calculates the total voltage change a MOS sensors has in response to DEET.

$$V_{max\ voltage} - V_{start\ voltage} = V_{total\ voltage\ change} \quad (5.1)$$

Each sensor has a total voltage change for each trial. MOS sensors grouped into seven quadrants correspond to the quadrants used in the mosquito tracking program (Figure A.51, A.52, A53). Sorting the sensors and corresponding quadrants by total voltage

change provides a list of sensors ranked by greatest voltage change. Generally, MOS sensors that have detected larger amounts of DEET are found at the top of these lists. The list created for each test breaks down total voltage change by DEET sample sizes. Table 5.21 shows the sorted sensors and quadrants of 1 ml, 2 ml, and 3 ml of DEET sample sizes for MOS sensor test 10-18-2017. The sensor column sorts the sensors by greatest voltage change of that test. The quadrant column displays the corresponding sensors quadrant location. Each of the eight data sets of MOS sensor voltage has a table.

The top 50%, 25% and 10% of sensors and quadrants with the greatest voltage change are found. Table 5.29 shows a list of sensors with counts associated with them. Each count shows how many times a specific sensor was found in the top 50% of sensors. As there are eight data sets, any sensor with eight counts has a higher voltage change than the bottom 50% of remaining sensors. Sensors with lower count totals have some total voltage change that rank within the bottom 50% of sensors. Total voltage change correlates to amount of DEET dissipation detected. Sensors with higher count totals have stronger responses to DEET dissipation. Table 5.1 shows a list of quadrants with counts associated with them. Each count shows how many times a sensor within the quadrants was found in the top 50% of sensors. Quadrants with higher total counts have sensors within them with higher total voltage change. The quadrants with higher counts have areas with higher DEET dissipation. This provides a way to compare mosquito movement to MOS voltage response. Table 5.30 and Table 5.31 provide the sensors with greatest voltage change of the top 25% and 10% of sensors. Table 5.2 and Table 5.3 provide the quadrant equivalent.

5.3.2 Mosquito Image Data Processing

Mosquito image data provides a view of the mosquito activity as DEET dissipates throughout the chamber. Seven data sets collected have four trials conducted with bait, 1ml, 2ml, and 3ml of DEET. These trials were conducted from 7-18-2017 to 7-22-2017. This produced a significant amount of image data. The image conversion and mosquito tracking programs processed the mosquito images collected.

Each mosquito trial produced 11400 captured mosquito images. The image conversion program reduces the storage requirements of each image. The mosquito tracking program processes the converted images. The program locates moving mosquitoes within an image. The coordinates of the moving mosquitoes are then found and stored. The image of the chamber divides into seven quadrants to better track the mosquito's locations. If there are any mosquito coordinates within any of the seven quadrants, a count increments for the corresponding quadrant (Figure A.54). This count keeps track of the number of mosquitoes that have moved through a quadrant from the start of the trial. The program generates a video and single heat map for each trial. The heat map compiles all detected mosquito movement into one image and displays areas of detected movement. The quadrants and quadrant counts are drawn on each heat map. The quadrant counts provide exact number of detected moving mosquitoes within the quadrant.

5.4 Results

5.4.1 MOS Sensor Test Results

Table 5.1 Compiled top 10% quadrants for sensor with greatest voltage response

Top 10% of quadrants with greatest voltage response			
Quadrant number	Number of times Quadrants was in top 10% for 1ml of DEET	Number of times Quadrants was in top 10% for 2ml of DEET	Number of times Quadrants was in top 10% for 3ml of DEET
Q1	0	1	1
Q2	6	5	1
Q3	14	16	16
Q4	1	1	1
Q5	3	1	5
Q6	0	0	0
Q7	0	0	0

Table 5.2 Compiled top 25% quadrants for sensor with greatest voltage response

Top 25% of quadrants with greatest voltage response			
Quadrant number	Number of times Quadrants was in top 25% for 1ml of DEET	Number of times Quadrants was in top 25% for 2ml of DEET	Number of times Quadrants was in top 25% for 3ml of DEET
Q1	6	10	9
Q2	13	12	9
Q3	37	31	35
Q4	7	9	8
Q5	8	9	10
Q6	1	1	1
Q7	0	0	0

Table 5.3 Compiled top 50% quadrants for sensor with greatest voltage response

Top 50% of quadrants with greatest voltage response			
Quadrant number	Number of times Quadrants was in top 50% for 1ml of DEET	Number of times Quadrants was in top 50% for 2ml of DEET	Number of times Quadrants was in top 50% for 3ml of DEET
Q1	19	19	21
Q2	21	21	17
Q3	55	53	60
Q4	22	24	25
Q5	19	18	14
Q6	3	3	3
Q7	5	6	4

Table 5.4 Compiled top 10% quadrants for sensor with greatest voltage response plot

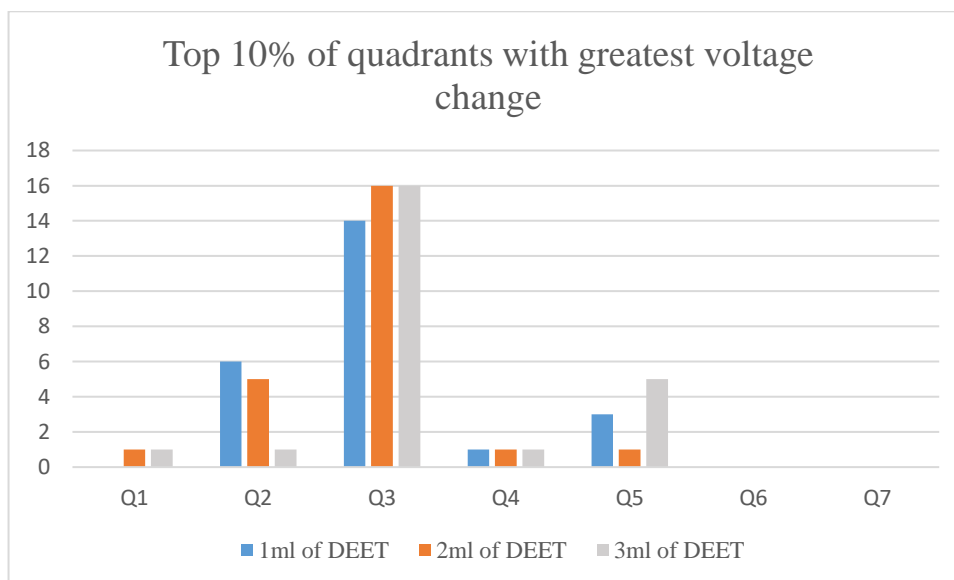


Table 5.5 Compiled top 25% quadrants for sensor with greatest voltage response plot

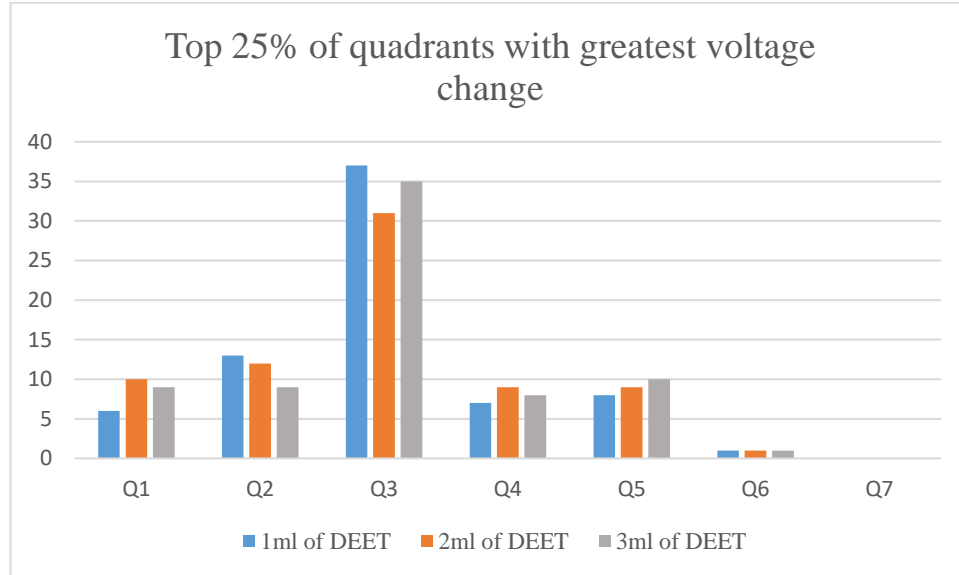
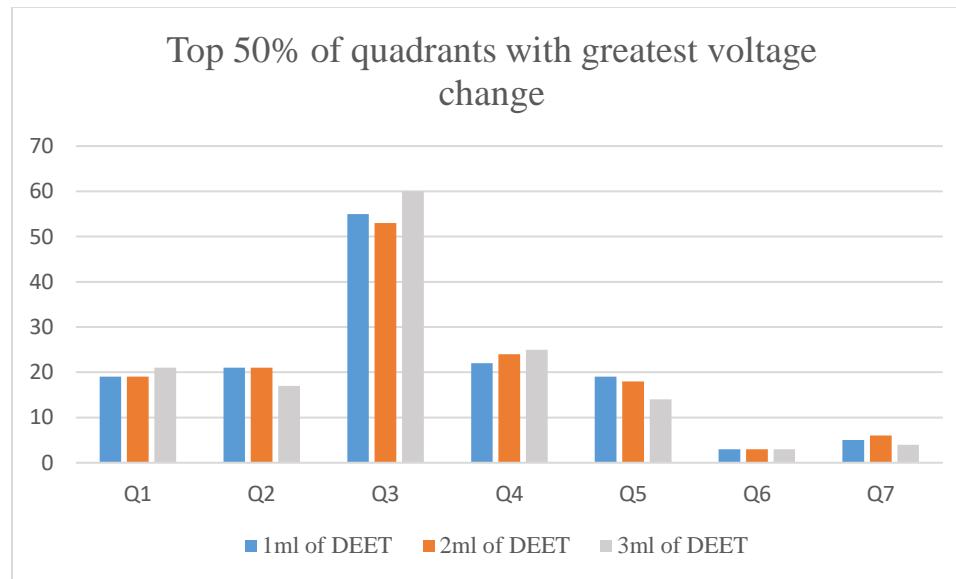


Table 5.6 Compiled top 50% quadrants for sensor with greatest voltage response plot



5.4.2 Mosquito Activity Results

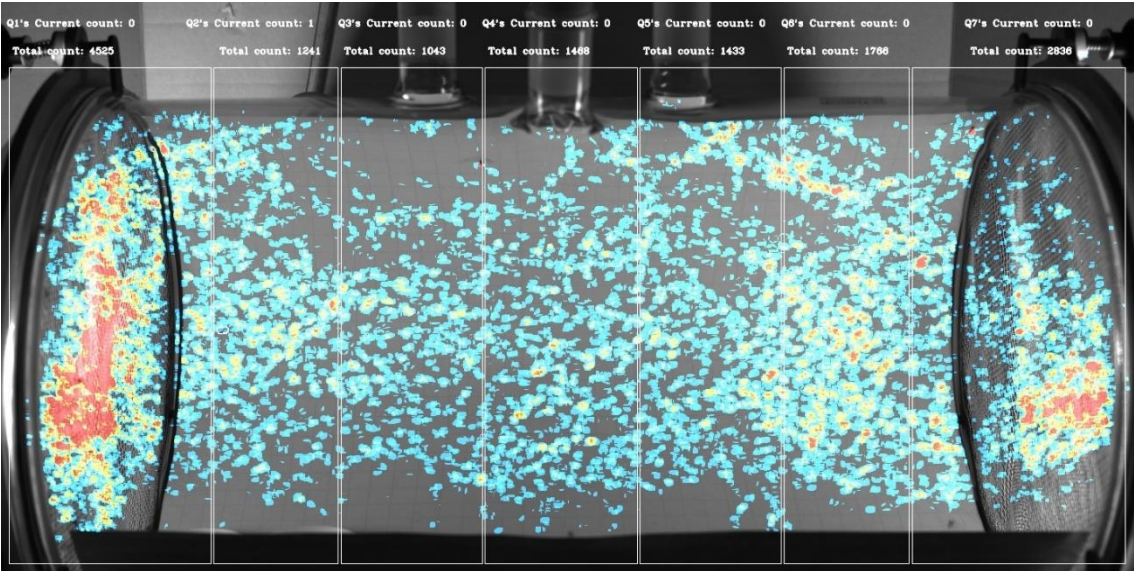
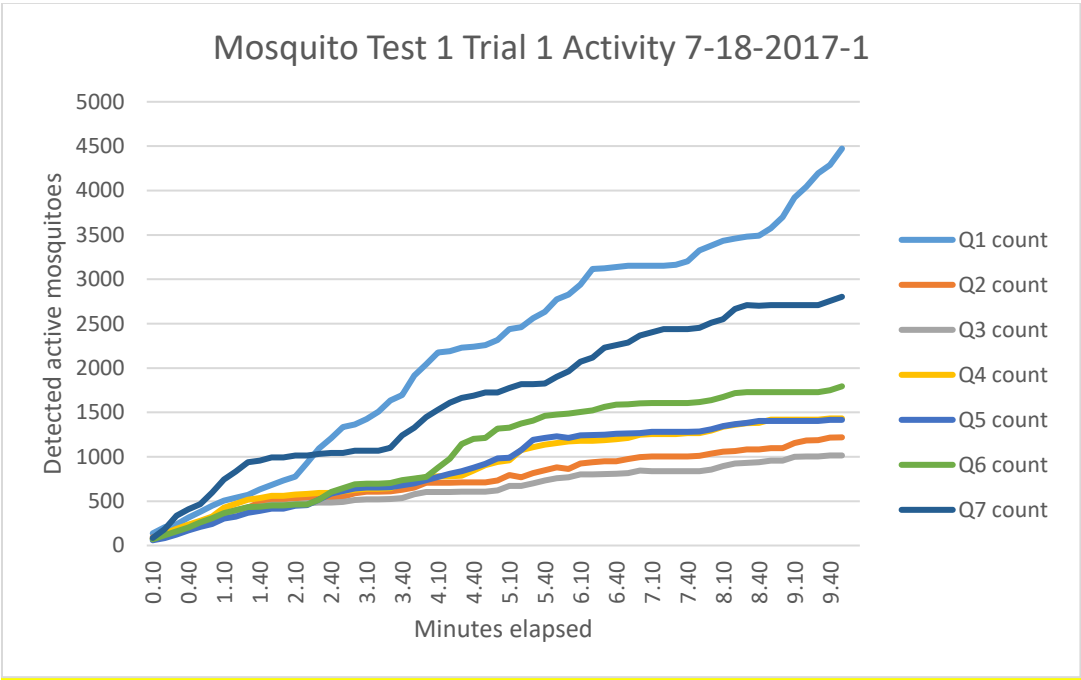


Figure 5.1 7-18-2017-1 test Bait trial mosquito heat map

Table 5.7 7-18-2017-1 test Bait trial mosquito activity during test



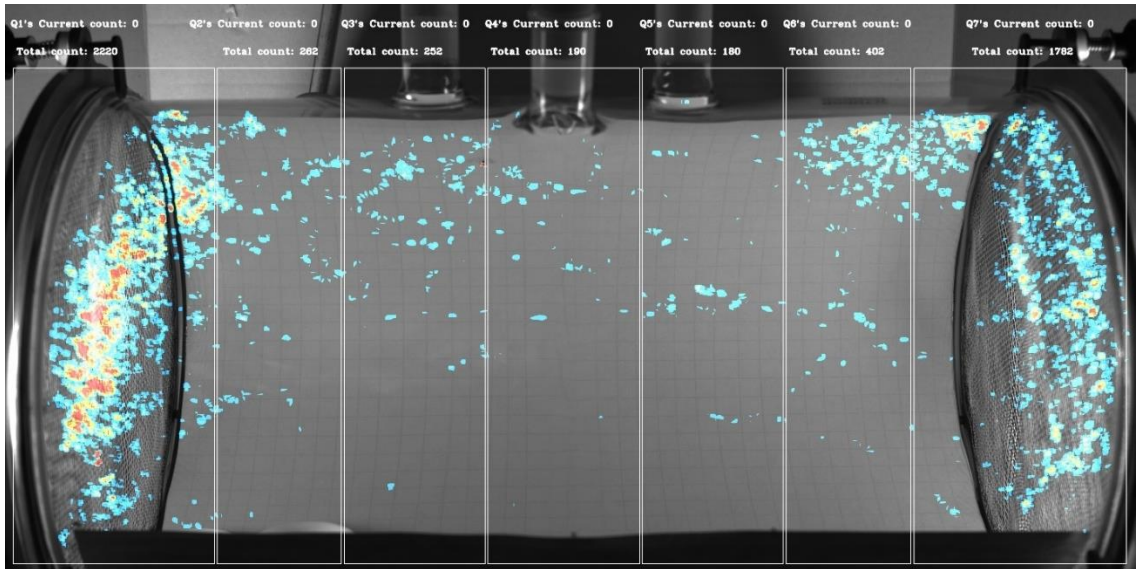
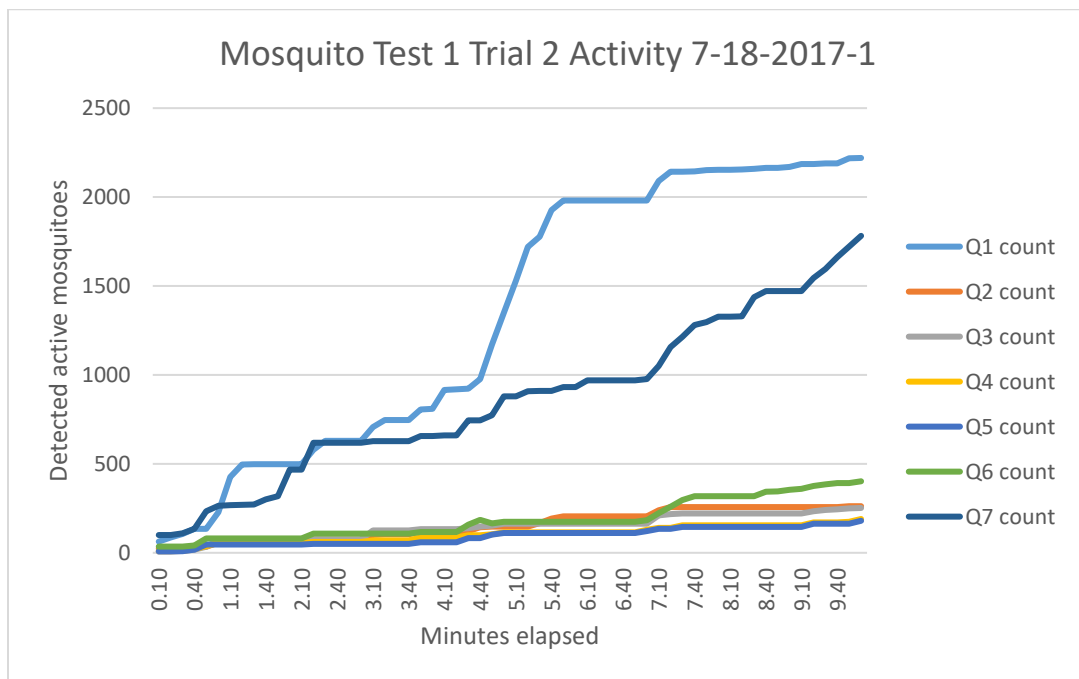


Figure 5.2 7-18-2017-1 test Bait + 1ml trial mosquito heat map

Table 5.8 7-18-2017-1 test Bait + 1ml trial mosquito activity during test



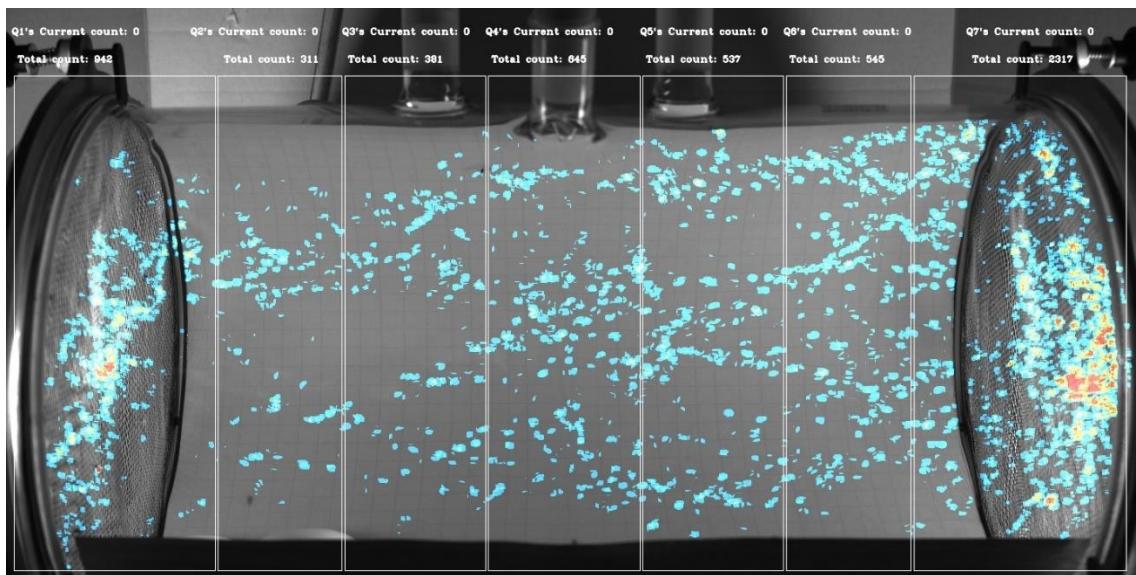
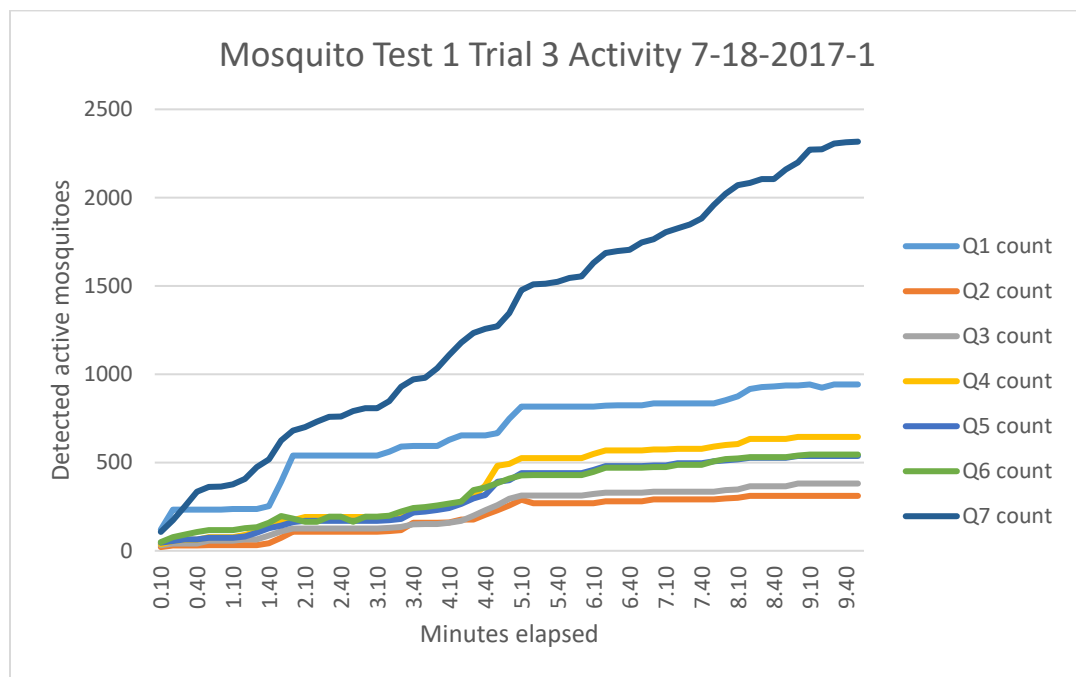


Figure 5.3 7-18-2017-1 test Bait + 2ml trial mosquito heat map

Table 5.9 7-18-2017-1 test Bait + 2ml trial mosquito activity during test



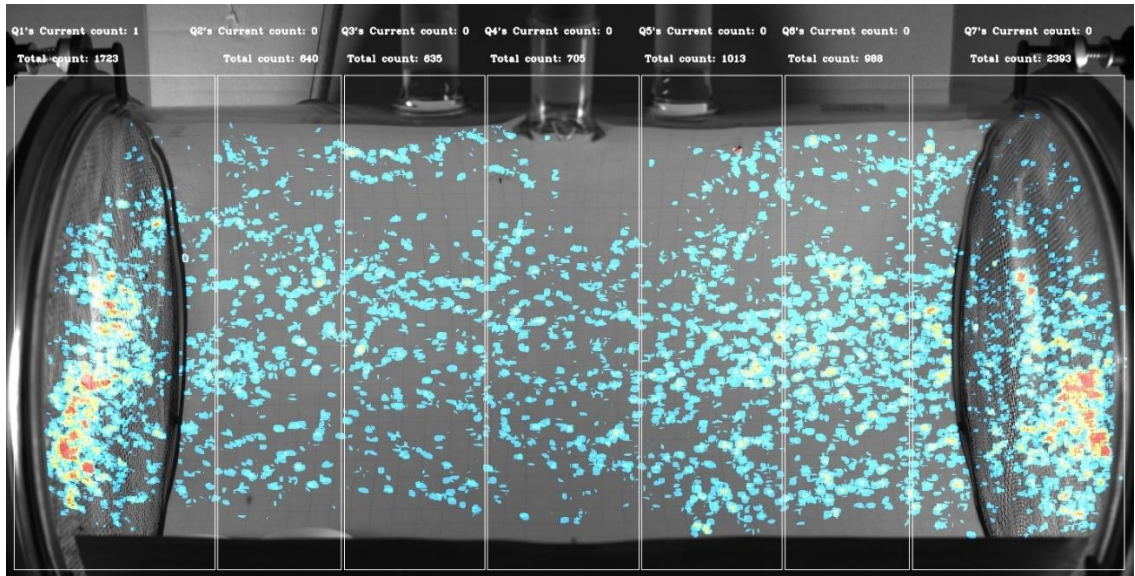


Figure 5.4 7-18-2017-1 test Bait + 3ml trial mosquito heat map

Table 5.10 7-18-2017-1 test Bait + 3ml trial mosquito activity during test

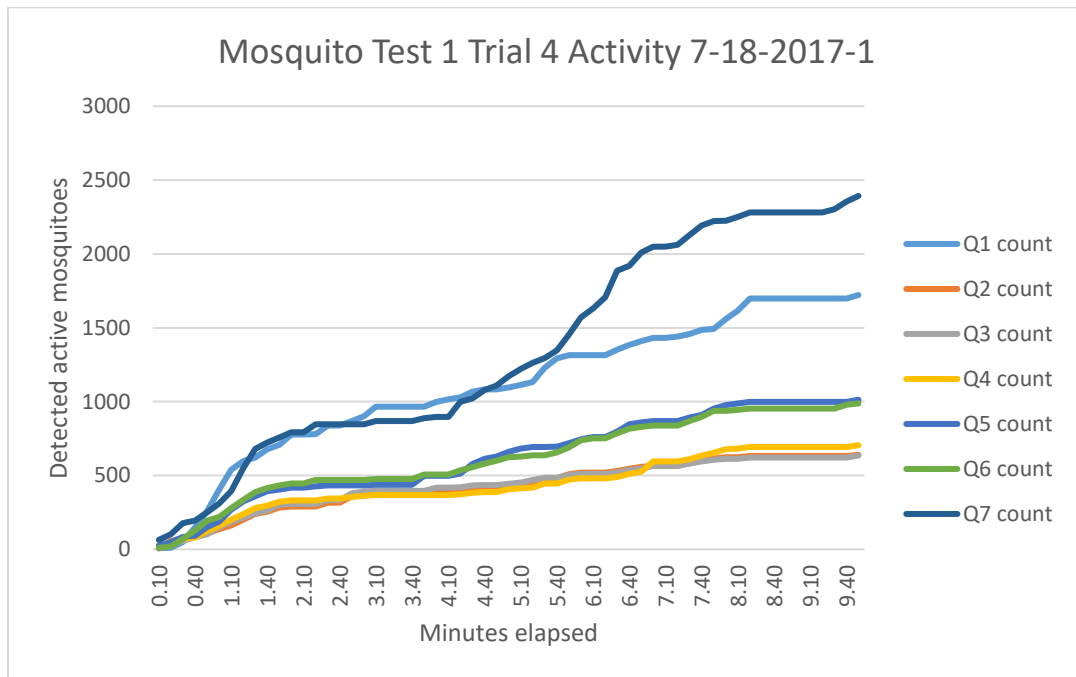
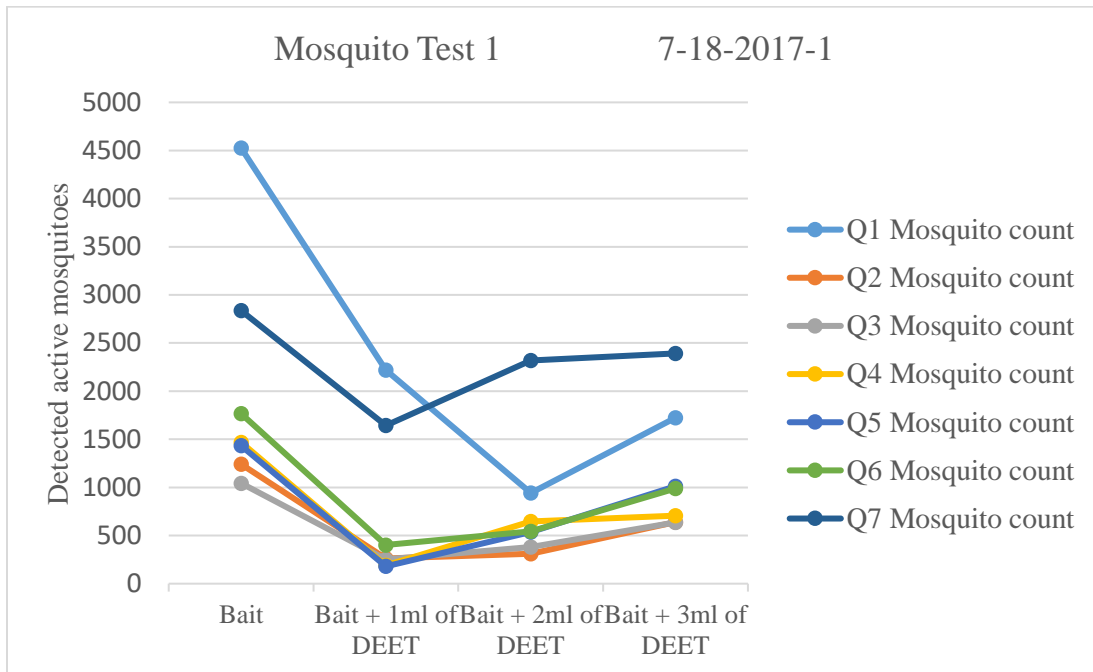


Table 5.11 7-18-2017-1 test quadrant mosquito count

Mosquito test 1		Date 7-18-2017-1						
Trial	Q1 count	Q2 count	Q3 count	Q4 count	Q5 count	Q6 count	Q7 count	Trial total
Bait	4525	1241	1043	1468	1433	1766	2836	14312
Bait + 1ml of DEET	2220	262	252	190	180	402	1643	5149
Bait + 2ml of DEET	942	311	381	645	537	545	2317	5678
Bait + 3ml of DEET	1723	640	635	705	1013	988	2393	8097
Quadrant total	9410	2454	2311	3008	3163	3701	9189	

Table 5.12 7-18-2017-1 test quadrant mosquito counts plotted



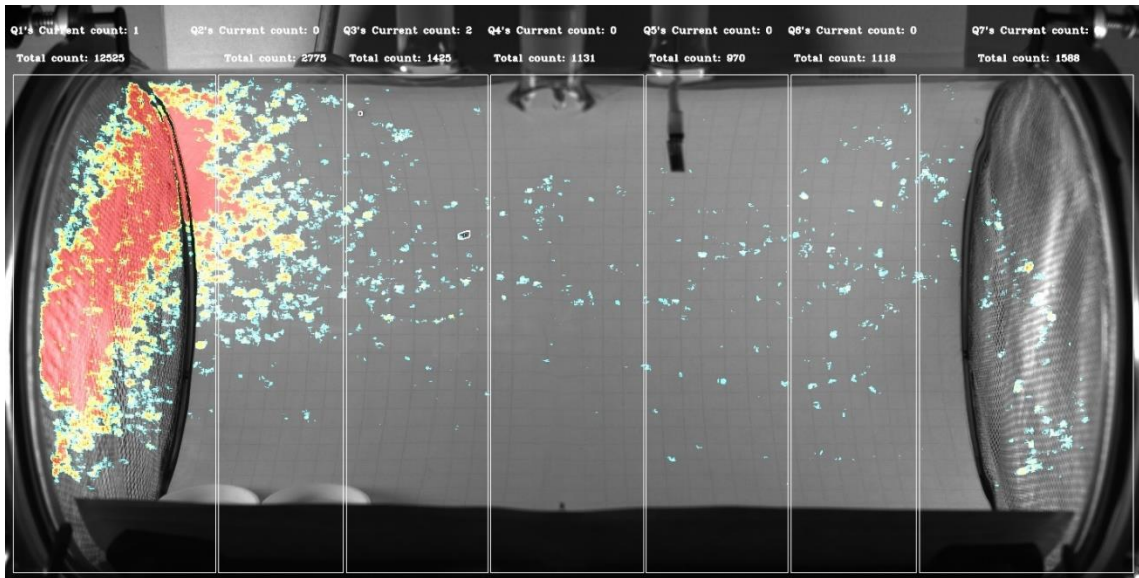
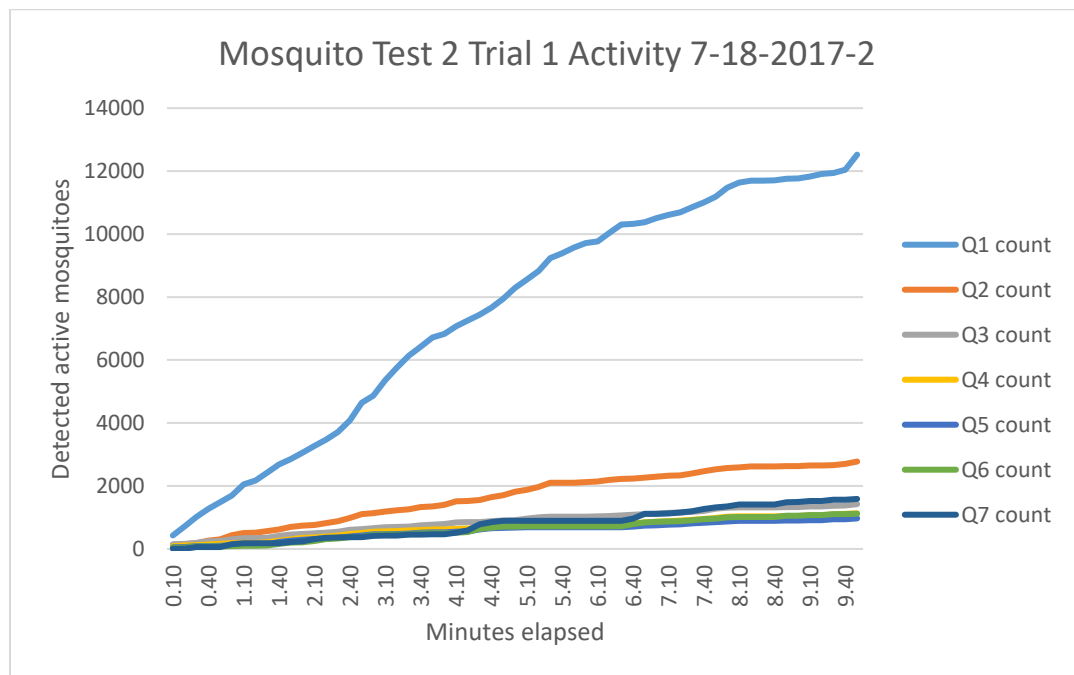


Figure 5.5 7-18-2017-2 test Bait trial mosquito heat map

Table 5.13 7-18-2017-2 test Bait trial mosquito activity during test



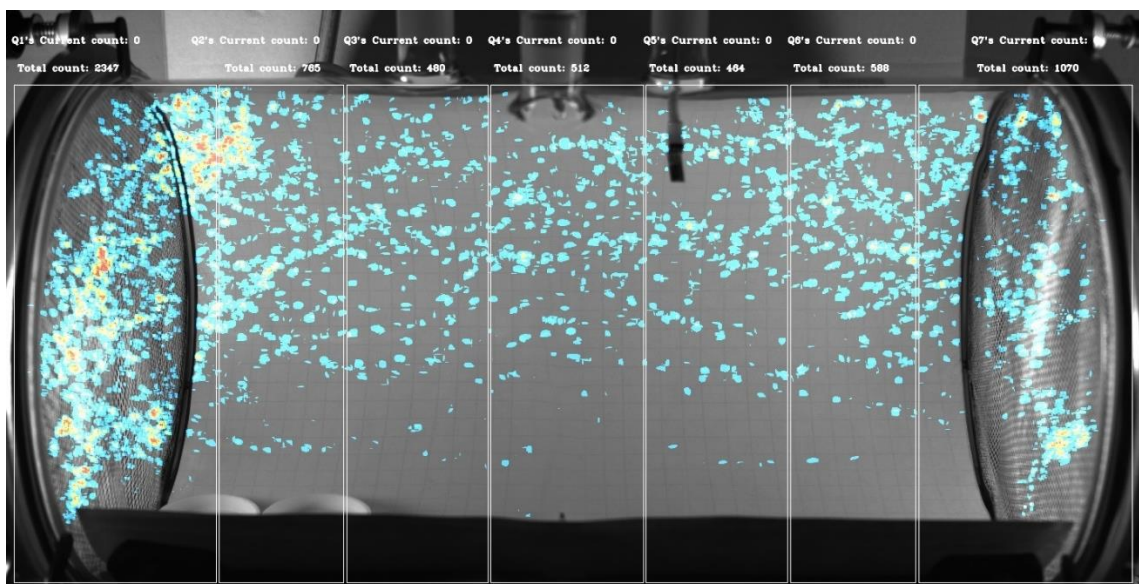
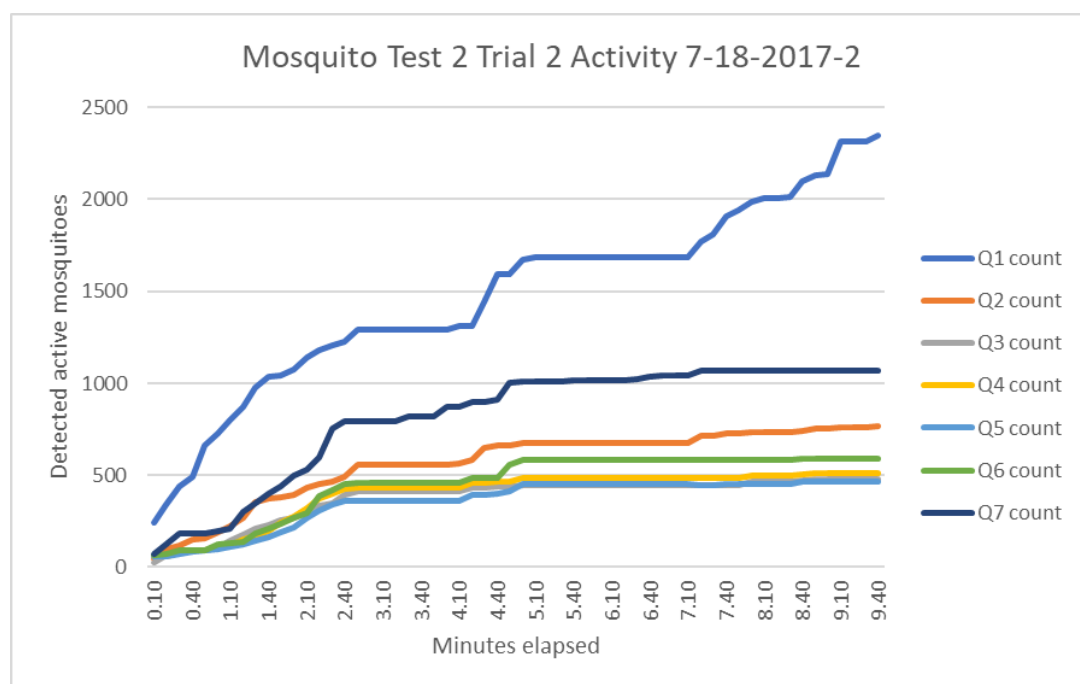


Figure 5.6 7-18-2017-2 test Bait + 1ml trial mosquito heat map

Table 5.14 7-18-2017-2 test Bait +1ml trial mosquito activity during test



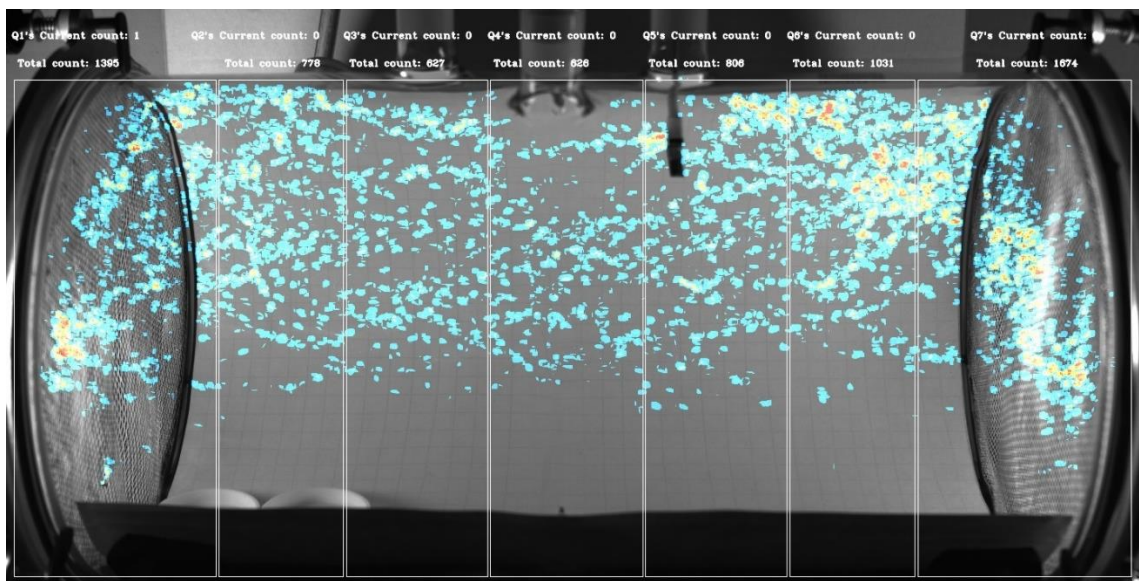
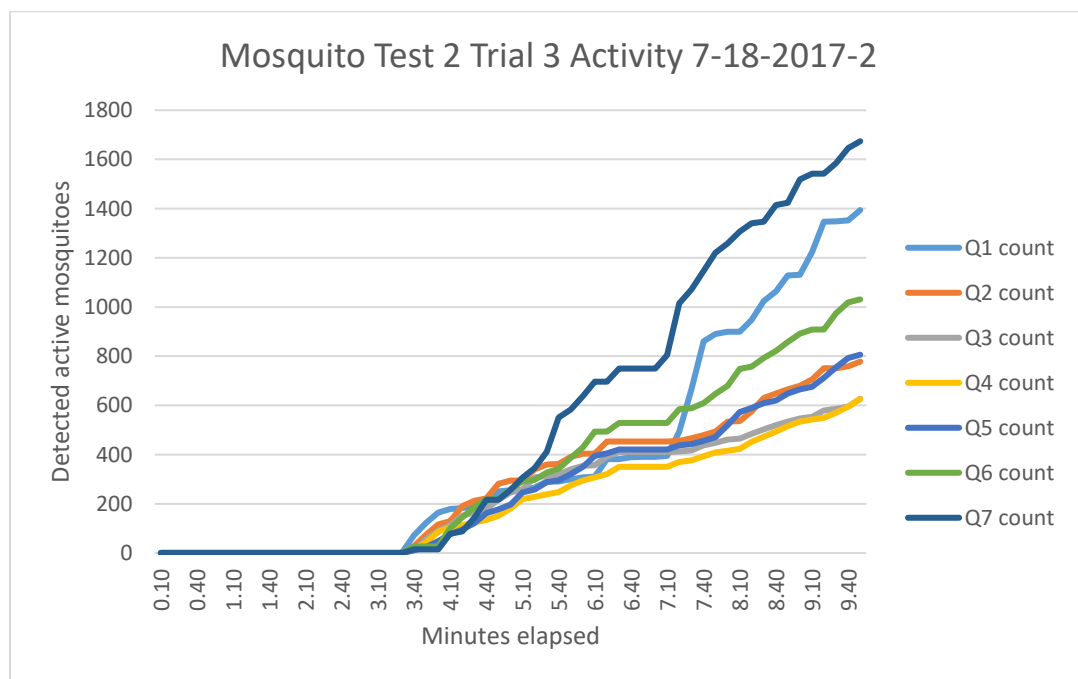


Figure 5.7 7-18-2017-2 test Bait + 2ml trial mosquito heat map

Table 5.15 7-18-2017-2 test Bait + 2ml trial mosquito activity during test



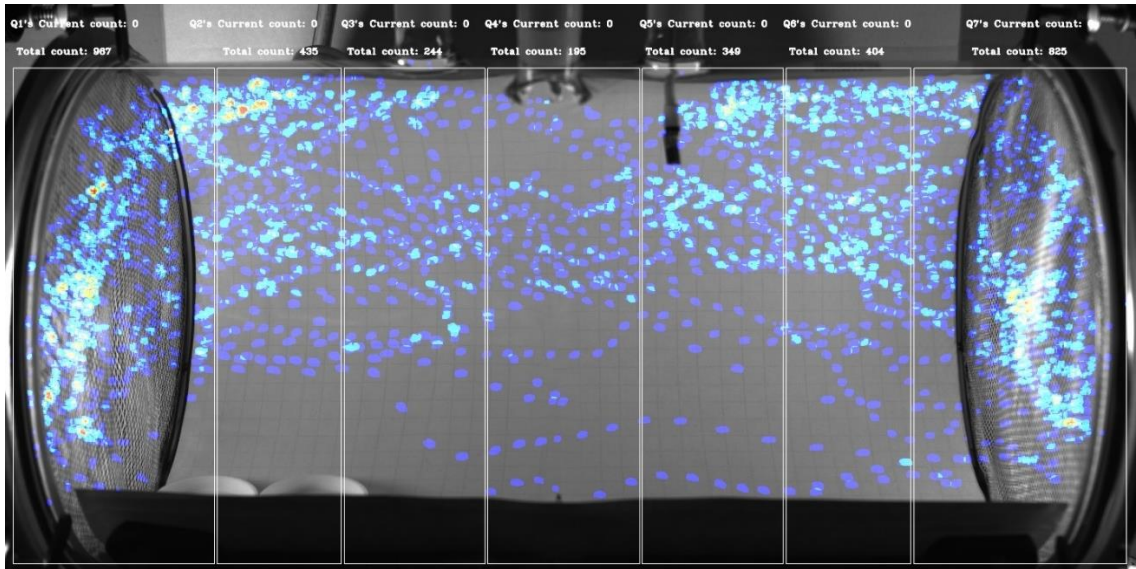


Figure 5.8 7-18-2017-2 test Bait + 3ml trial mosquito heat map

Table 5.16 7-18-2017-2 test Bait + 3ml trial mosquito activity during test

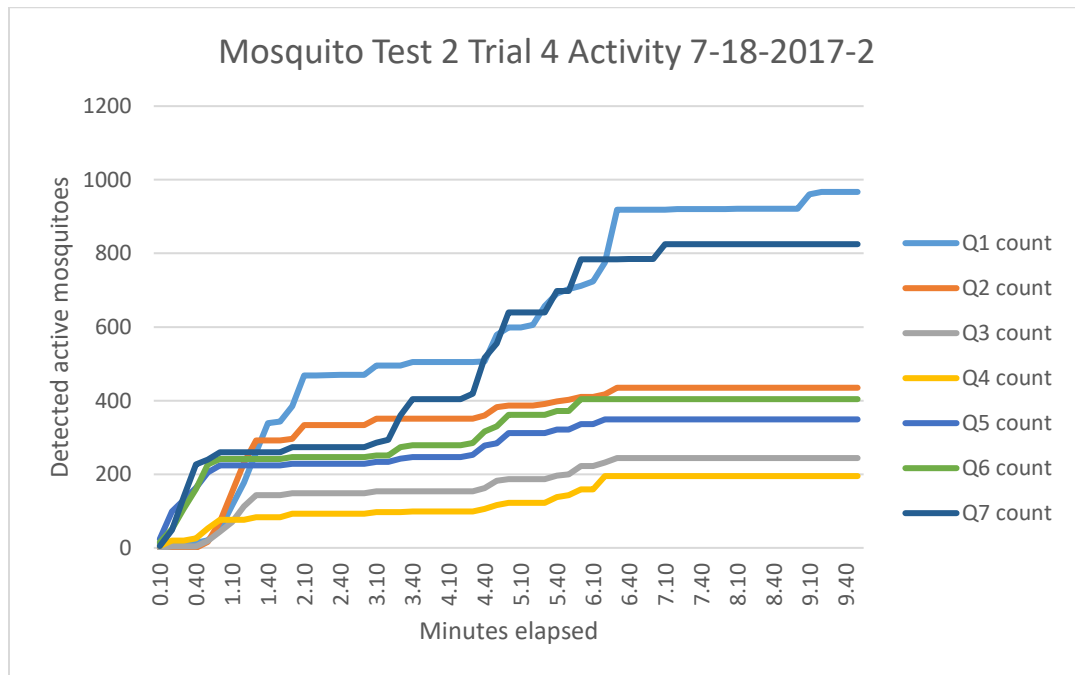
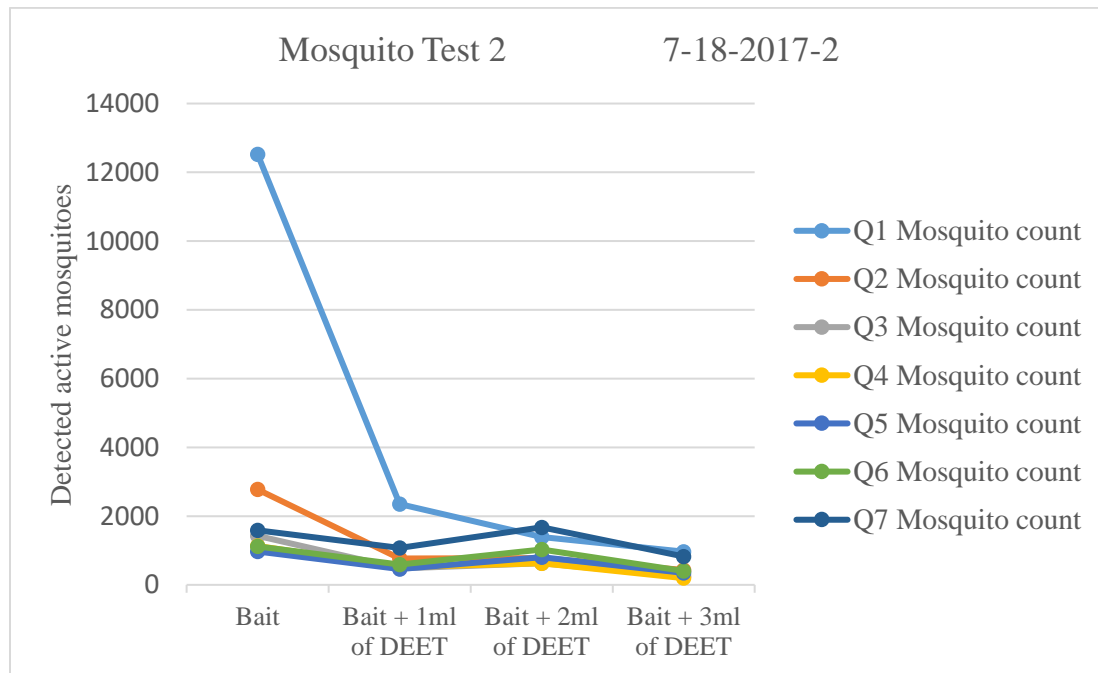


Table 5.17 7-18-2017-2 test quadrant mosquito counts

Mosquito test 2		Date 7-18-2017-2						
Trial	Q1 count	Q2 count	Q3 count	Q4 count	Q5 count	Q6 count	Q7 count	Trial total
Bait	12525	2775	1425	1131	970	1118	1588	21532
Bait + 1ml of DEET	2347	765	480	512	464	588	1070	6226
Bait + 2ml of DEET	1395	778	627	626	806	1031	1674	6937
Bait + 3ml of DEET	967	435	244	195	349	404	825	3419
Quadrant total	17234	4753	2776	2464	2589	3141	5157	

Table 5.18 7-18-2017-2 test quadrant mosquito counts plotted



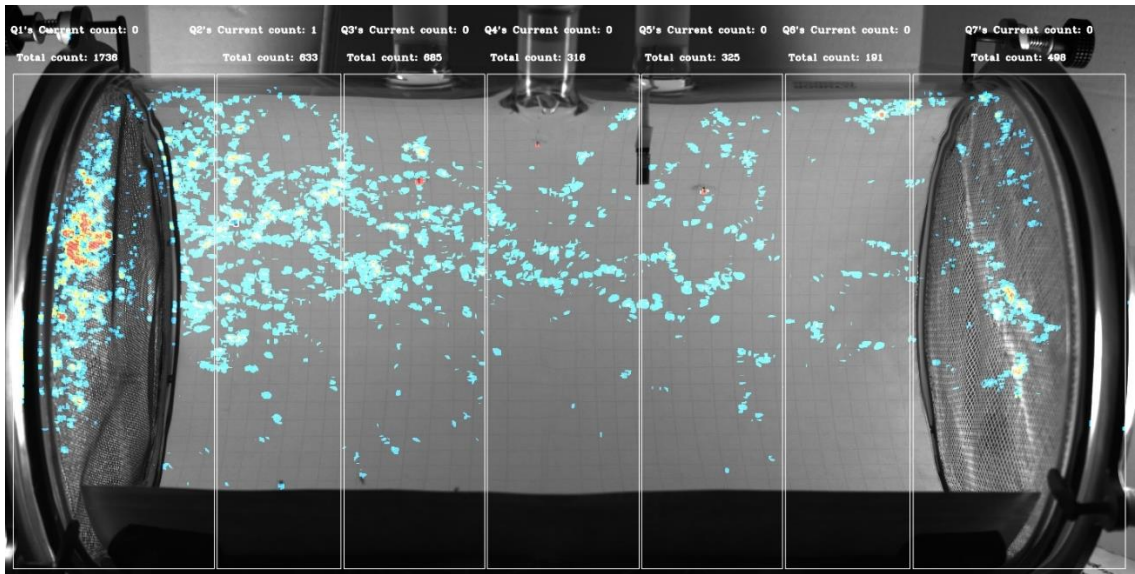


Figure 5.9 7-20-2017 test Bait trial mosquito heat map

Table 5.19 7-20-2017 test Bait trial mosquito activity during test

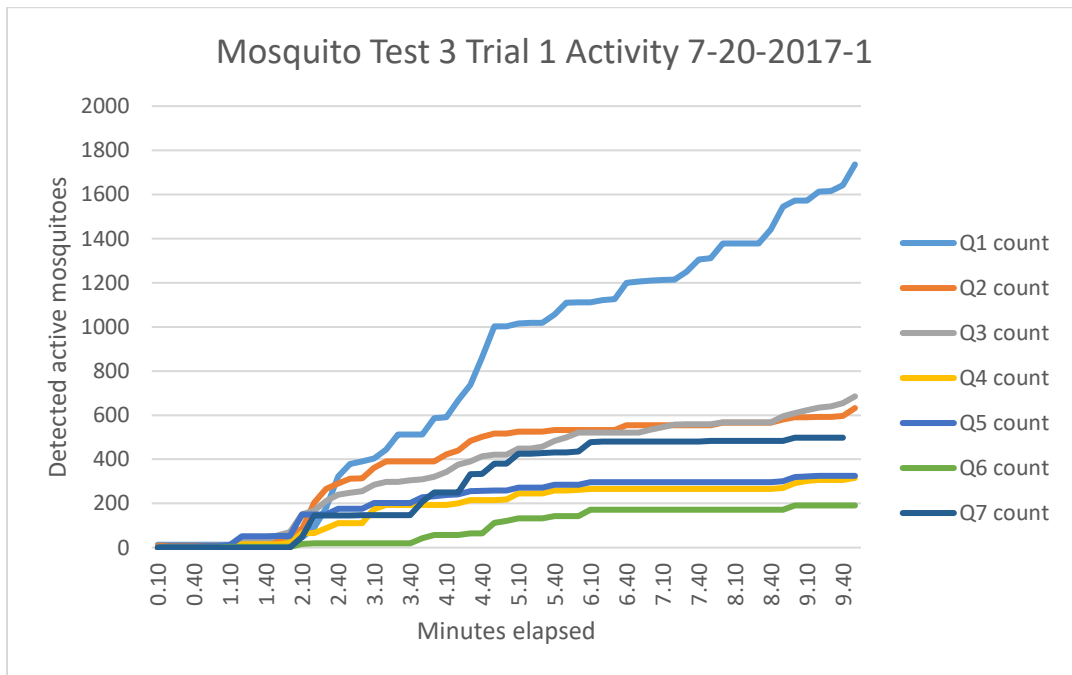
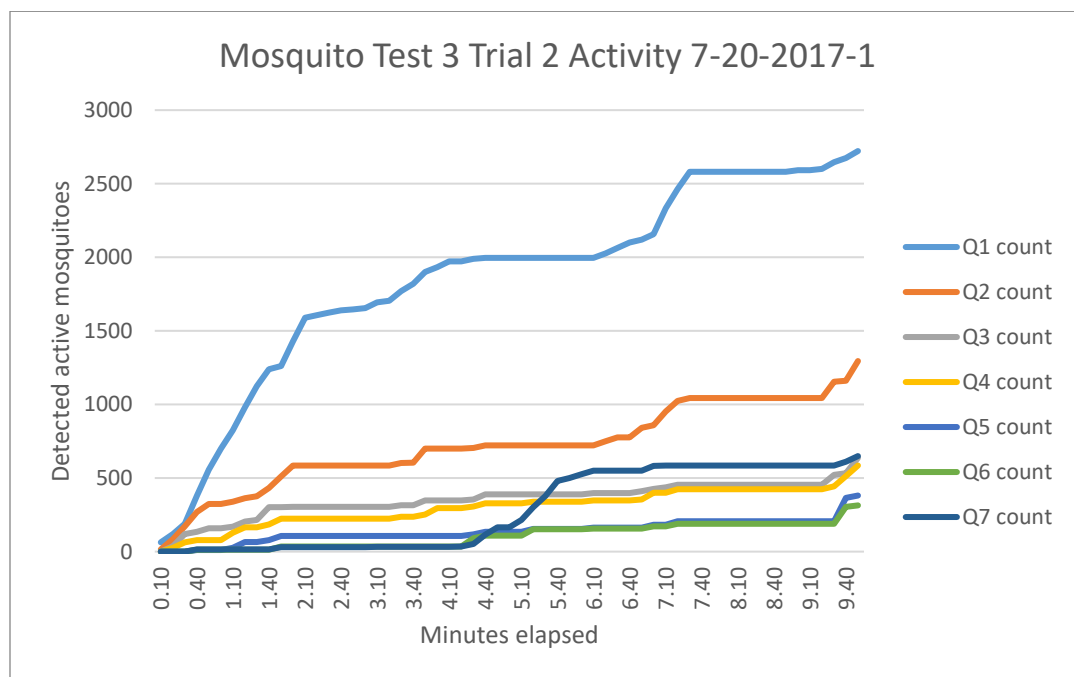




Figure 5.10 7-20-2017 test Bait + 1ml trial mosquito heat map

Table 5.20 7-20-2017 test Bait + 1ml trial mosquito activity during test



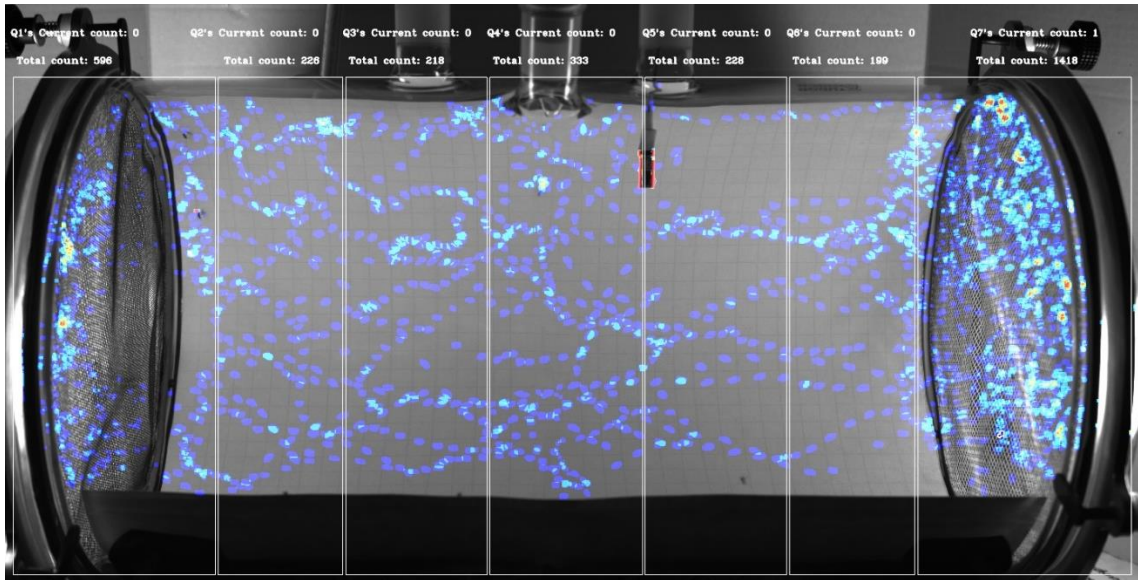
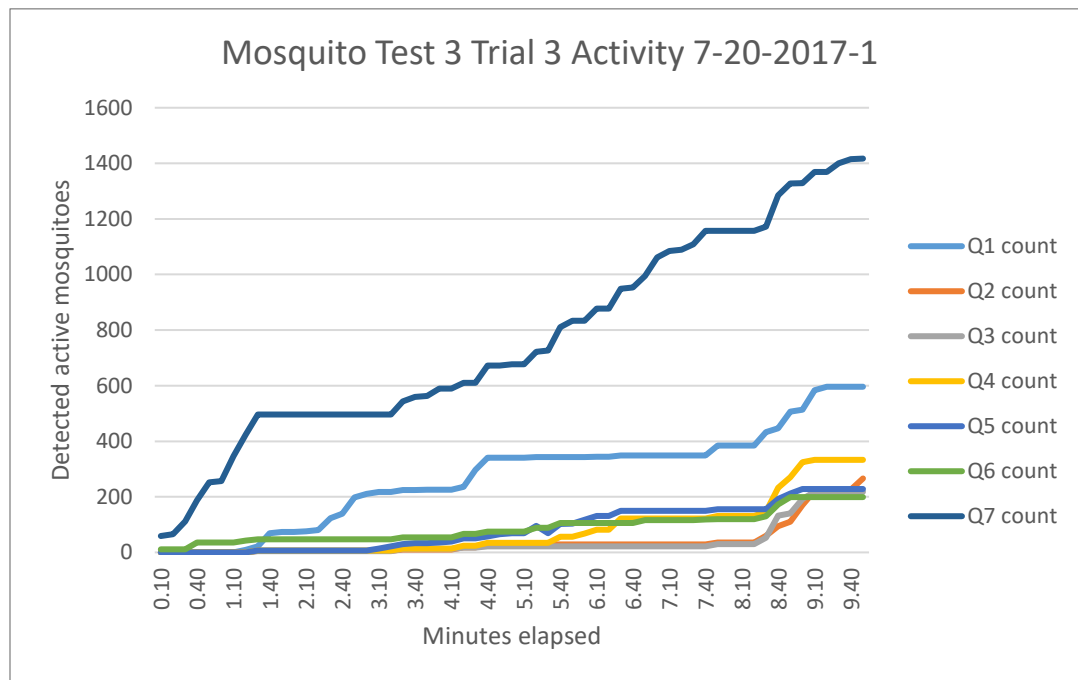


Figure 5.11 7-20-2017 test Bait + 2ml trial mosquito heat map

Table 5.21 7-20-2017 test Bait + 2ml trial mosquito activity during test



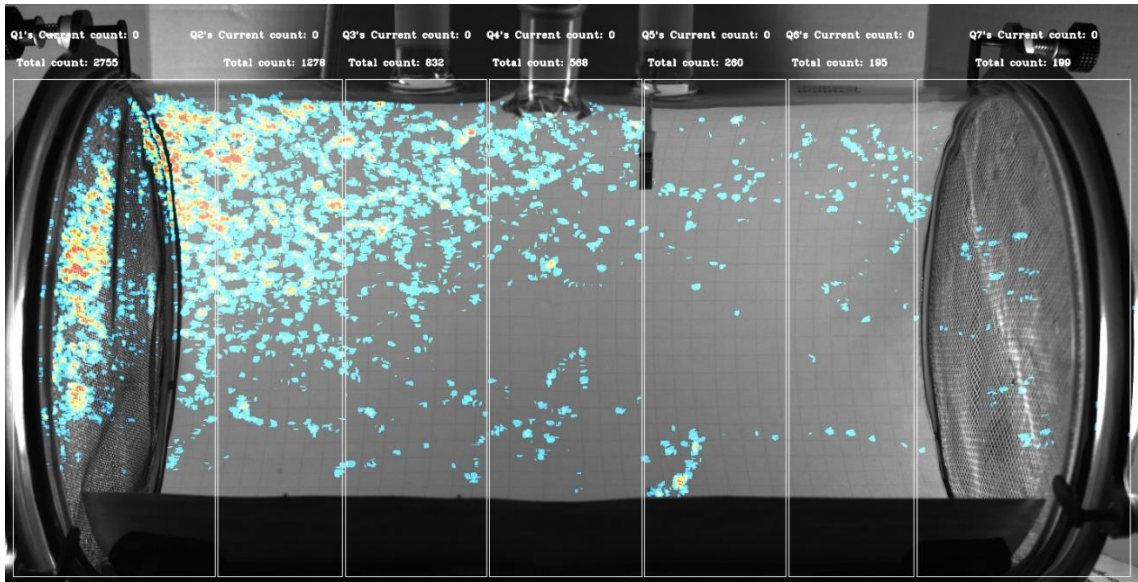


Figure 5.12 7-20-2017 test Bait + 3ml trial mosquito heat map

Table 5.22 7-20-2017 test Bait + 3ml trial mosquito activity during test

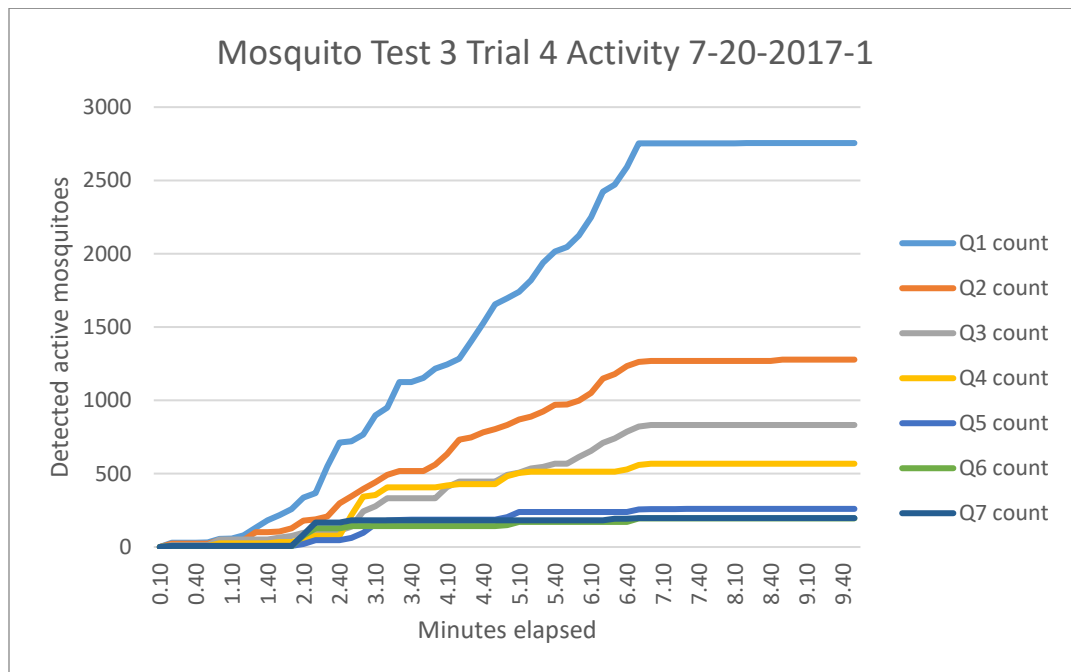
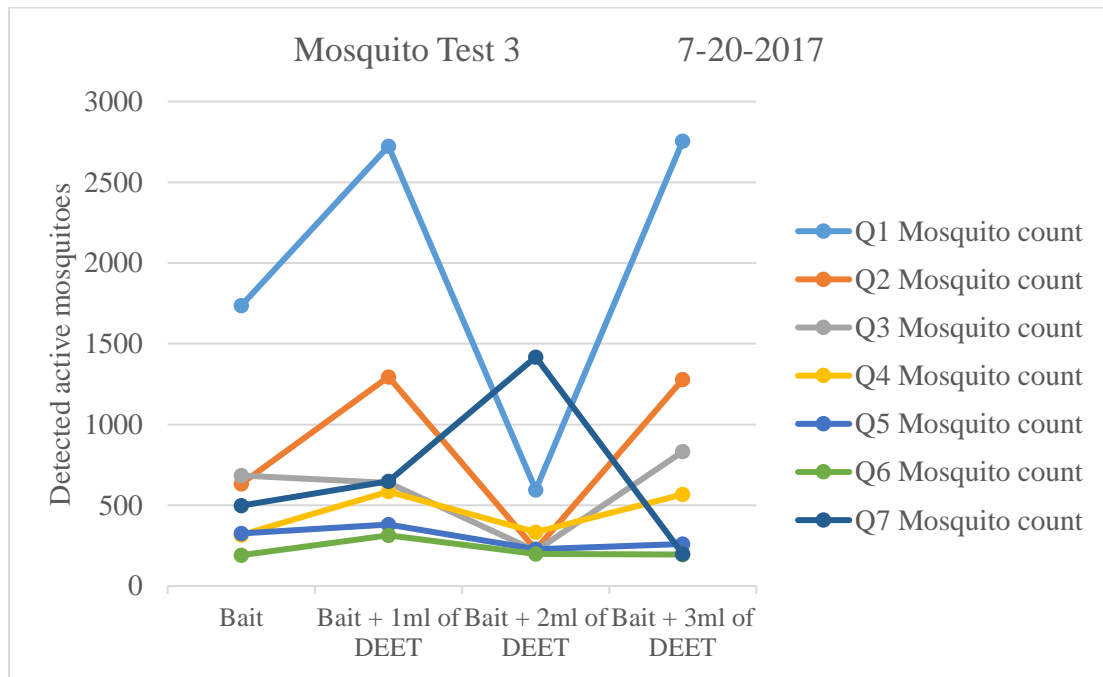


Table 5.23 7-20-2017 test quadrant mosquito counts

Mosquito test 3		Date 7-20-2017						
Trial	Q1 count	Q2 count	Q3 count	Q4 count	Q5 count	Q6 count	Q7 count	Trial total
Bait	1736	633	685	316	325	191	498	4384
Bait + 1ml of DEET	2722	1295	638	585	381	314	649	6584
Bait + 2ml of DEET	596	226	218	333	228	199	1418	3218
Bait + 3ml of DEET	2755	1278	832	568	260	195	199	6087
Quadrant total	7809	3432	2373	1802	1194	899	2764	

Table 5.24 7-20-2017 test quadrant mosquito counts plotted



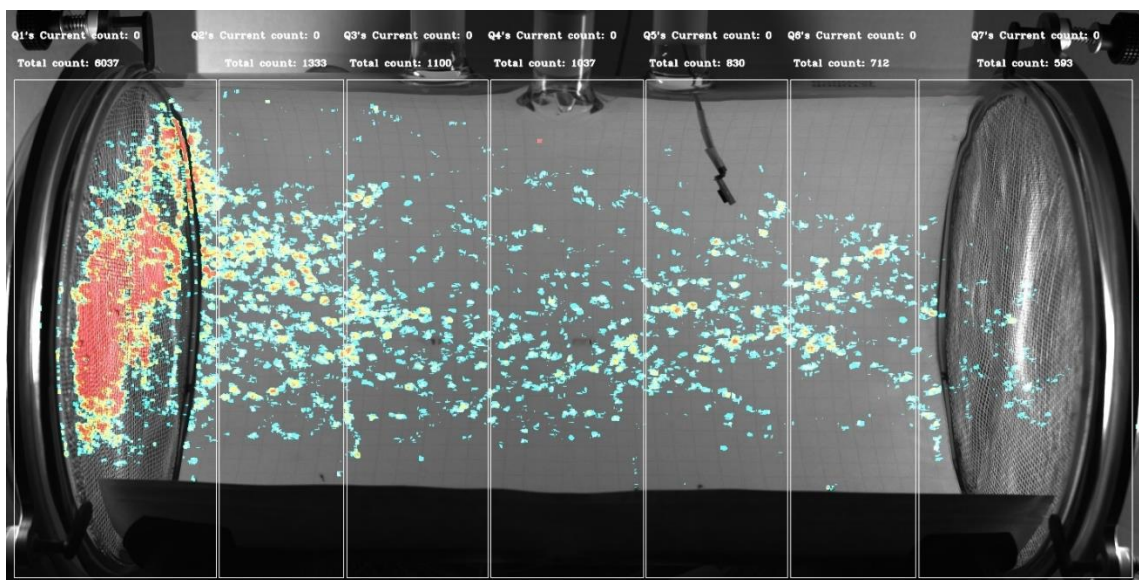
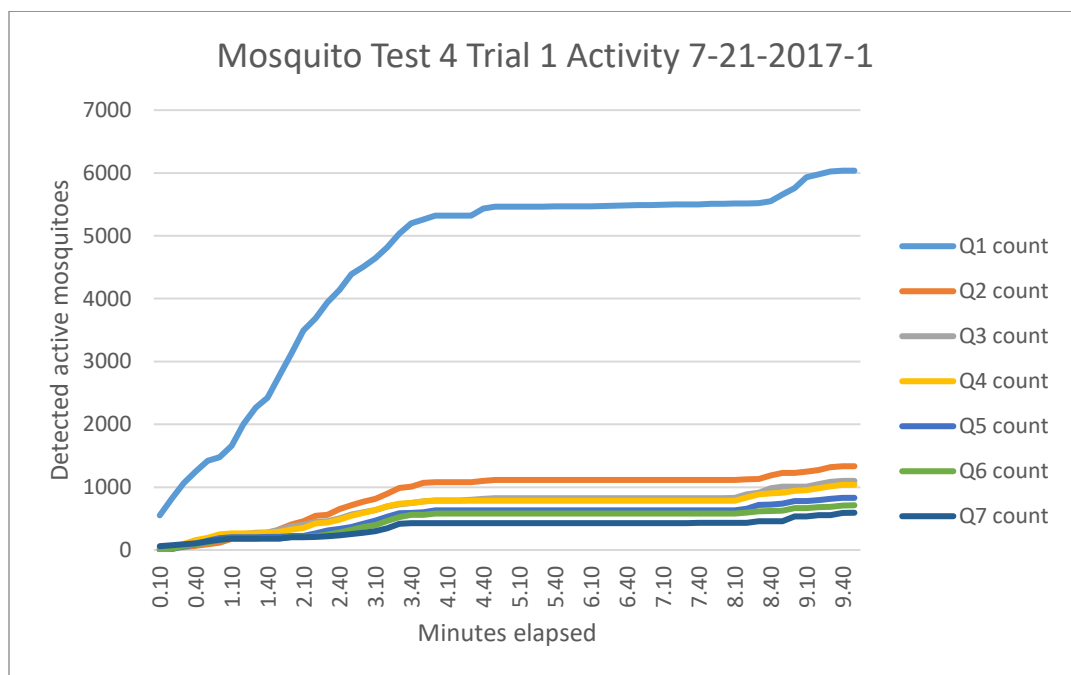


Figure 5.13 7-21-2017-1 test Bait trial mosquito heat map

Table 5.25 7-21-2017-1 test Bait trial mosquito activity during test



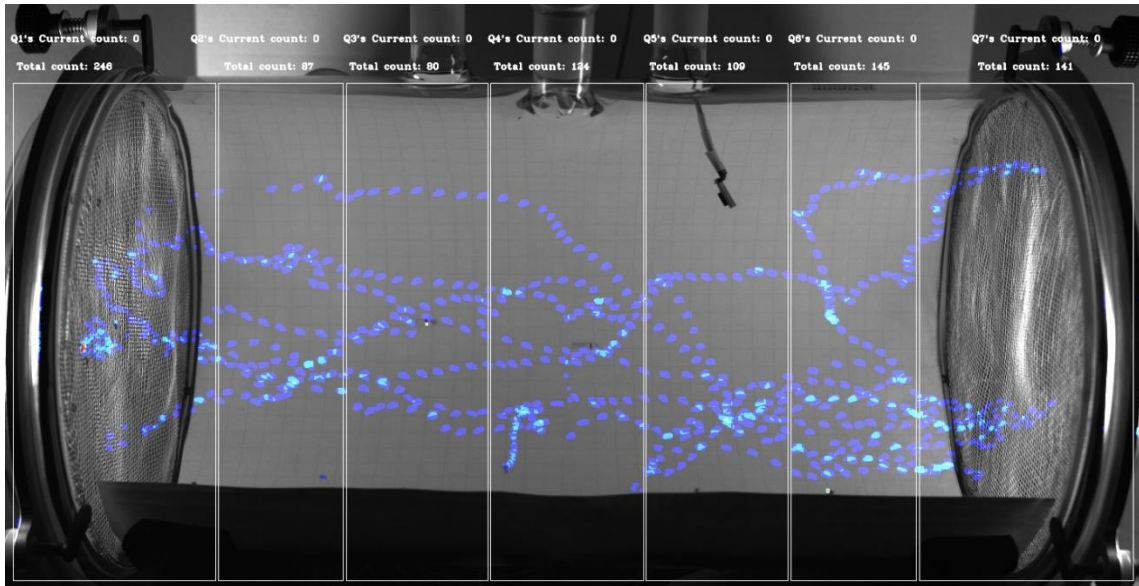
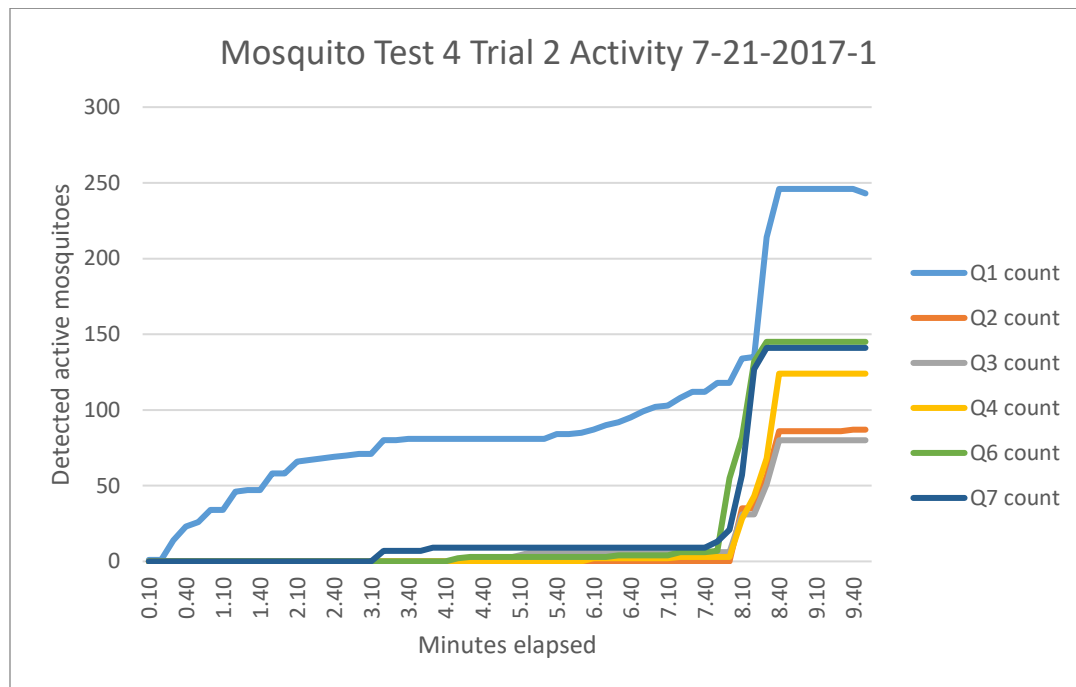


Figure 5.14 7-21-2017-1 test Bait + 1ml trial mosquito heat map

Table 5.26 7-21-2017-1 test Bait + 1ml trial mosquito activity during test



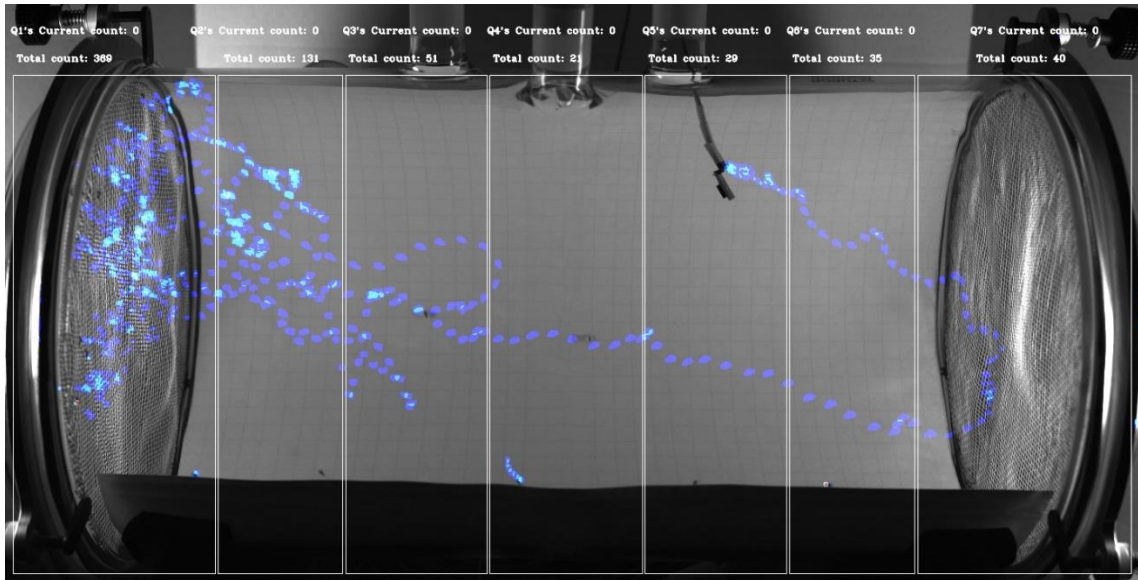
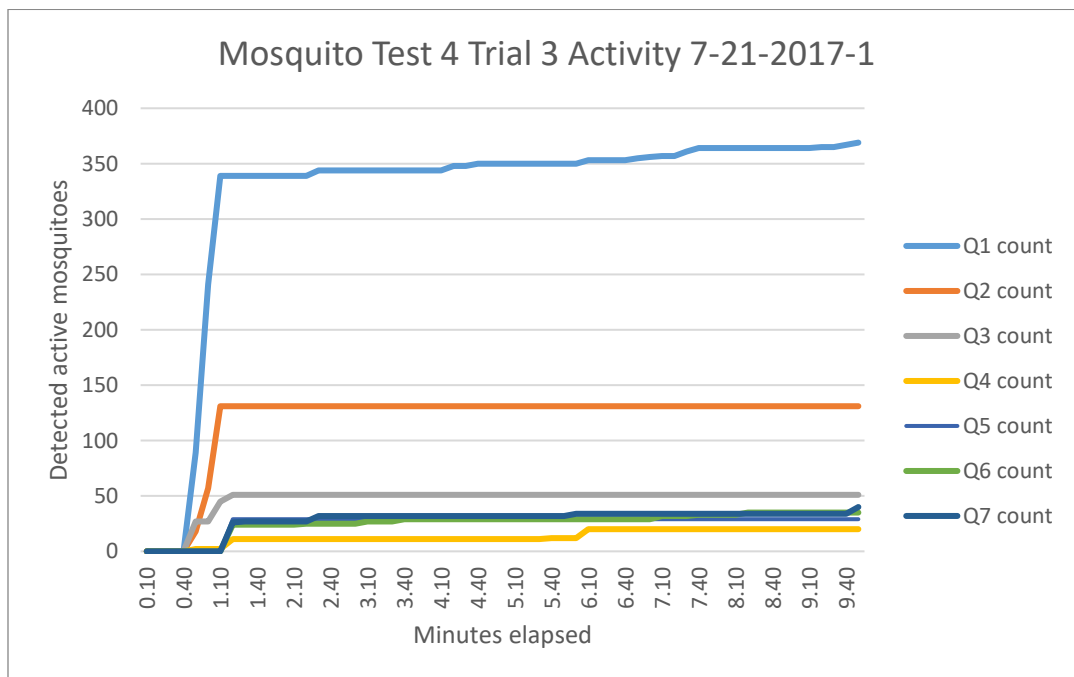


Figure 5.15 7-21-2017-1 test Bait + 2ml trial mosquito heat map

Table 5.27 7-21-2017-1 test Bait + 2ml trial mosquito activity during test



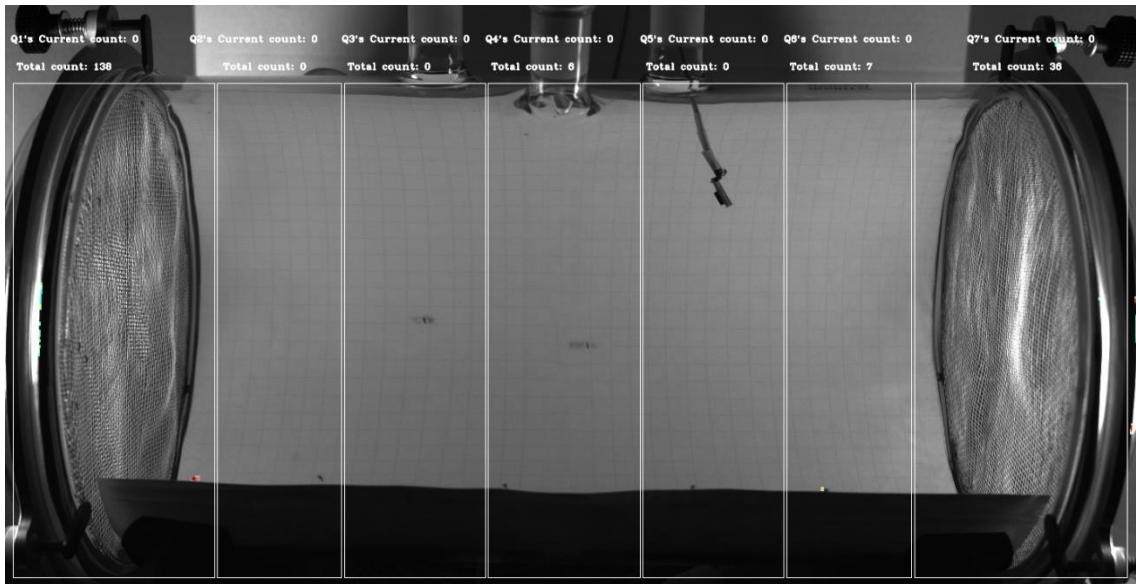


Figure 5.16 7-21-2017-1 test Bait + 3ml trial mosquito heat map

Table 5.28 7-21-2017-1 test Bait + 3ml trial mosquito activity during test

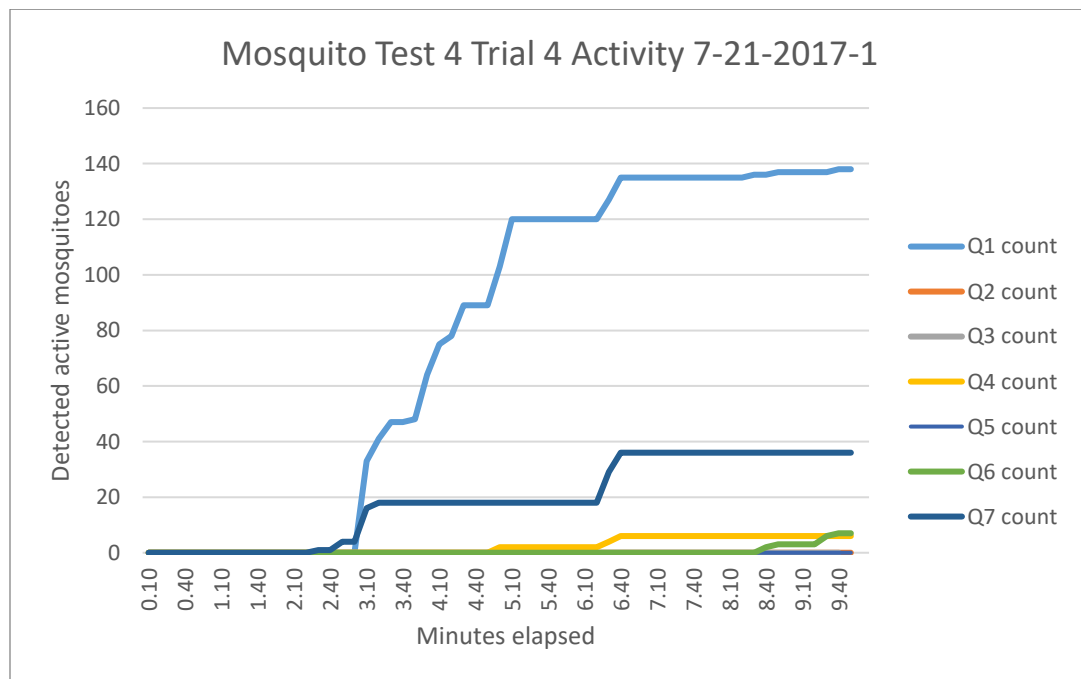
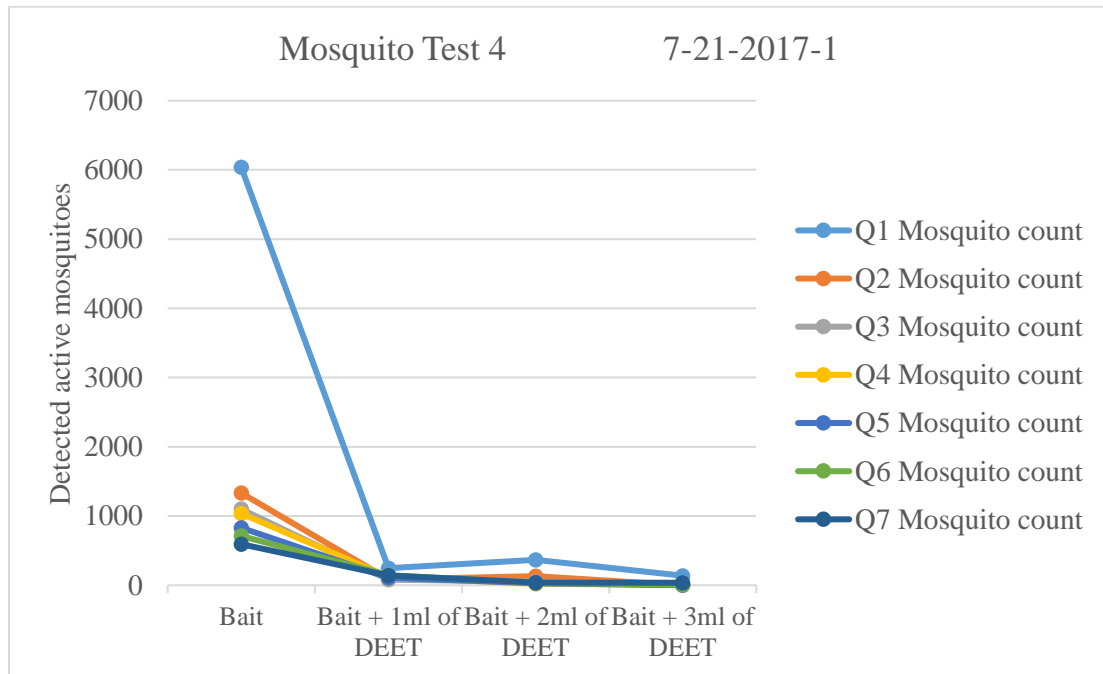


Table 5.29 7-21-2017-1 test quadrant mosquito counts

Mosquito test 4		Date 7-21-2017-1						
Trial	Q1 count	Q2 count	Q3 count	Q4 count	Q5 count	Q6 count	Q7 count	Trial total
Bait	6037	1333	1100	1037	830	712	593	11642
Bait + 1ml of DEET	246	87	80	124	109	145	141	932
Bait + 2ml of DEET	369	131	51	21	29	35	40	676
Bait + 3ml of DEET	138	0	0	6	0	7	36	187
Quadrant total	6790	1551	1231	1188	968	899	810	

Table 5.30 7-21-2017-1 test quadrant mosquito counts plotted



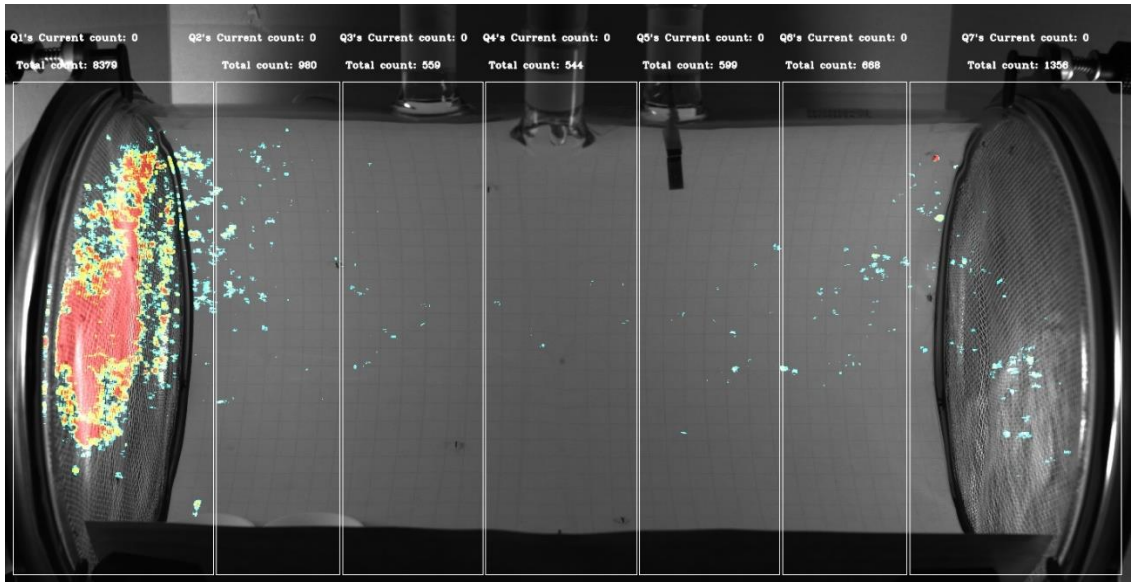
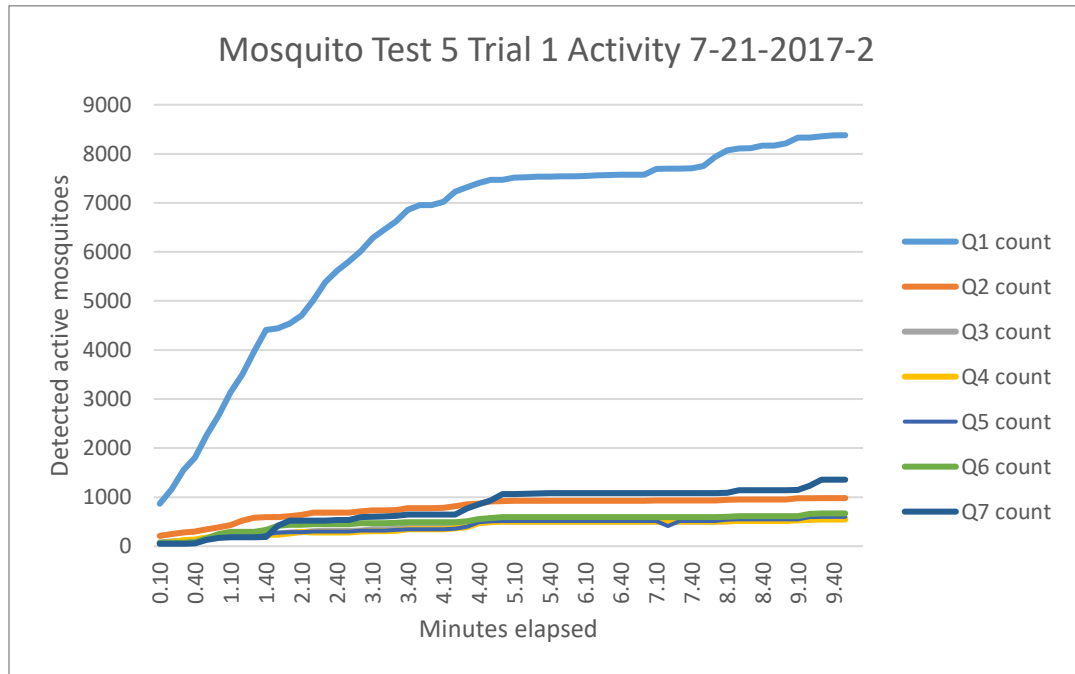


Figure 5.17 7-21-2017-2 test Bait trial mosquito heat map

Table 5.31 7-21-2017-2 test Bait trial mosquito activity during test



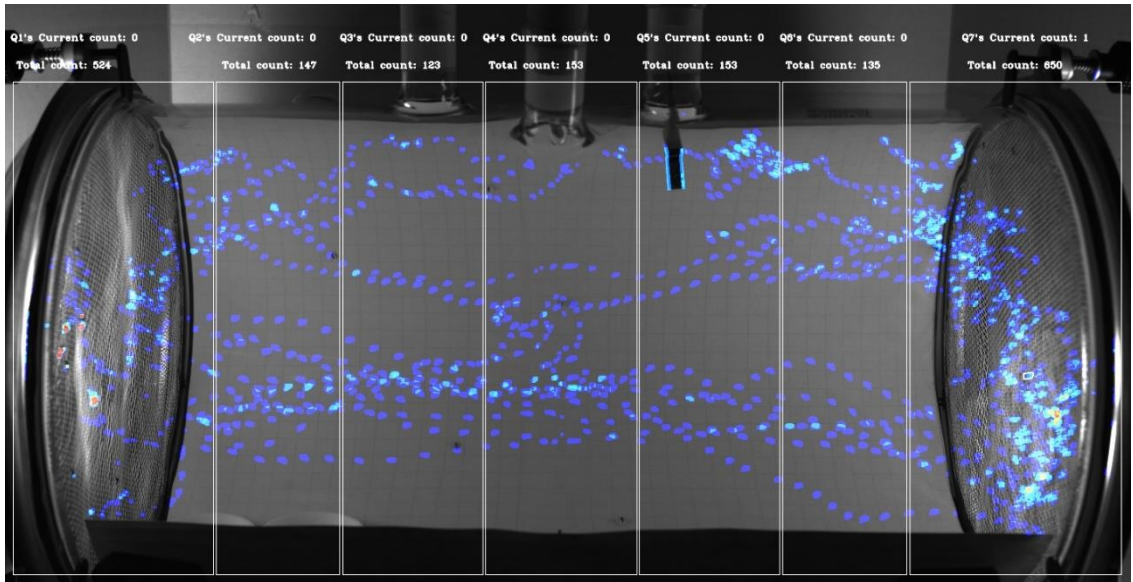
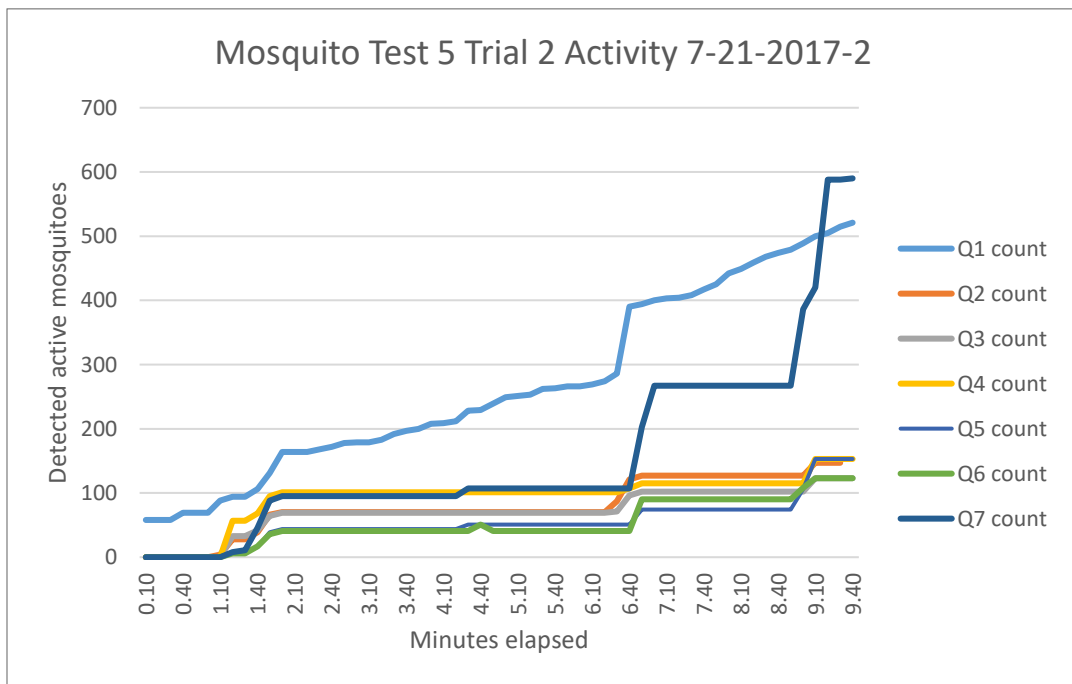


Figure 5.18 7-21-2017-2 test Bait + 1ml trial mosquito heat map

Table 5.32 7-21-2017-2 test Bait + 1ml trial mosquito activity during test



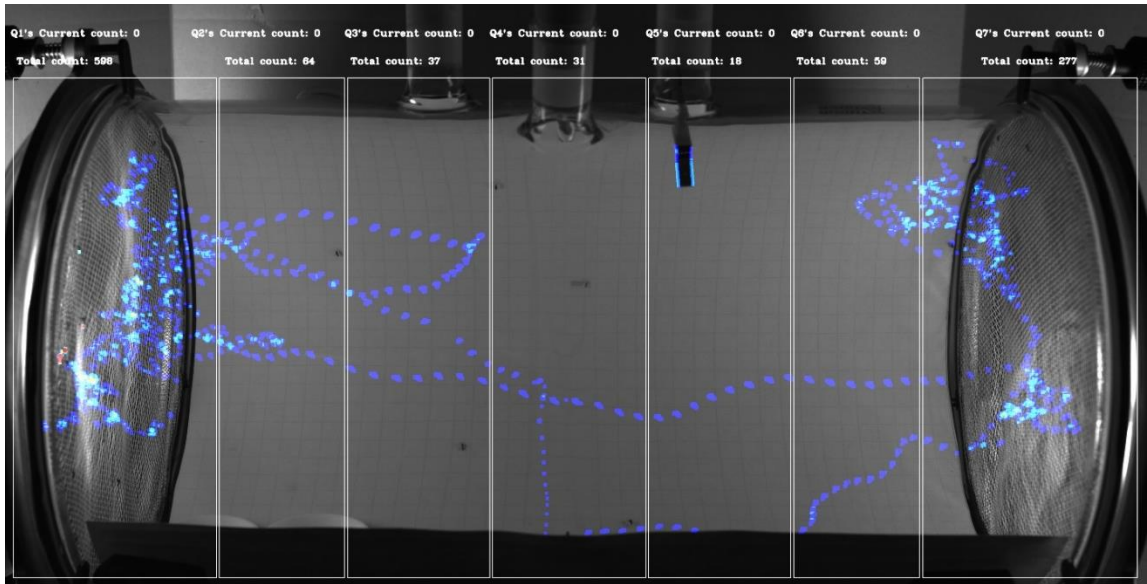
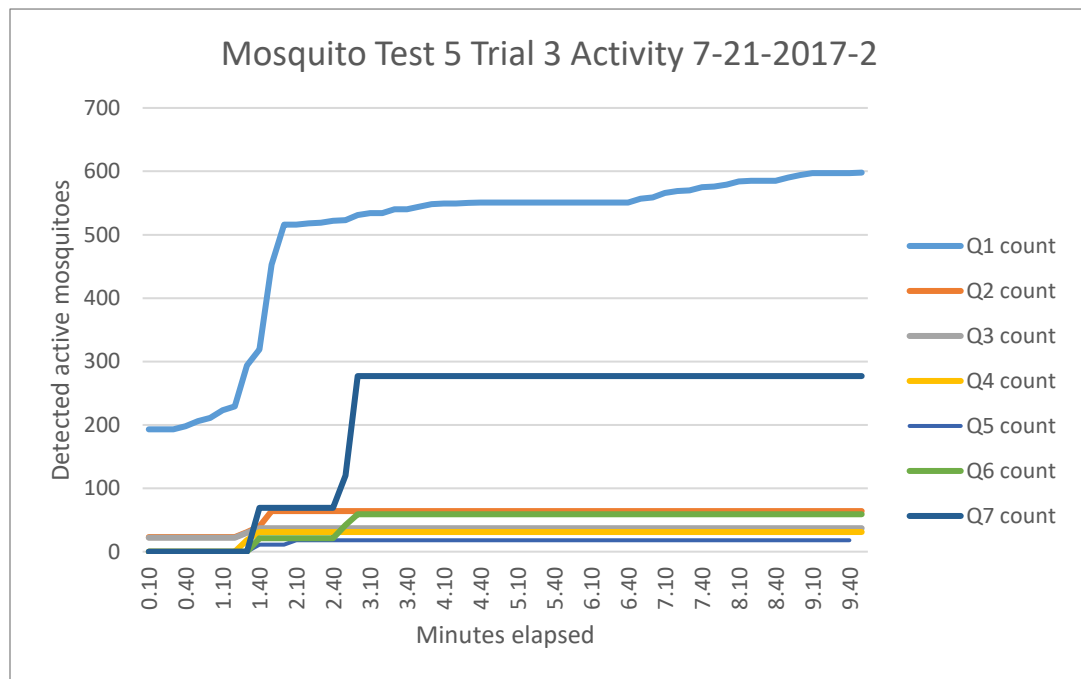


Figure 5.19 7-21-2017-2 test Bait + 2ml trial mosquito heat map

Table 5.33 7-21-2017-2 test Bait + 2ml trial mosquito activity during test



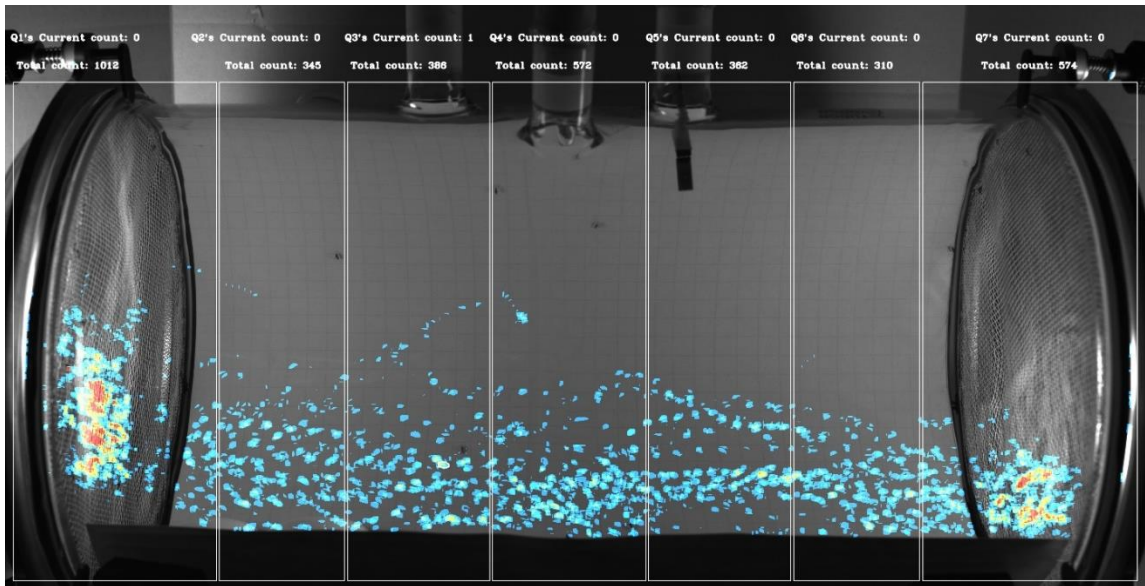


Figure 5.20 7-21-2017-2 test Bait + 3ml trial mosquito heat map

Table 5.34 7-21-2017-2 test Bait + 3ml trial mosquito activity during test

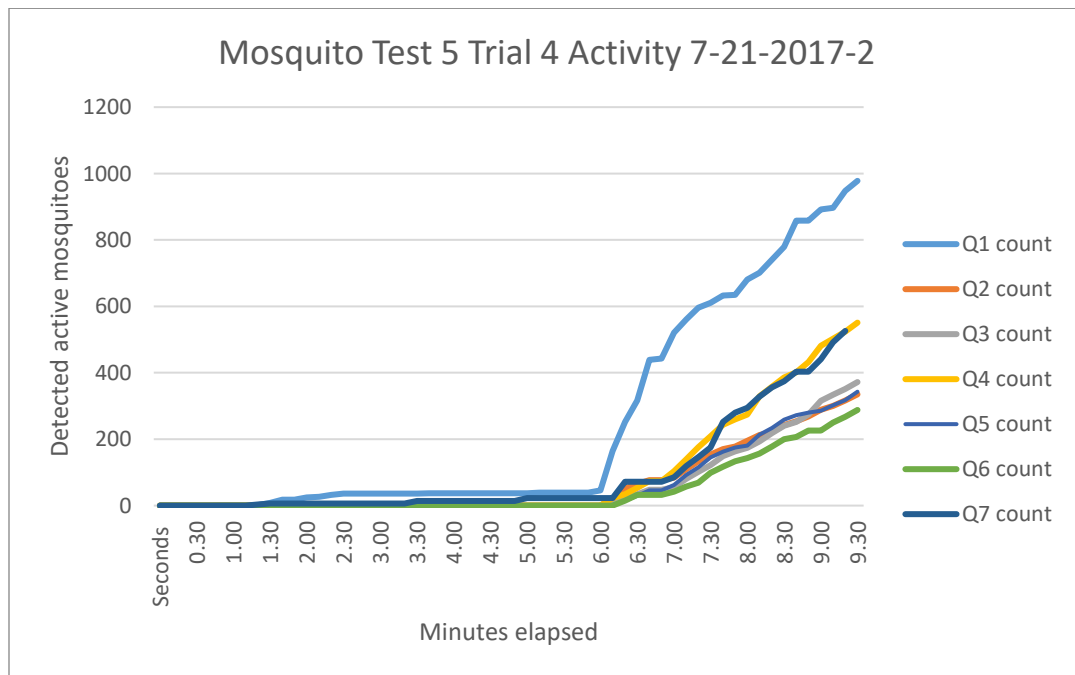
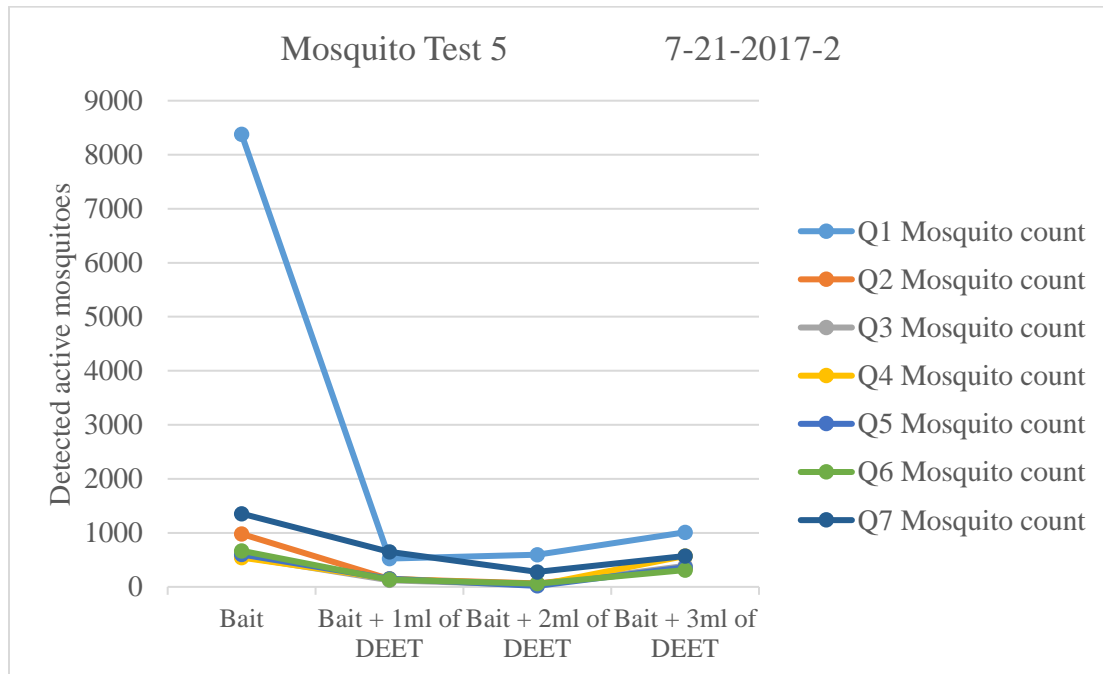


Table 5.35 7-21-2017-1 test quadrant mosquito counts

Mosquito test 5		Date 7-21-2017-2						
Trial	Q1 count	Q2 count	Q3 count	Q4 count	Q5 count	Q6 count	Q7 count	Trial total
Bait	8379	980	559	544	599	668	1356	13085
Bait + 1ml of DEET	524	147	123	153	153	135	650	1885
Bait + 2ml of DEET	598	64	37	31	18	59	277	1084
Bait + 3ml of DEET	1012	345	386	572	362	310	574	3561
Quadrant total	10513	1536	1105	1300	1132	1172	2857	

Table 5.36 7-21-2017-1 test quadrant mosquito counts plotted



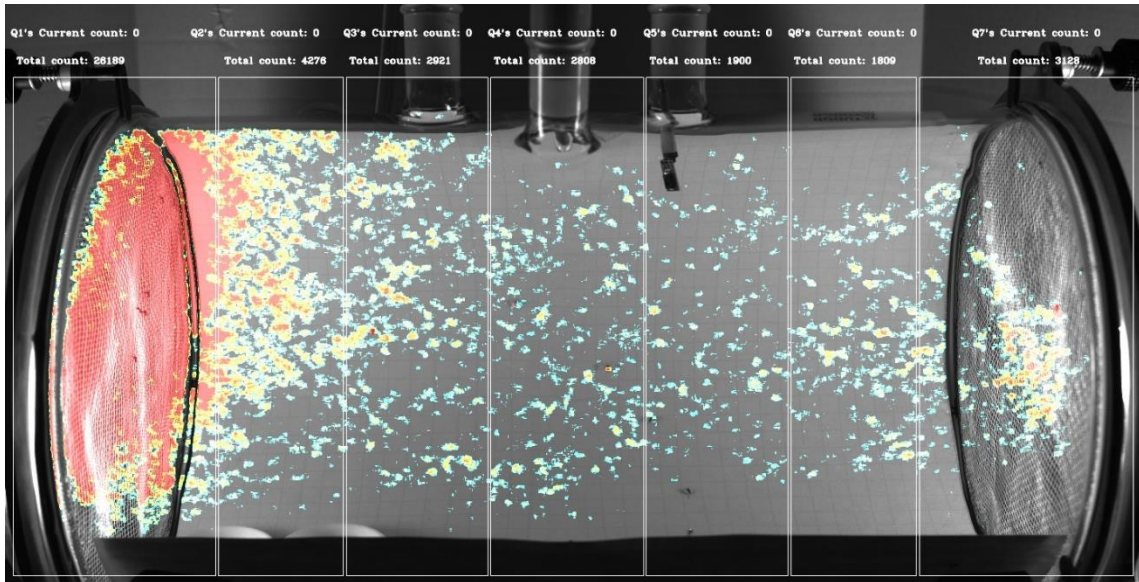
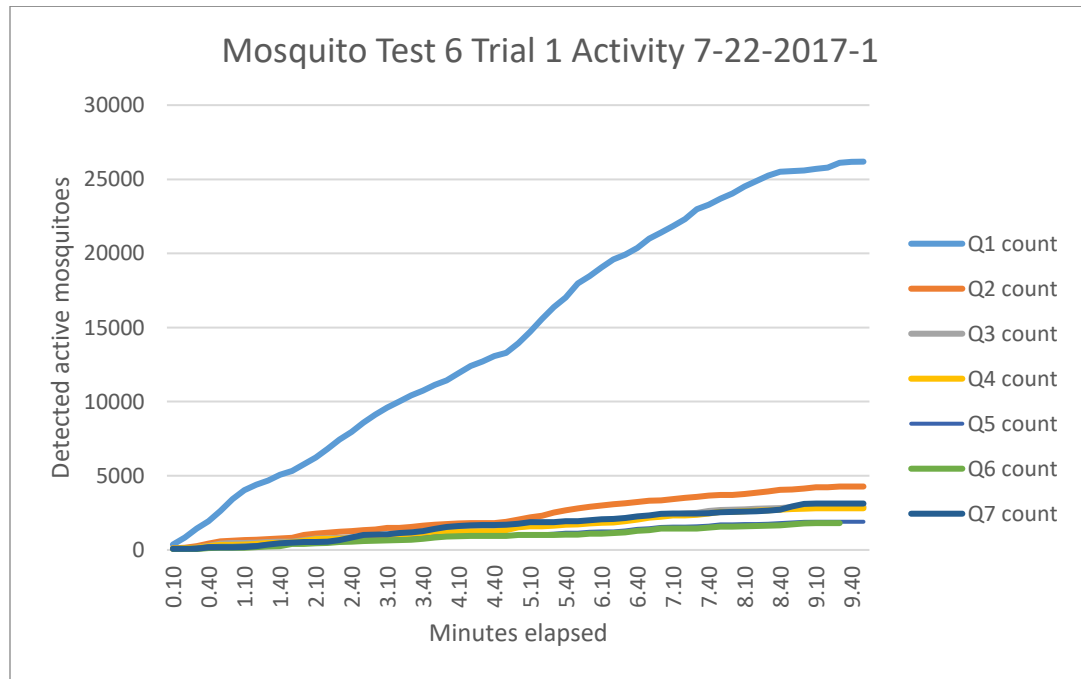


Figure 5.21 7-22-2017-1 test Bait trial mosquito heat map

Table 5.37 7-22-2017-1 test Bait trial mosquito activity during test



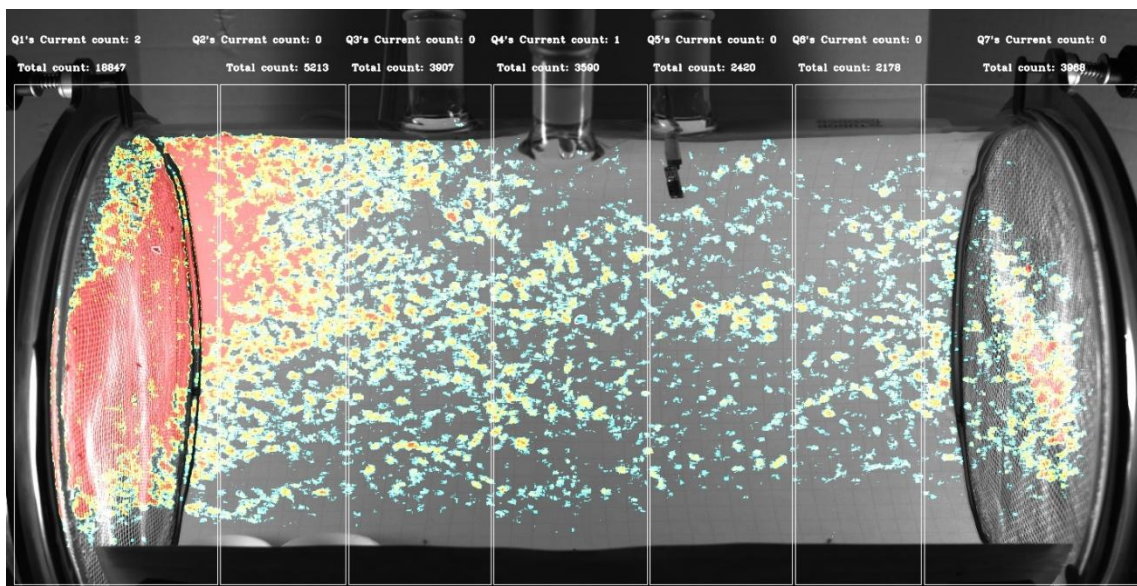
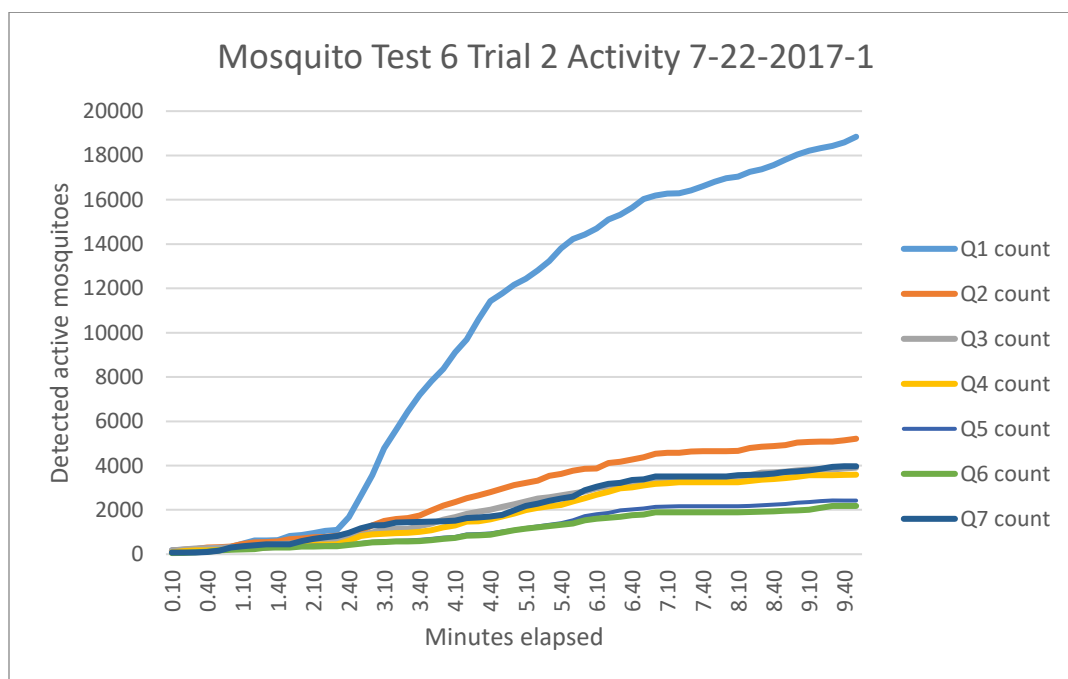


Figure 5.22 7-22-2017-1 test Bait + 1ml trial mosquito heat map

Table 5.38 7-22-2017-1 test Bait + 1ml trial mosquito activity during test



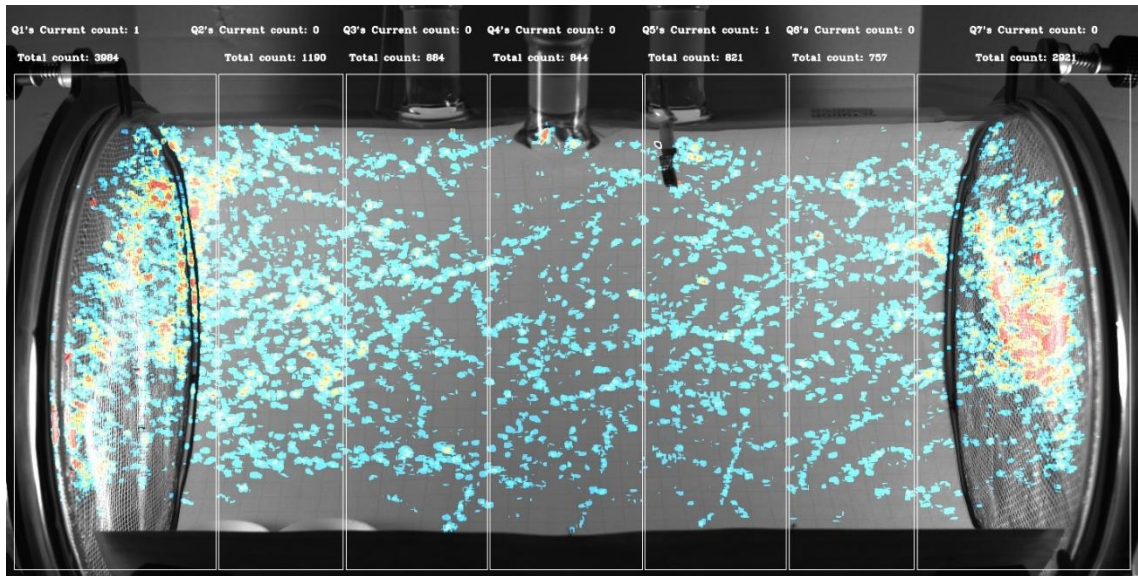
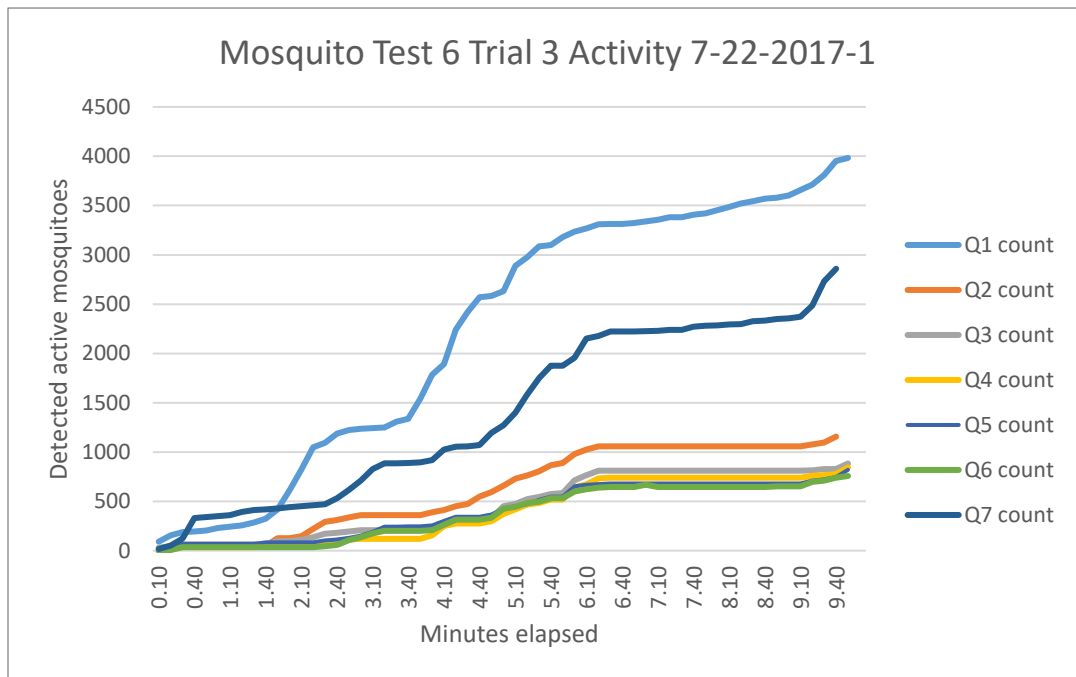


Figure 5.23 7-22-2017-1 test Bait + 2ml trial mosquito heat map

Table 5.39 7-22-2017-1 test Bait + 2ml trial mosquito activity during test



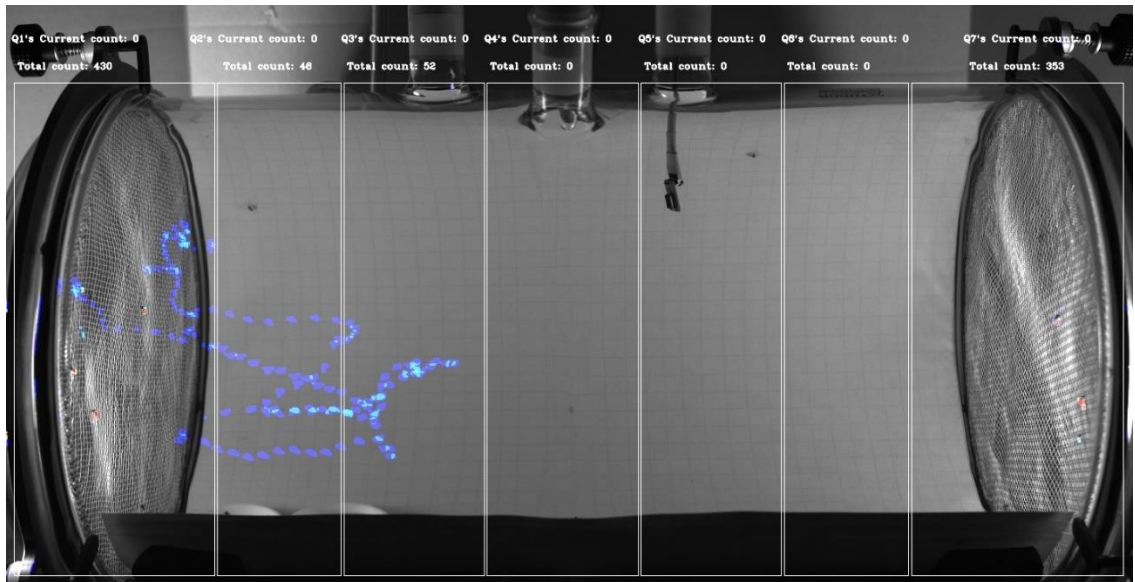


Figure 5.24 7-22-2017-1 test Bait + 3ml trial mosquito heat map

Table 5.40 7-22-2017-1 test Bait + 3ml trial mosquito activity during test

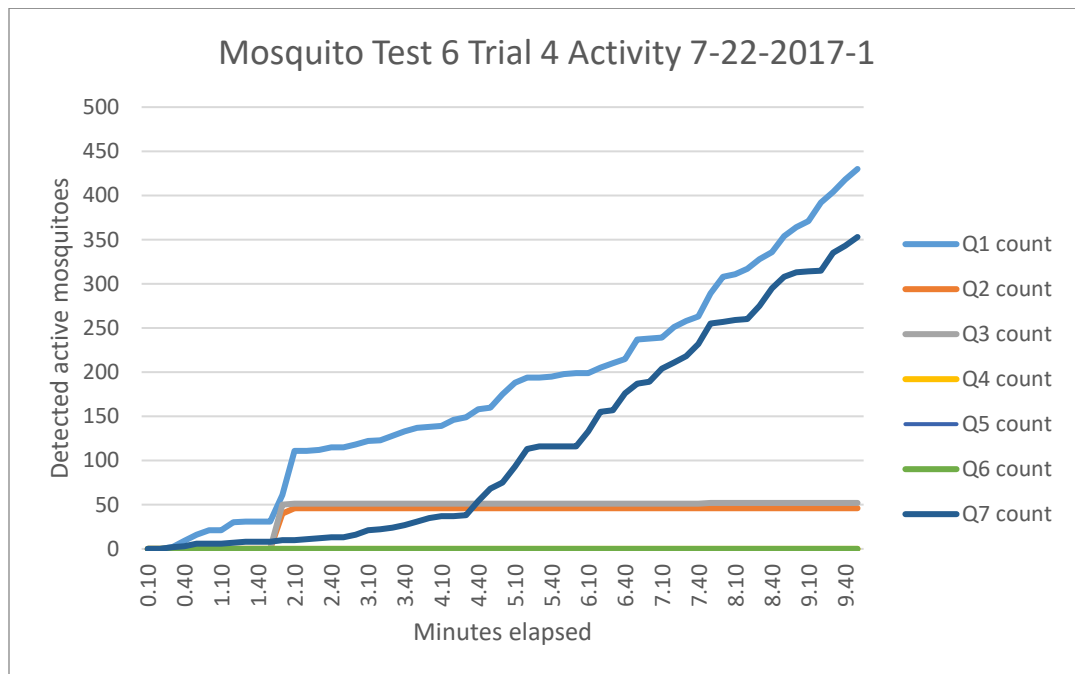
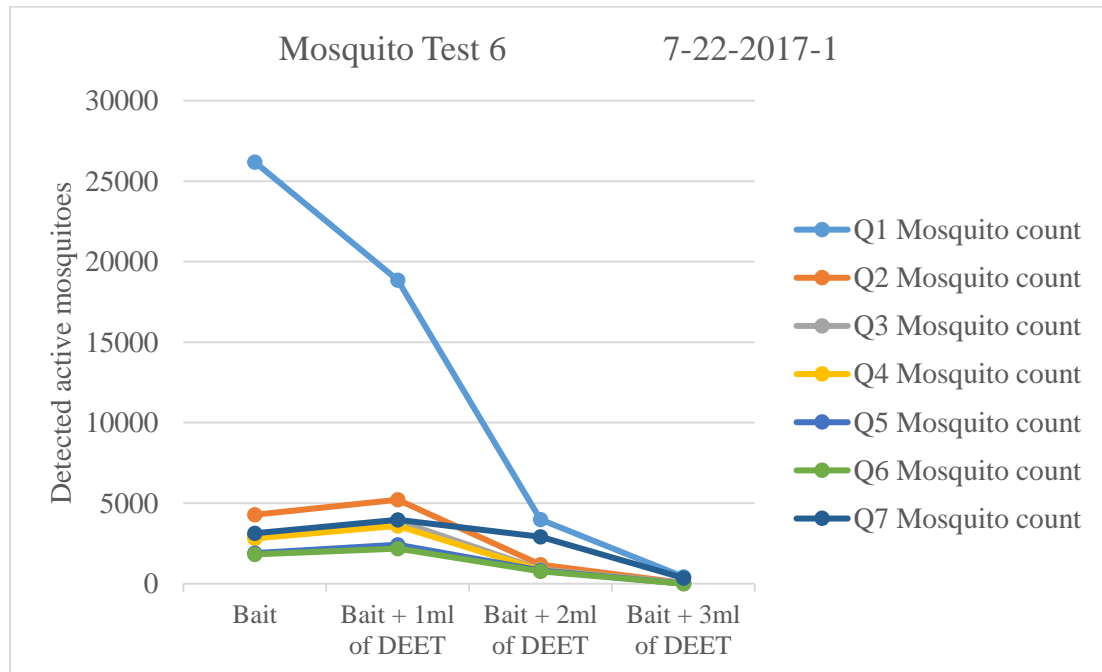


Table 5.41 7-22-2017-1 test quadrant mosquito counts

Mosquito test 6		Date 7-22-2017-1						
Trial	Q1 count	Q2 count	Q3 count	Q4 count	Q5 count	Q6 count	Q7 count	Trial total
Bait	26189	4276	2921	2808	1900	1809	3128	43031
Bait + 1ml of DEET	18847	5213	3907	3590	2420	2178	3968	40123
Bait + 2ml of DEET	3984	1190	884	844	821	757	2921	11401
Bait + 3ml of DEET	430	46	52	0	0	0	353	881
Quadrant total	49450	10725	7764	7242	5141	4744	10370	

Table 5.42 7-22-2017-1 test quadrant mosquito counts plotted



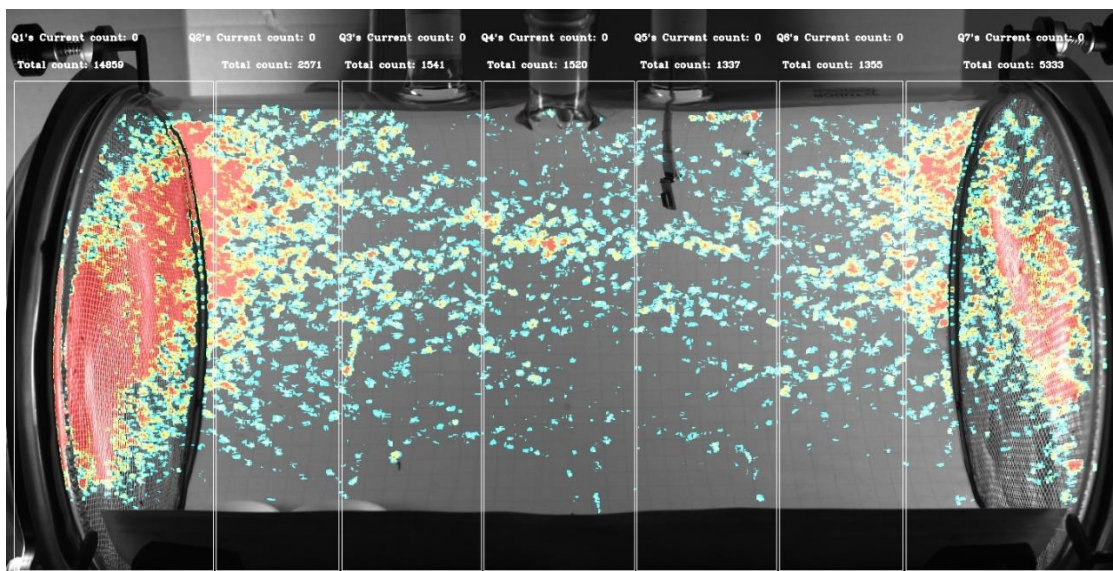
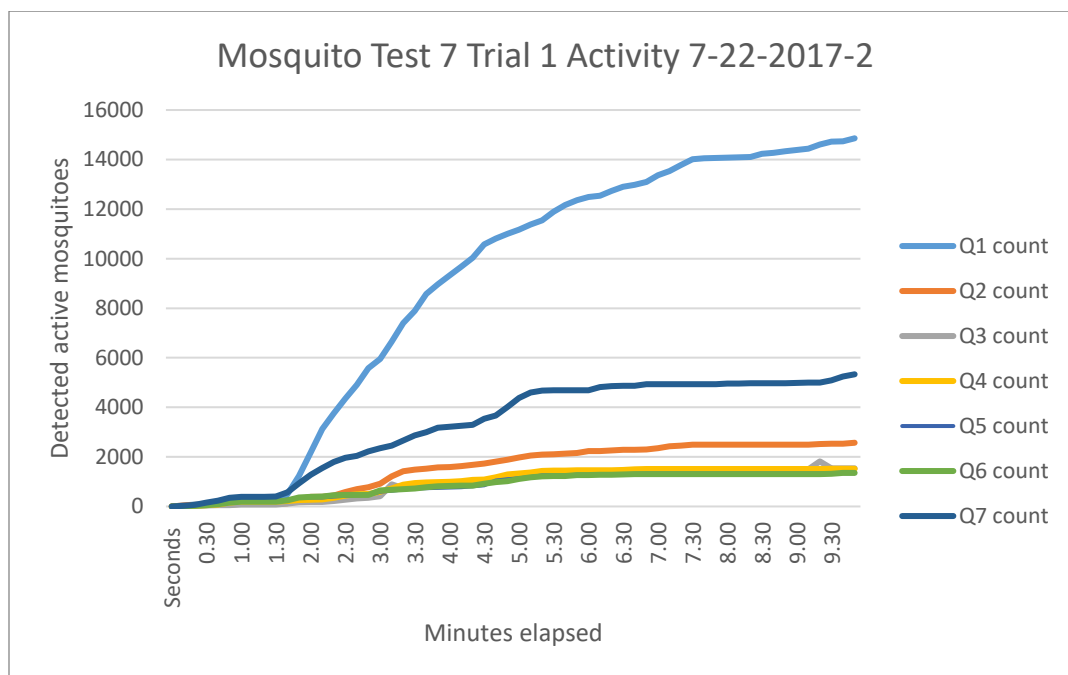


Figure 5.25 7-22-2017-2 test Bait trial mosquito heat map

Table 5.43 7-22-2017-2 test Bait trial mosquito activity during test



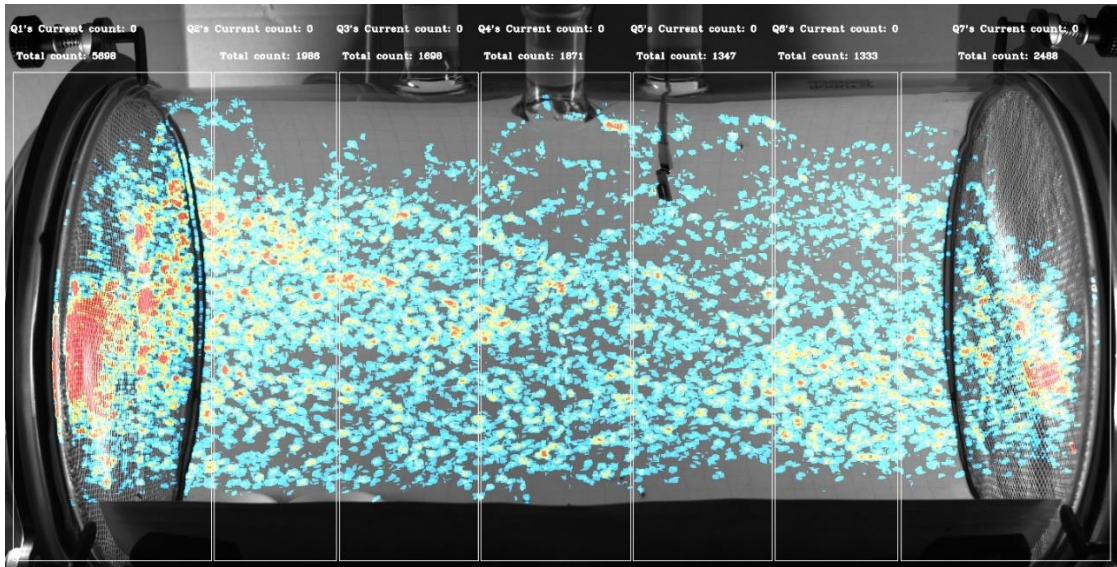
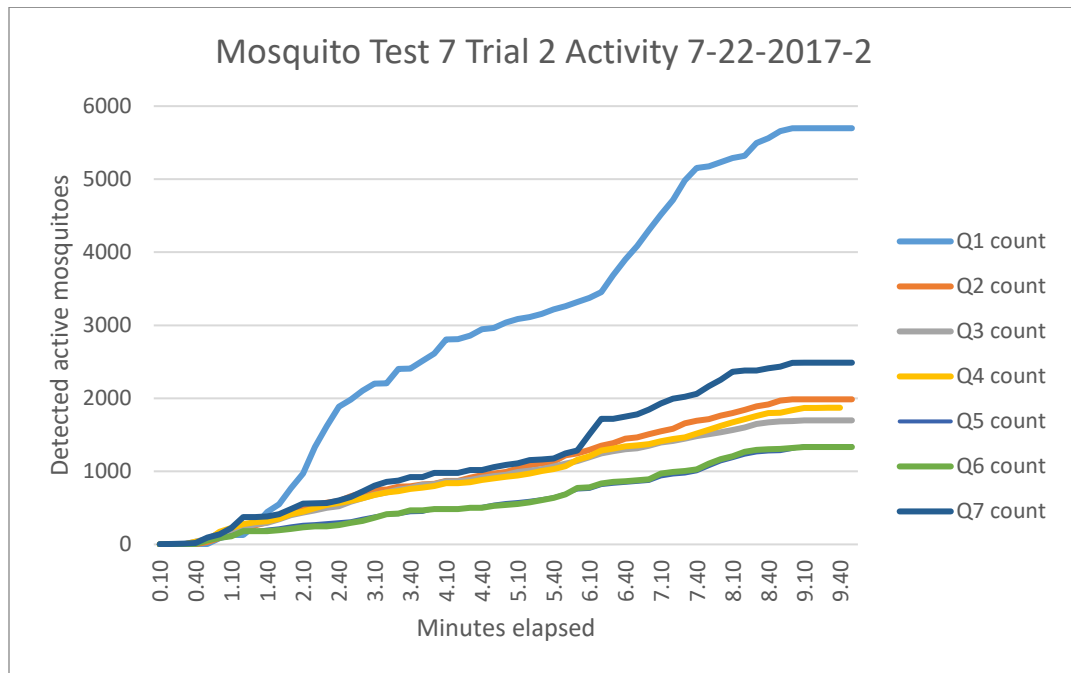


Figure 5.26 7-22-2017-2 test Bait + 1ml trial mosquito heat map

Table 5.44 7-22-2017-2 test Bait + 1ml trial mosquito activity during test



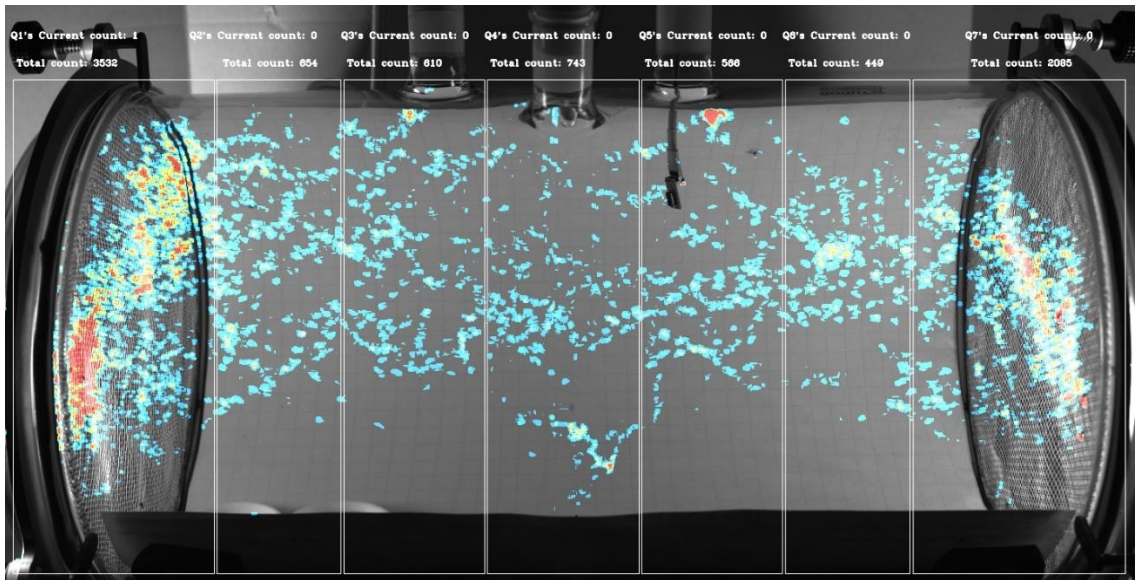
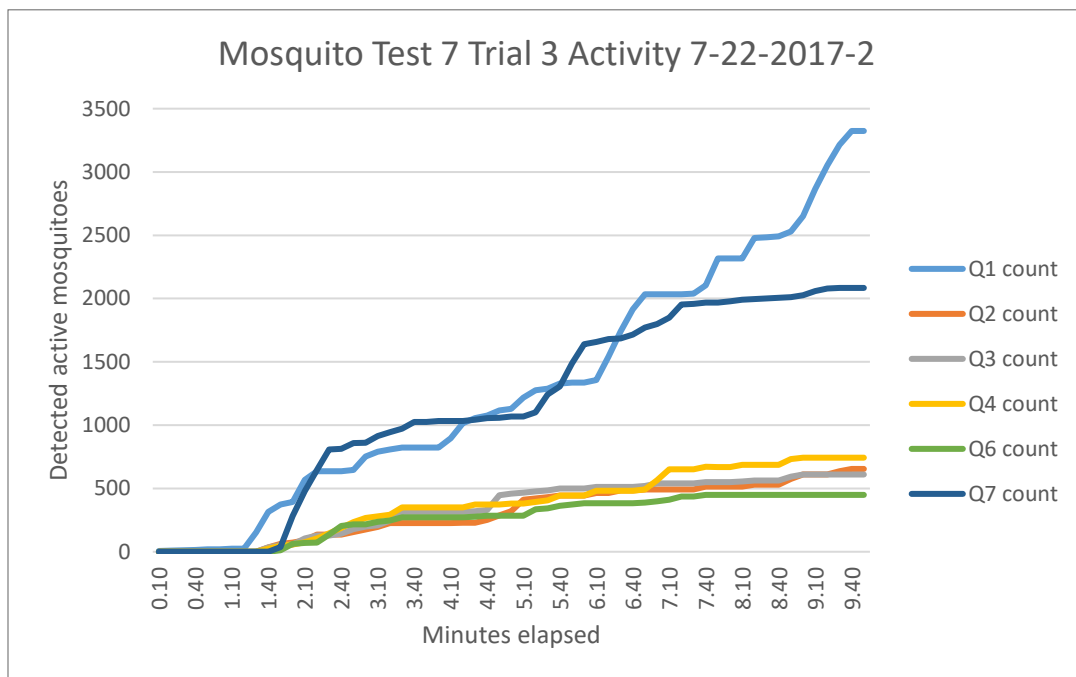


Figure 5.27 7-22-2017-2 test Bait + 2ml trial mosquito heat map

Table 5.45 7-22-2017-2 test Bait + 2ml trial mosquito activity during test



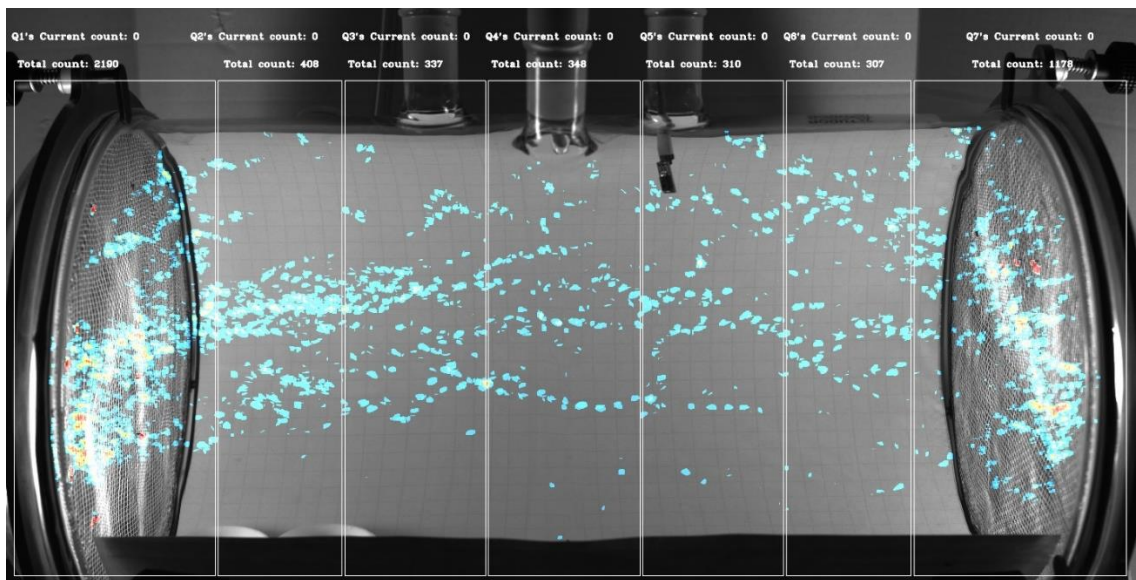


Figure 5.28 7-22-2017-2 test Bait + 3ml trial mosquito heat map

Table 5.46 7-22-2017-2 test Bait + 3ml trial mosquito activity during test

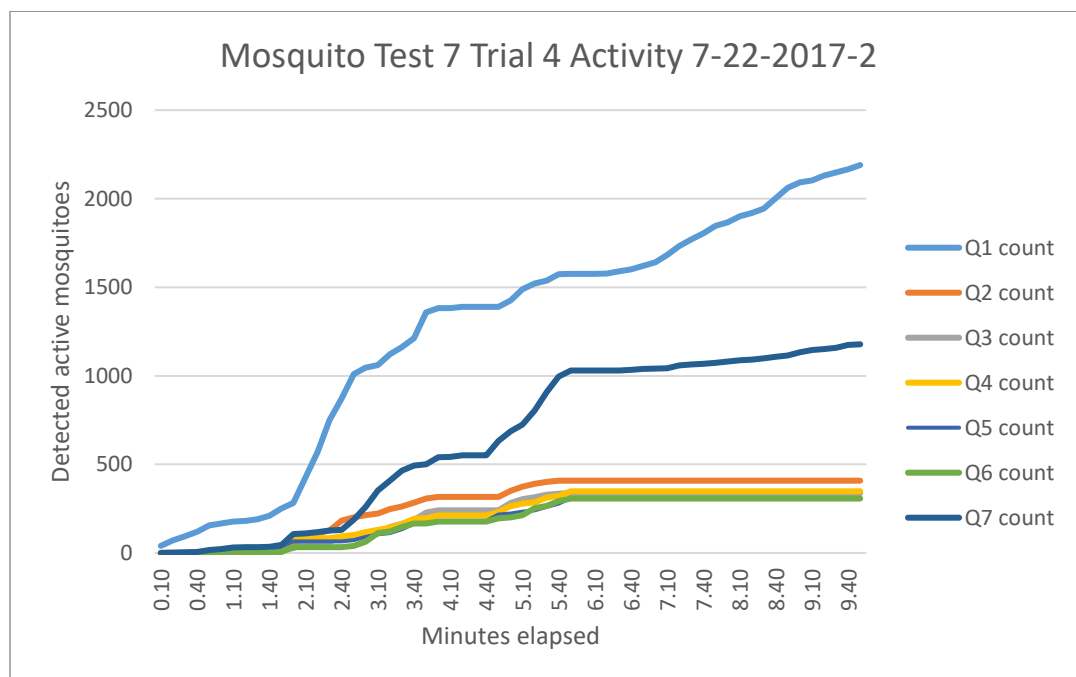
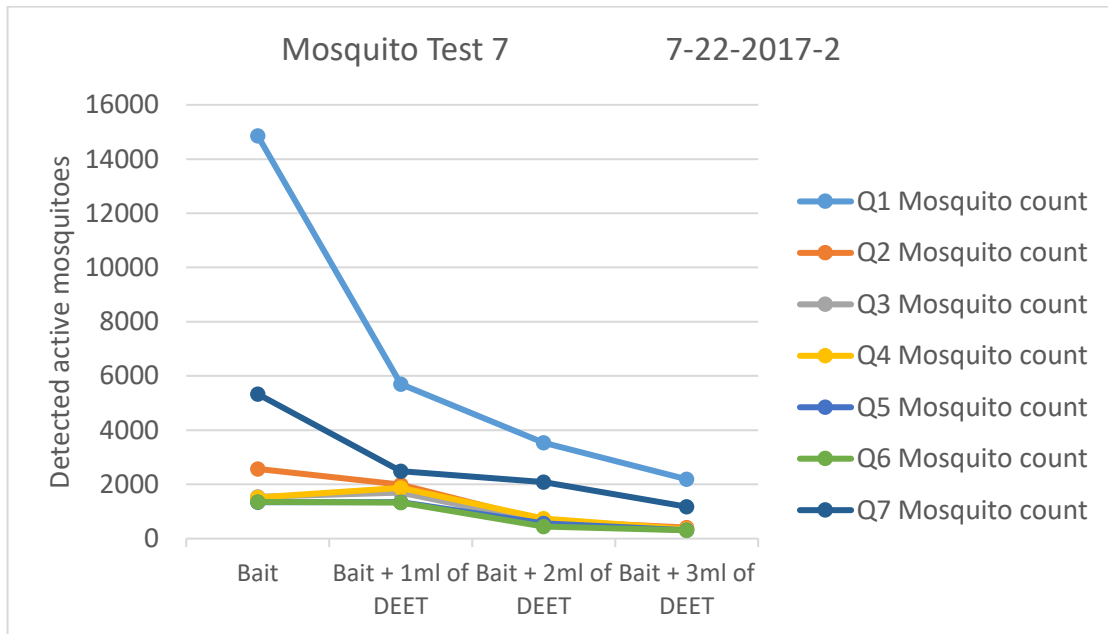


Table 5.47 7-22-2017-2 test quadrant mosquito counts

Mosquito test 7		Date 7-22-2017-2						
Trial	Q1 count	Q2 count	Q3 count	Q4 count	Q5 count	Q6 count	Q7 count	Trial total
Bait	14859	2571	1541	1520	1337	1355	5333	28516
Bait + 1ml of DEET	5698	1986	1698	1871	1347	1333	2488	16421
Bait + 2ml of DEET	3532	654	610	743	566	449	2085	8639
Bait + 3ml of DEET	2190	408	337	348	310	307	1178	5078
Quadrant total	26279	5619	4186	4482	3560	3444	11084	

Table 5.48 7-22-2017-2 test quadrant mosquito counts plotted



CHAPTER VI – DISCUSSION AND CONCLUSION

6.1 Discussion

6.1.1 MOS Sensor Data

Understanding the MOS sensor data can provide insight into how DEET dissipates into the chamber. Following the process outlined in data processing correlating the data to mosquito activity is possible. Sorting the MOS sensors by greatest voltage change provides the sensors with the greatest response to DEET. Quadrants provide a way to include multiple MOS sensor responses to an area of the chamber. Sensors and quadrants that consistently have the greater voltage responses display where the most DEET dissipation within the chamber occurs.

The top 10%, 25% and 50% of sensors and quadrants with greater voltage response provided a view of DEET dissipation. The top 10% of sensors include three of the top responding MOS sensors of each test. Compiled data sets of 1 ml, 2 ml and 3 ml displayed in Table 5.1 show quadrant 3 having the most MOS sensors with greatest voltage response. Quadrants 2 and 5 have a smaller number of sensors responding. The remaining quadrants have less to none. Quadrant 3 contains nearly all MOS sensors with greatest voltage response when only looking at the top 10% of responding sensors.

The top 25% of sensors include nine of the top responding MOS sensors of each test. Table 5.2 shows quadrant 3 still having the most MOS sensors with greatest voltage response. Quadrant 2 appears to have the second largest amount of MOS sensors. Quadrants 1, 4, and 5 have similar amounts of MOS sensors. Quadrant 3 contains the majority of the MOS sensors with greatest voltage response with the top 25% considered. Other quadrants such as 1, 2, 4, and 5 do contain sensors responding to DEET.

The top 50% of sensors include eighteen of the top responding MOS sensors of each test. Table 5.3 shows quadrant 3 with the most MOS sensors with greatest voltage response. Quadrant 4 has the second largest amount of MOS sensors with voltage response. Quadrants 1, 2, and 5 have less than quadrants 3 and 4 but all have similar amounts of responding sensors.

Quadrant 3 appears to have the strongest MOS voltage response to DEET dissipation. This is observed in the top 10% 25% and 50% of responding sensors. Quadrants 1, 2, 4, and 5 show less response. Viewing the top 50% of responding sensors provides a picture of DEET dissipation within the chamber. Sensors of quadrant 3 detects the greatest amount of DEET while sensors of quadrant 2 detect the next greatest amount. Quadrants 1,4, and 5 have comparable responses to each other. As the quadrants move away from quadrant 3 the number of sensors with greater responses decreases.

6.1.2 Mosquito Activity Data

Mosquito activity data can show how DEET affects mosquito activity within the chamber. Heat maps and quadrant counts of mosquito activity provide areas of greatest activity. Heat maps show most active areas of the chamber. Areas of red, orange, yellow have the greatest activity while areas of cyan to blue show areas of less activity. Each quadrant counts the number of mosquitoes moving within the quadrant them during a test.

Detected mosquito activity is very dependent on the mosquitoes. Mosquitoes can be active or inactive during a test. Quadrant count tables such as Table 5.7 show quadrant counts of each quadrant for each trial. Plots of mosquito counts such as Table 5.8 show decreases or increases between each trial. A total of seven mosquito tests show decreased

mosquito activity as the sample size of DEET increases. The order of testing trials follows bait only, bait with 1 ml DEET, bait with 2 ml of DEET and bait with 3ml of DEET.

Bait only trials have the greatest activity in all quadrants. The bait encourages host-seeking behavior and increases mosquito activity. The location of the Teflon dish with the bait sample is quadrant 1. Each of the bait only tests has varying amounts of mosquito activity in quadrant 1. However, activity is greatest in quadrant 1 in bait only trials. This is true in all mosquito tests but test 3 on 7-20-2017. Mosquito test 3 has greater mosquito activity during the bait with 1 ml of DEET trial.

Upon injecting 1 ml of DEET into the chamber mosquito activity within all quadrants decreased. Quadrant 1 has the greatest reduction in mosquito activity. This is due to quadrant 1's increased activity over all other quadrants. Quadrants 2 through 7 have more moderate reductions in activity. Despite being exposed to DEET mosquito activity does not cease completely, however this initial exposure to DEET does reduce activity. This reduction from the bait only trial to bait with 1ml of DEET trial is displayed in mosquito tests 1, 2, 4, 5, and 7. Mosquito test 3 has an increase in activity in the bait with 1 ml of DEET trial. Mosquito test 6 has an increase in activity in all quadrants except 1 in the bait with 1ml of DEET trial.

Increasing the amount of DEET to 2 ml has mixed results. Not all tests show a reduction of mosquito activity. Quadrant 1 of most tests has a reduction of activity. This can be seen in mosquito tests 1, 2, 3, 6 and 7. This could be due to quadrant 1's increased mosquito activity over all quadrants. Tests 4 and 5 show an increase in mosquito activity for quadrant 1. Following the first DEET trial some tests continues to show a reduction in

mosquito activity after introducing 2 ml of DEET. This can be seen in mosquito tests 3, 4, 5, 6, and 7. In some tests with reduced mosquito activity from 1 ml of DEET have an increase in activity after 2 ml of DEET is introduced. This can be seen in mosquito tests 1 and 2. Despite the increase in DEET mosquito activity does not cease completely.

3 ml of DEET trials continue to show mixed results. Three mosquito tests show mosquito activity increases during 3 ml DEET trials. They are mosquito tests 1, 3, and 5. Quadrant 1 of these tests shows increase in mosquito activity along with the majority of other quadrants. The remaining mosquito tests 2, 4, 6, and 7 show decreases in mosquito activity. All quadrants of these test show decrease in mosquito activity. Mosquito tests 4 and 6 show no mosquito activity in three quadrants.

6.1.3 Combined Data

The MOS sensor data shows that quadrant 3 has the highest responding sensors. Quadrant 3 has the most DEET dissipated within it. The Teflon dish containing the DEET sample is located within quadrant 2. Due to the airflow in the chamber the MOS sensors in quadrant 3 detect more DEET than MOS sensors in quadrant 2. MOS sensors in Quadrants 1, 2, 4, and 5 also have a response to DEET. The further away a quadrant is from quadrant 3 the less DEET is detected by the MOS sensors. The MOS sensor data shows what quadrants DEET dissipation is the strongest. Mosquito activity data of specific quadrants is not as accurate. Mosquito activity in quadrant 3 or any of the quadrants where MOS sensors detected the largest amount of DEET does not cease. A decrease in mosquito activity occurs when DEET is introduced into the chamber. This decrease in activity is not localized to one quadrant of the chamber. As the DEET sample is increased in sequential trials mosquito activity continues to decline. It is possible that

the DEET inhibits the mosquito's ability to detect the bait sample. This causes mosquitoes to shift from host seeking behavior and they become less active. In some mosquito tests a shift in activity from quadrant 1 to quadrant 7 occurs. This can be seen in the test's heatmaps. Quadrant 7 is the furthest away from the bait and DEET sample. The MOS sensors in quadrants 6 and 7 detect the least amount of DEET. This could indicate mosquitoes moving away from quadrants with greatest amount of DEET detected by the MOS sensors. In some mosquito tests activity begins to increase as the final 1 ml of DEET is introduced into the chamber. After continuous and increasing exposure to DEET it could be possible that the mosquitoes become less affected by it.

6.2 Conclusion

In conclusion, it has been shown that it is possible to measure the dissipation of DEET and observe the mosquito behavioral response using the developed system. Two separate test types completed using the system provide data supporting this. The system can measure DEET dissipation via MOS sensors as well as observing mosquito activity within a controlled environment. The system can maintain the controlled environment with specialized equipment and circuitry. Developed software processes captured mosquito images to provide a computational representation of mosquito activity. Comparing MOS sensor response and mosquito activity displays evidence of DEET's effects on mosquitoes. A reduction in mosquito activity occurs when mosquitoes are exposed to DEET.

APPENDIX A – Tables and Figures

Table A.1 10-18-2017 MOS sensor and quadrants sorted by greatest voltage						
	1ml		2ml		3ml	
Sensor Rank from total voltage	Sensor	Quadrant	Sensor	Quadrant	Sensor	Quadrant
1	S15	Q3	S3	Q3	S6	Q5
2	S6	Q5	S27	Q3	S3	Q3
3	S3	Q3	S26	Q2	S27	Q3
4	S7	Q3	S6	Q5	S7	Q3
5	S4	Q3	S2	Q2	S4	Q3
6	S27	Q3	S13	Q1	S2	Q2
7	S5	Q4	S4	Q3	S5	Q4
8	S2	Q2	S7	Q3	S28	Q3
9	S16	Q3	S5	Q4	S8	Q4
10	S8	Q4	S24	Q7	S1	Q1
11	S28	Q3	S25	Q1	S15	Q3
12	S20	Q4	S1	Q1	S20	Q4
13	S13	Q1	S8	Q4	S13	Q1
14	S1	Q1	S15	Q3	S16	Q3
15	S26	Q2	S31	Q3	S31	Q3
16	S14	Q2	S16	Q3	S19	Q3
17	S21	Q5	S14	Q2	S32	Q4
18	S18	Q5	S28	Q3	S25	Q1
19	S31	Q3	S20	Q4	S21	Q5
20	S25	Q1	S9	Q5	S29	Q4
21	S17	Q4	S11	Q6	S14	Q2
22	S29	Q4	S19	Q3	S11	Q6
23	S24	Q7	S10	Q5	S30	Q5
24	S30	Q5	S30	Q5	S10	Q5
25	S10	Q5	S29	Q4	S24	Q7
26	S32	Q4	S23	Q6	S18	Q5
27	S11	Q6	S18	Q5	S17	Q4
28	S23	Q6	S21	Q5	S26	Q2
29	S22	Q5	S32	Q4	S23	Q6
30	S9	Q5	S36	Q7	S9	Q5
31	S19	Q3	S17	Q4	S22	Q5
32	S36	Q7	S22	Q5	S36	Q7
33	S35	Q6	S35	Q6	S35	Q6
34	S33	Q5	S33	Q5	S33	Q5
35	S12	Q7	S12	Q7	S34	Q5
36	S34	Q5	S34	Q5	S12	Q7

Table A.2 10-19-2017 MOS sensor and quadrants sorted by greatest voltage						
	1ml		2ml		3ml	
Sensor Rank from total voltage	Sensor	Quadrant	Sensor	Quadrant	Sensor	Quadrant
1	S3	Q3	S3	Q3	S3	Q3
2	S26	Q2	S27	Q3	S27	Q3
3	S6	Q5	S26	Q2	S6	Q5
4	S2	Q2	S6	Q5	S13	Q1
5	S4	Q3	S2	Q2	S2	Q2
6	S7	Q3	S13	Q1	S7	Q3
7	S13	Q1	S4	Q3	S4	Q3
8	S5	Q4	S7	Q3	S1	Q1
9	S27	Q3	S5	Q4	S15	Q3
10	S1	Q1	S24	Q7	S31	Q3
11	S8	Q4	S25	Q1	S28	Q3
12	S24	Q7	S1	Q1	S5	Q4
13	S25	Q1	S8	Q4	S20	Q4
14	S20	Q4	S15	Q3	S8	Q4
15	S31	Q3	S31	Q3	S24	Q7
16	S28	Q3	S16	Q3	S14	Q2
17	S15	Q3	S14	Q2	S25	Q1
18	S16	Q3	S28	Q3	S16	Q3
19	S14	Q2	S20	Q4	S26	Q2
20	S9	Q5	S9	Q5	S9	Q5
21	S23	Q6	S11	Q6	S21	Q5
22	S18	Q5	S19	Q3	S32	Q4
23	S19	Q3	S10	Q5	S11	Q6
24	S10	Q5	S30	Q5	S19	Q3
25	S30	Q5	S29	Q4	S23	Q6
26	S11	Q6	S23	Q6	S29	Q4
27	S29	Q4	S18	Q5	S30	Q5
28	S32	Q4	S21	Q5	S10	Q5
29	S21	Q5	S32	Q4	S18	Q5
30	S17	Q4	S36	Q7	S33	Q5
31	S22	Q5	S17	Q4	S22	Q5
32	S33	Q5	S22	Q5	S17	Q4
33	S35	Q6	S35	Q6	S36	Q7
34	S12	Q7	S33	Q5	S12	Q7
35	S36	Q7	S12	Q7	S35	Q6
36	S34	Q5	S34	Q5	S34	Q5

Table A.3 10-31-2017 MOS sensor and quadrants sorted by greatest voltage						
	1ml		2ml		3ml	
Sensor Rank from total voltage	Sensor	Quadrant	Sensor	Quadrant	Sensor	Quadrant
1	S31	Q3	S27	Q3	S27	Q3
2	S27	Q3	S20	Q4	S20	Q4
3	S20	Q4	S28	Q3	S6	Q5
4	S28	Q3	S16	Q3	S13	Q1
5	S16	Q3	S6	Q5	S2	Q2
6	S6	Q5	S29	Q4	S1	Q1
7	S29	Q4	S13	Q1	S29	Q4
8	S26	Q2	S26	Q2	S16	Q3
9	S2	Q2	S15	Q3	S28	Q3
10	S15	Q3	S2	Q2	S31	Q3
11	S13	Q1	S31	Q3	S18	Q5
12	S14	Q2	S14	Q2	S15	Q3
13	S1	Q1	S8	Q4	S21	Q5
14	S18	Q5	S21	Q5	S8	Q4
15	S8	Q4	S24	Q7	S19	Q3
16	S30	Q5	S30	Q5	S25	Q1
17	S21	Q5	S25	Q1	S4	Q3
18	S25	Q1	S18	Q5	S32	Q4
19	S19	Q3	S4	Q3	S22	Q5
20	S3	Q3	S3	Q3	S14	Q2
21	S4	Q3	S23	Q6	S11	Q6
22	S10	Q5	S5	Q4	S23	Q6
23	S23	Q6	S11	Q6	S17	Q4
24	S9	Q5	S19	Q3	S3	Q3
25	S11	Q6	S1	Q1	S26	Q2
26	S17	Q4	S9	Q5	S9	Q5
27	S5	Q4	S22	Q5	S30	Q5
28	S24	Q7	S17	Q4	S5	Q4
29	S22	Q5	S32	Q4	S36	Q7
30	S32	Q4	S33	Q5	S24	Q7
31	S33	Q5	S35	Q6	S10	Q5
32	S36	Q7	S10	Q5	S35	Q6
33	S35	Q6	S36	Q7	S33	Q5
34	S7	Q3	S7	Q3	S12	Q7
35	S12	Q7	S34	Q5	S7	Q3
36	S34	Q5	S12	Q7	S34	Q5

Table A.4 11-1-2017-1 MOS sensor and quadrants sorted by greatest voltage						
	1ml		2ml		3ml	
Sensor Rank from total voltage	Sensor	Quadrant	Sensor	Quadrant	Sensor	Quadrant
1	S27	Q3	S27	Q3	S27	Q3
2	S26	Q2	S26	Q2	S15	Q3
3	S15	Q3	S15	Q3	S16	Q3
4	S6	Q5	S1	Q1	S6	Q5
5	S2	Q2	S6	Q5	S1	Q1
6	S28	Q3	S13	Q1	S20	Q4
7	S16	Q3	S16	Q3	S13	Q1
8	S31	Q3	S20	Q4	S26	Q2
9	S1	Q1	S18	Q5	S18	Q5
10	S13	Q1	S2	Q2	S28	Q3
11	S4	Q3	S31	Q3	S31	Q3
12	S3	Q3	S3	Q3	S3	Q3
13	S20	Q4	S28	Q3	S2	Q2
14	S18	Q5	S29	Q4	S29	Q4
15	S24	Q7	S21	Q5	S8	Q4
16	S8	Q4	S24	Q7	S21	Q5
17	S25	Q1	S8	Q4	S11	Q6
18	S30	Q5	S17	Q4	S19	Q3
19	S29	Q4	S14	Q2	S17	Q4
20	S14	Q2	S4	Q3	S30	Q5
21	S5	Q4	S25	Q1	S23	Q6
22	S11	Q6	S19	Q3	S25	Q1
23	S21	Q5	S11	Q6	S22	Q5
24	S17	Q4	S5	Q4	S14	Q2
25	S23	Q6	S30	Q5	S24	Q7
26	S22	Q5	S23	Q6	S5	Q4
27	S32	Q4	S22	Q5	S4	Q3
28	S10	Q5	S36	Q7	S32	Q4
29	S19	Q3	S9	Q5	S9	Q5
30	S9	Q5	S32	Q4	S36	Q7
31	S36	Q7	S33	Q5	S33	Q5
32	S33	Q5	S7	Q3	S10	Q5
33	S7	Q3	S10	Q5	S35	Q6
34	S35	Q6	S35	Q6	S7	Q3
35	S34	Q5	S12	Q7	S12	Q7
36	S12	Q7	S34	Q5	S34	Q5

Table A.5 11-1-2017-2 MOS sensor and quadrants sorted by greatest voltage						
	1ml		2ml		3ml	
Sensor Rank from total voltage	Sensor	Quadrant	Sensor	Quadrant	Sensor	Quadrant
1	S27	Q3	S27	Q3	S27	Q3
2	S26	Q2	S1	Q1	S1	Q1
3	S15	Q3	S28	Q3	S15	Q3
4	S3	Q3	S6	Q5	S20	Q4
5	S6	Q5	S13	Q1	S6	Q5
6	S28	Q3	S26	Q2	S26	Q2
7	S13	Q1	S2	Q2	S18	Q5
8	S2	Q2	S31	Q3	S28	Q3
9	S1	Q1	S15	Q3	S2	Q2
10	S31	Q3	S3	Q3	S24	Q7
11	S20	Q4	S17	Q4	S31	Q3
12	S16	Q3	S20	Q4	S16	Q3
13	S8	Q4	S24	Q7	S8	Q4
14	S24	Q7	S8	Q4	S19	Q3
15	S5	Q4	S16	Q3	S13	Q1
16	S18	Q5	S14	Q2	S3	Q3
17	S23	Q6	S30	Q5	S4	Q3
18	S4	Q3	S5	Q4	S14	Q2
19	S30	Q5	S18	Q5	S30	Q5
20	S11	Q6	S29	Q4	S29	Q4
21	S14	Q2	S19	Q3	S23	Q6
22	S21	Q5	S25	Q1	S5	Q4
23	S25	Q1	S4	Q3	S21	Q5
24	S29	Q4	S32	Q4	S32	Q4
25	S19	Q3	S10	Q5	S17	Q4
26	S17	Q4	S21	Q5	S25	Q1
27	S32	Q4	S33	Q5	S22	Q5
28	S10	Q5	S9	Q5	S36	Q7
29	S9	Q5	S23	Q6	S35	Q6
30	S36	Q7	S11	Q6	S7	Q3
31	S22	Q5	S36	Q7	S11	Q6
32	S33	Q5	S7	Q3	S9	Q5
33	S35	Q6	S35	Q6	S33	Q5
34	S7	Q3	S22	Q5	S10	Q5
35	S12	Q7	S12	Q7	S34	Q5
36	S34	Q5	S34	Q5	S12	Q7

Table A.6 12-8-2017-1 MOS sensor and quadrants sorted by greatest voltage						
	1ml		2ml		3ml	
Sensor Rank from total voltage	Sensor	Quadrant	Sensor	Quadrant	Sensor	Quadrant
1	S27	Q3	S26	Q2	S26	Q2
2	S26	Q2	S27	Q3	S27	Q3
3	S15	Q3	S28	Q3	S15	Q3
4	S28	Q3	S20	Q4	S20	Q4
5	S13	Q1	S15	Q3	S13	Q1
6	S14	Q2	S13	Q1	S28	Q3
7	S29	Q4	S6	Q5	S29	Q4
8	S6	Q5	S4	Q3	S21	Q5
9	S31	Q3	S29	Q4	S16	Q3
10	S4	Q3	S22	Q5	S3	Q3
11	S2	Q2	S21	Q5	S31	Q3
12	S3	Q3	S14	Q2	S4	Q3
13	S24	Q7	S2	Q2	S1	Q1
14	S20	Q4	S1	Q1	S2	Q2
15	S30	Q5	S5	Q4	S14	Q2
16	S23	Q6	S3	Q3	S23	Q6
17	S8	Q4	S16	Q3	S6	Q5
18	S1	Q1	S23	Q6	S36	Q7
19	S25	Q1	S30	Q5	S25	Q1
20	S16	Q3	S11	Q6	S18	Q5
21	S18	Q5	S18	Q5	S11	Q6
22	S19	Q3	S19	Q3	S5	Q4
23	S21	Q5	S8	Q4	S8	Q4
24	S7	Q3	S31	Q3	S17	Q4
25	S11	Q6	S7	Q3	S22	Q5
26	S9	Q5	S25	Q1	S24	Q7
27	S17	Q4	S24	Q7	S19	Q3
28	S36	Q7	S17	Q4	S7	Q3
29	S5	Q4	S33	Q5	S30	Q5
30	S22	Q5	S36	Q7	S33	Q5
31	S33	Q5	S9	Q5	S32	Q4
32	S35	Q6	S32	Q4	S9	Q5
33	S32	Q4	S35	Q6	S35	Q6
34	S10	Q5	S10	Q5	S10	Q5
35	S34	Q5	S34	Q5	S34	Q5
36	S12	Q7	S12	Q7	S12	Q7

Table A.7 12-8-2017-2 MOS sensor and quadrants sorted by greatest voltage						
	1ml		2ml		3ml	
Sensor Rank from total voltage	Sensor	Quadrant	Sensor	Quadrant	Sensor	Quadrant
1	S27	Q3	S26	Q2	S6	Q5
2	S26	Q2	S27	Q3	S7	Q3
3	S15	Q3	S15	Q3	S27	Q3
4	S6	Q5	S13	Q1	S4	Q3
5	S32	Q4	S6	Q5	S26	Q2
6	S4	Q3	S1	Q1	S15	Q3
7	S5	Q4	S2	Q2	S28	Q3
8	S28	Q3	S28	Q3	S19	Q3
9	S31	Q3	S14	Q2	S31	Q3
10	S2	Q2	S3	Q3	S25	Q1
11	S20	Q4	S4	Q3	S24	Q7
12	S14	Q2	S16	Q3	S13	Q1
13	S33	Q5	S25	Q1	S29	Q4
14	S19	Q3	S23	Q6	S8	Q4
15	S24	Q7	S29	Q4	S20	Q4
16	S25	Q1	S20	Q4	S2	Q2
17	S13	Q1	S5	Q4	S14	Q2
18	S22	Q5	S22	Q5	S1	Q1
19	S23	Q6	S8	Q4	S16	Q3
20	S29	Q4	S31	Q3	S21	Q5
21	S3	Q3	S18	Q5	S23	Q6
22	S1	Q1	S17	Q4	S22	Q5
23	S16	Q3	S30	Q5	S5	Q4
24	S17	Q4	S24	Q7	S3	Q3
25	S18	Q5	S21	Q5	S30	Q5
26	S10	Q5	S11	Q6	S18	Q5
27	S8	Q4	S19	Q3	S17	Q4
28	S21	Q5	S9	Q5	S9	Q5
29	S30	Q5	S32	Q4	S35	Q6
30	S36	Q7	S33	Q5	S32	Q4
31	S7	Q3	S36	Q7	S36	Q7
32	S35	Q6	S7	Q3	S11	Q6
33	S9	Q5	S35	Q6	S10	Q5
34	S11	Q6	S10	Q5	S33	Q5
35	S34	Q5	S12	Q7	S34	Q5
36	S12	Q7	S34	Q5	S12	Q7

Table A.8 12-9-2017 MOS sensor and quadrants sorted by greatest voltage						
	1ml		2ml		3ml	
Sensor Rank from total voltage	Sensor	Quadrant	Sensor	Quadrant	Sensor	Quadrant
1	S6	Q5	S27	Q3	S6	Q5
2	S7	Q3	S26	Q2	S7	Q3
3	S26	Q2	S15	Q3	S27	Q3
4	S27	Q3	S28	Q3	S4	Q3
5	S4	Q3	S6	Q5	S26	Q2
6	S13	Q1	S13	Q1	S13	Q1
7	S15	Q3	S29	Q4	S15	Q3
8	S23	Q6	S23	Q6	S23	Q6
9	S28	Q3	S7	Q3	S28	Q3
10	S31	Q3	S3	Q3	S25	Q1
11	S29	Q4	S31	Q3	S16	Q3
12	S1	Q1	S4	Q3	S20	Q4
13	S16	Q3	S25	Q1	S29	Q4
14	S20	Q4	S16	Q3	S2	Q2
15	S19	Q3	S20	Q4	S5	Q4
16	S3	Q3	S24	Q7	S31	Q3
17	S14	Q2	S5	Q4	S1	Q1
18	S2	Q2	S30	Q5	S8	Q4
19	S8	Q4	S2	Q2	S3	Q3
20	S24	Q7	S8	Q4	S18	Q5
21	S25	Q1	S14	Q2	S24	Q7
22	S11	Q6	S21	Q5	S17	Q4
23	S5	Q4	S1	Q1	S19	Q3
24	S32	Q4	S11	Q6	S30	Q5
25	S17	Q4	S18	Q5	S21	Q5
26	S18	Q5	S33	Q5	S14	Q2
27	S30	Q5	S9	Q5	S32	Q4
28	S36	Q7	S19	Q3	S33	Q5
29	S21	Q5	S36	Q7	S10	Q5
30	S22	Q5	S10	Q5	S11	Q6
31	S33	Q5	S22	Q5	S36	Q7
32	S35	Q6	S32	Q4	S22	Q5
33	S10	Q5	S35	Q6	S9	Q5
34	S9	Q5	S17	Q4	S35	Q6
35	S34	Q5	S34	Q5	S12	Q7
36	S12	Q7	S12	Q7	S34	Q5

Table A.9 Top 50% of MOS sensors with greatest voltage response			
Sensor number	Number of times sensor was in top 50% for 1ml of DEET	Number of times sensor was in top 50% for 2ml of DEET	Number of times sensor was in top 50% for 3ml of DEET
S1	7	6	8
S2	8	7	8
S3	6	7	5
S4	7	5	7
S5	4	6	3
S6	8	8	8
S7	3	3	4
S8	6	5	7
S9	0	0	0
S10	0	0	0
S11	0	0	1
S12	0	0	0
S13	8	8	8
S14	5	6	4
S15	8	8	8
S16	6	8	7
S17	0	2	0
S18	4	2	3
S19	2	0	5
S20	8	6	8
S21	2	3	3
S22	1	2	0
S23	3	3	2
S24	5	6	3
S25	4	5	5
S26	8	8	5
S27	8	8	8
S28	8	8	8
S29	3	5	5
S30	3	3	0
S31	7	6	8
S32	1	0	2
S33	1	0	0
S34	0	0	0
S35	0	0	0
S36	0	0	1

Table A.10 Top 25% of MOS sensors with greatest voltage response			
Sensor number	Number of times sensor was in top 25% for 1ml of DEET	Number of times sensor was in top 25% for 2ml of DEET	Number of times sensor was in top 25% for 3ml of DEET
S1	2	3	4
S2	5	4	4
S3	3	2	2
S4	4	3	4
S5	3	2	1
S6	8	8	7
S7	3	3	4
S8	0	1	1
S9	0	0	0
S10	0	0	0
S11	0	0	0
S12	0	0	0
S13	4	7	5
S14	1	1	0
S15	6	7	6
S16	3	3	3
S17	0	0	0
S18	0	1	2
S19	0	0	1
S20	1	3	4
S21	0	0	1
S22	0	0	0
S23	1	1	1
S24	0	0	0
S25	0	0	0
S26	7	7	5
S27	8	7	8
S28	6	5	6
S29	2	3	2
S30	0	0	0
S31	4	1	1
S32	1	0	0
S33	0	0	0
S34	0	0	0
S35	0	0	0
S36	0	0	0

Table A.11 Top 10% of MOS sensors with greatest voltage response			
Sensor number	Number of times sensor was in top 10% for 1ml of DEET	Number of times sensor was in top 10% for 2ml of DEET	Number of times sensor was in top 10% for 3ml of DEET
S1	0	1	1
S2	0	0	0
S3	2	2	2
S4	0	0	0
S5	0	0	0
S6	3	1	5
S7	1	1	2
S8	0	0	0
S9	0	0	0
S10	0	0	0
S11	0	0	0
S12	0	0	0
S13	0	0	0
S14	0	0	0
S15	5	3	3
S16	0	0	1
S17	0	0	0
S18	0	0	0
S19	0	0	0
S20	1	1	1
S21	0	0	0
S22	0	0	0
S23	0	0	0
S24	0	0	0
S25	0	0	0
S26	6	5	1
S27	5	7	8
S28	0	3	0
S29	0	0	0
S30	0	0	0
S31	1	0	0
S32	0	0	0
S33	0	0	0
S34	0	0	0
S35	0	0	0
S36	0	0	0

Table A.12 Compiled top 10% of MOS sensors with greatest voltage change

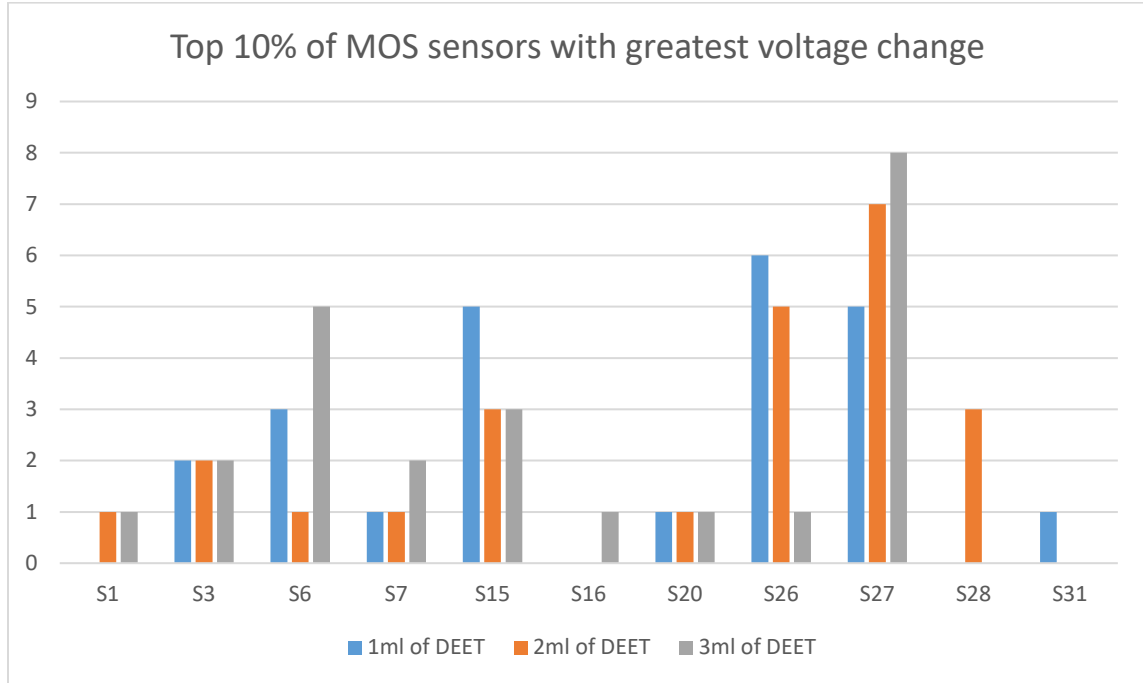


Table A.13 Compiled top 25% of MOS sensors with greatest voltage change

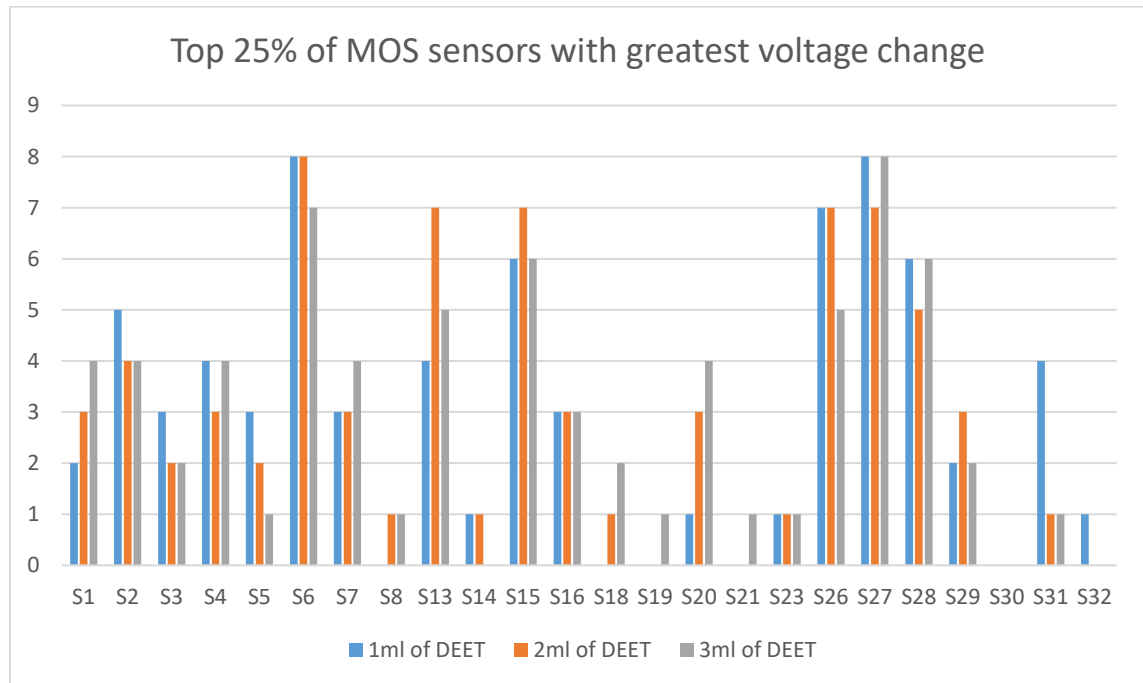


Table A.14 Compiled top 50% of MOS sensors with greatest voltage change

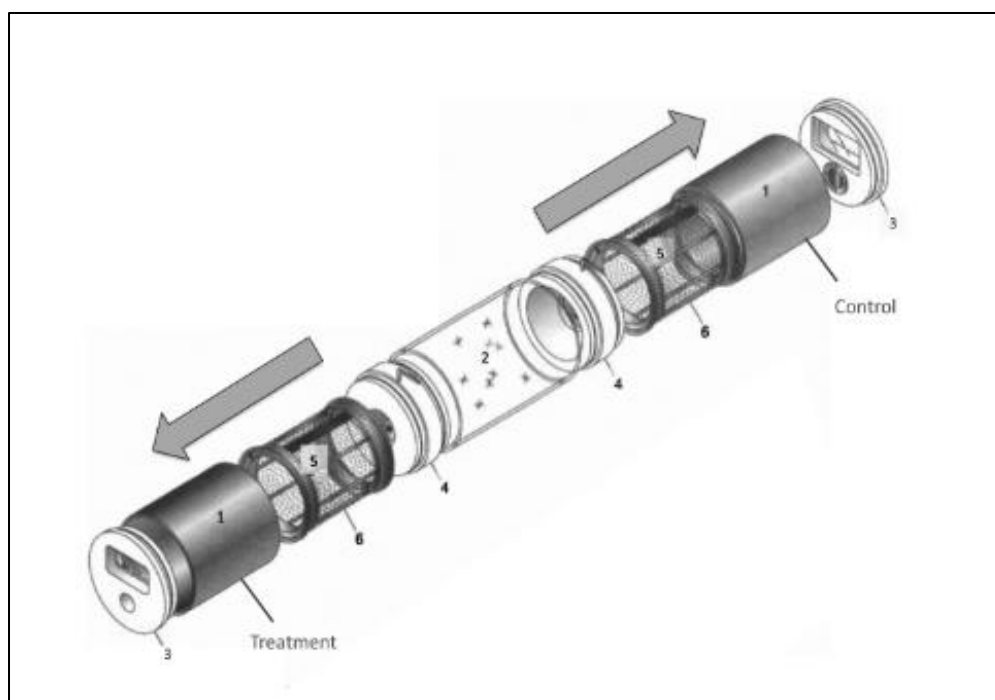
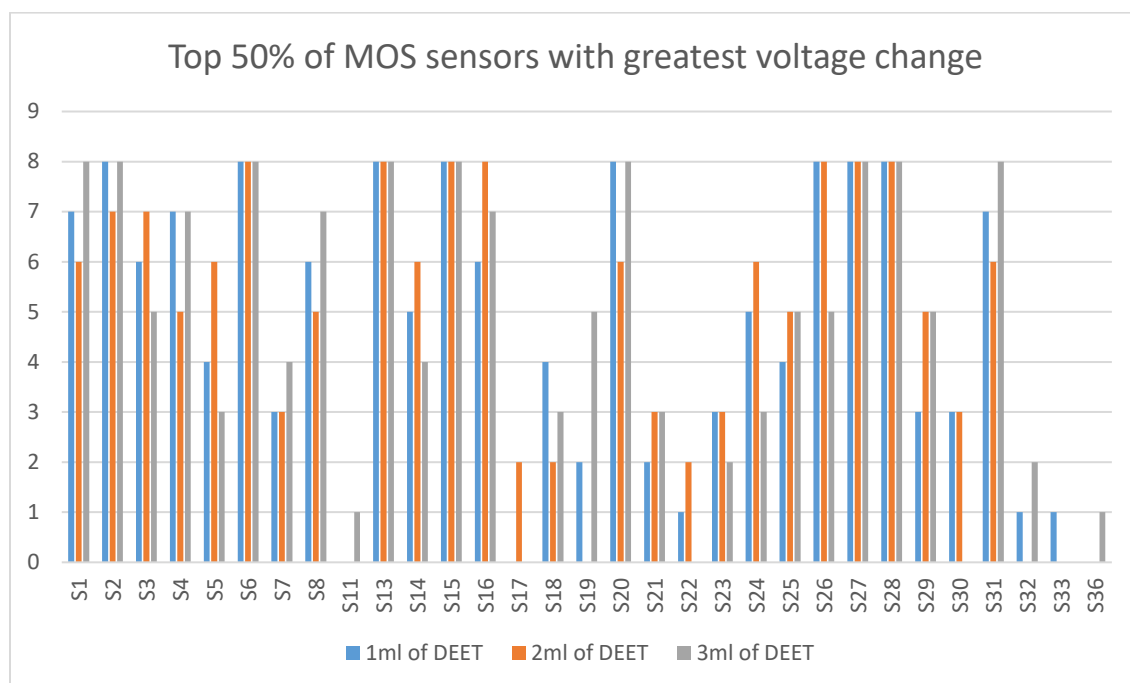


Figure A.1 Cylinder apparatus from Guidelines for Efficacy Testing of Spatial Repellents

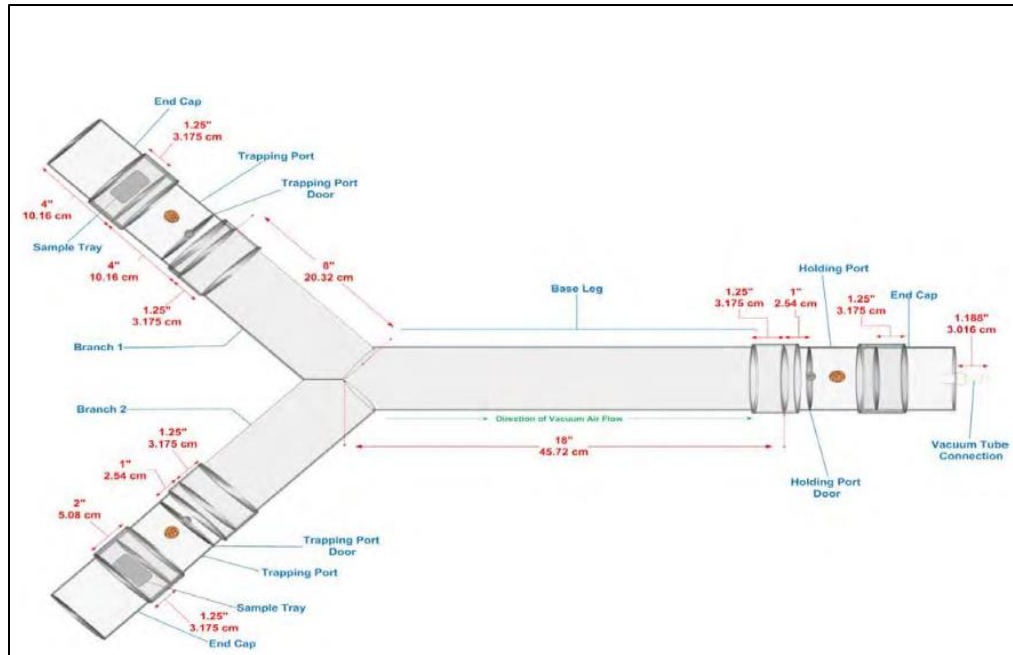


Figure A.2 Y-tube olfactometer Guidelines for Efficacy Testing of Spatial Repellents



Figure A.3 Chamber with chamber ends removed with three tier sensor arm inside



Figure A.4 Image of chamber with chamber end show together



Figure A.5 Image of chamber with chamber end held together with bracket.



Figure A.6 Image of chamber end with septa sealing 29/42 ground glass joint

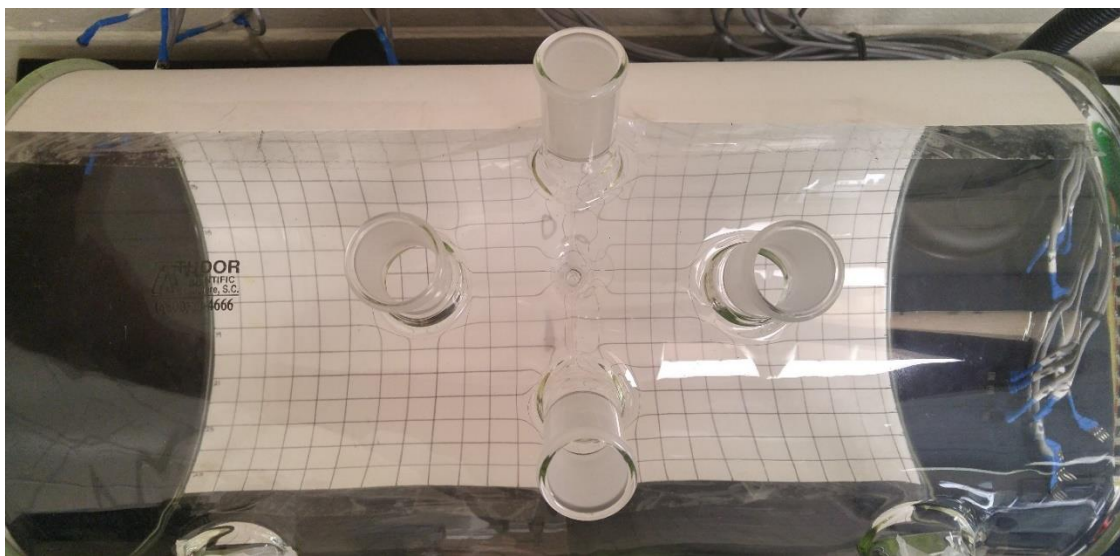


Figure A.7 Image of four 29/42 ground glass joint at top of chamber

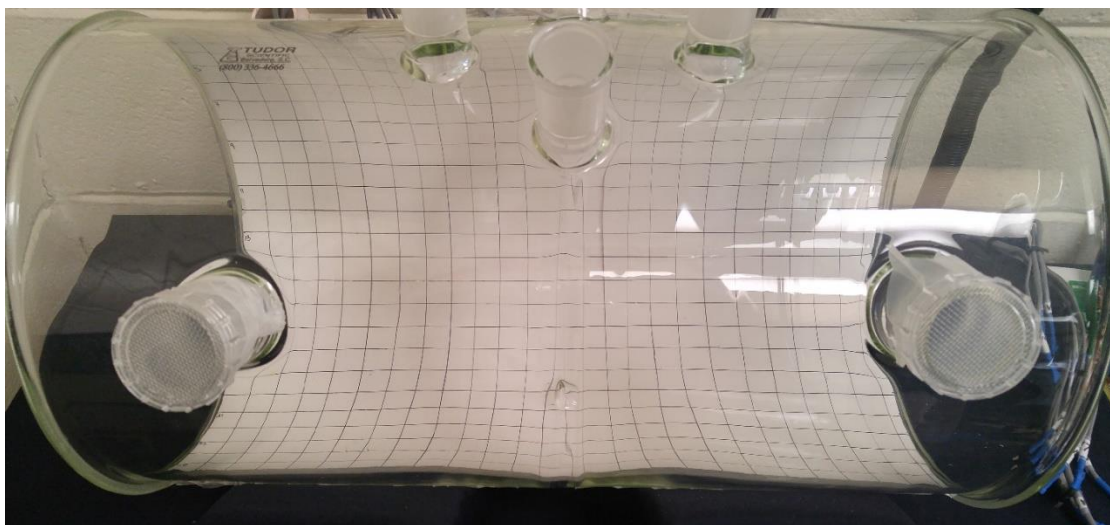


Figure A.8 Image of mosquito introduction ports

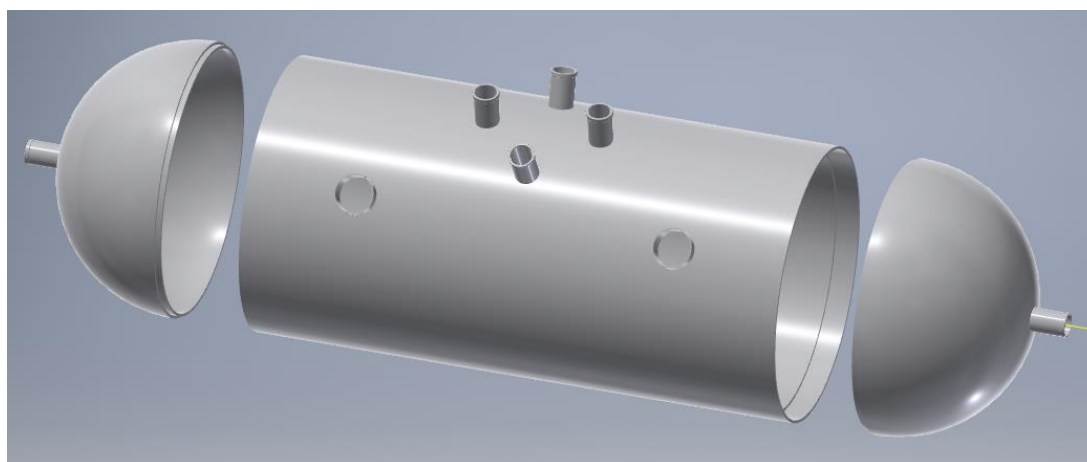


Figure A.9 CAD of the prototype chamber provided to TUDOR scientific

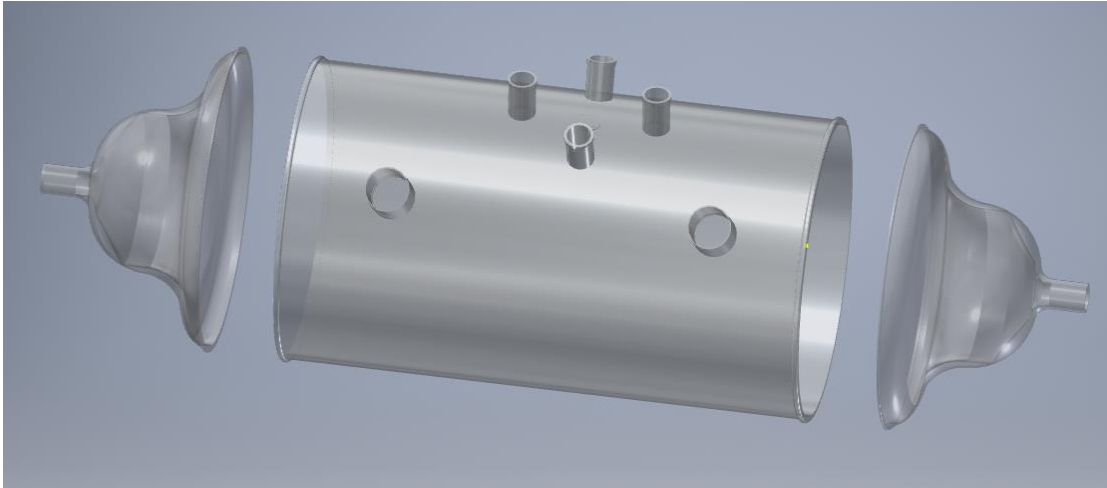


Figure A.10 CAD of the prototype chamber that TUDOR Scientific produced



Figure A.11 Notch place at the top of the chamber for expanding rod



Figure A.12 Notch placed at the bottom of the chamber for the expandable rod

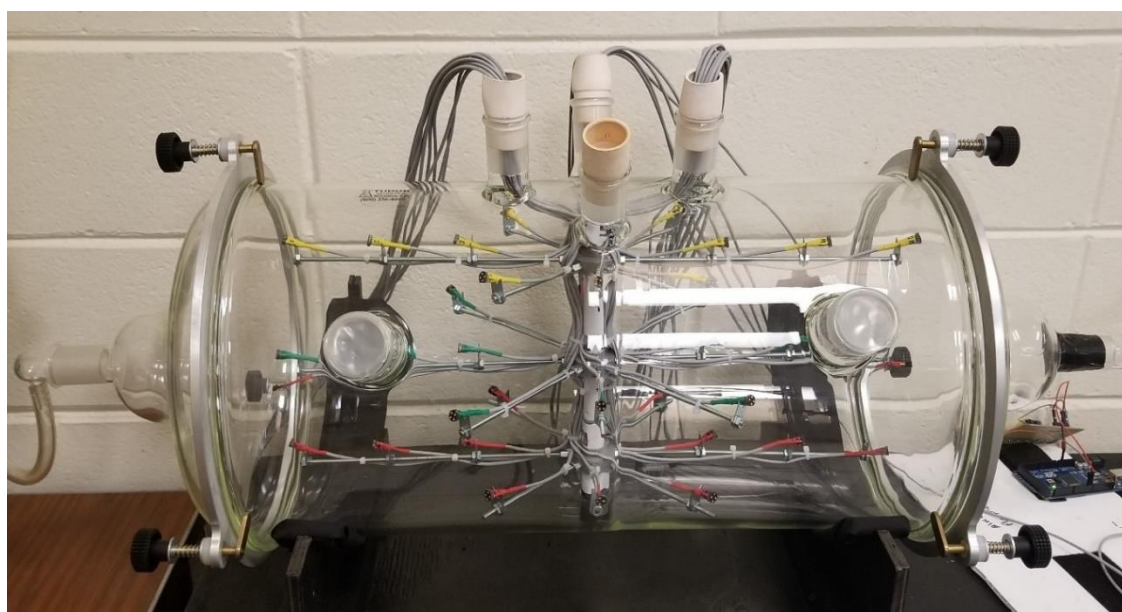


Figure A.13 Standard chamber setup



Figure A.14 TGS 2602 metal oxide semiconductor sensor

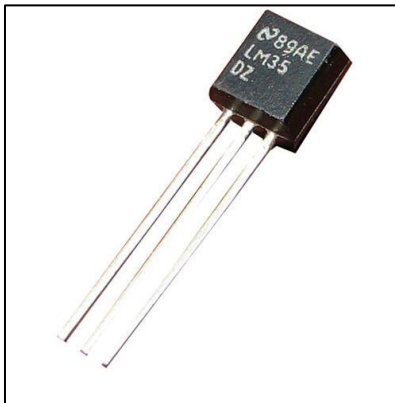


Figure A.15 LM35DZ temperature sensor

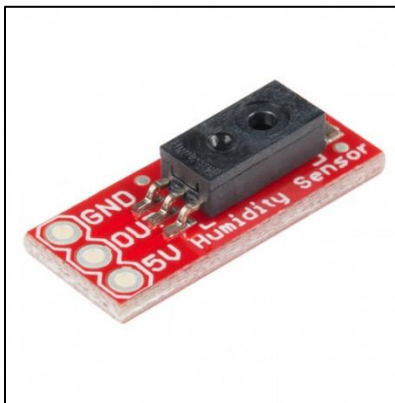


Figure A.16 HIH-4030 humidity sensor

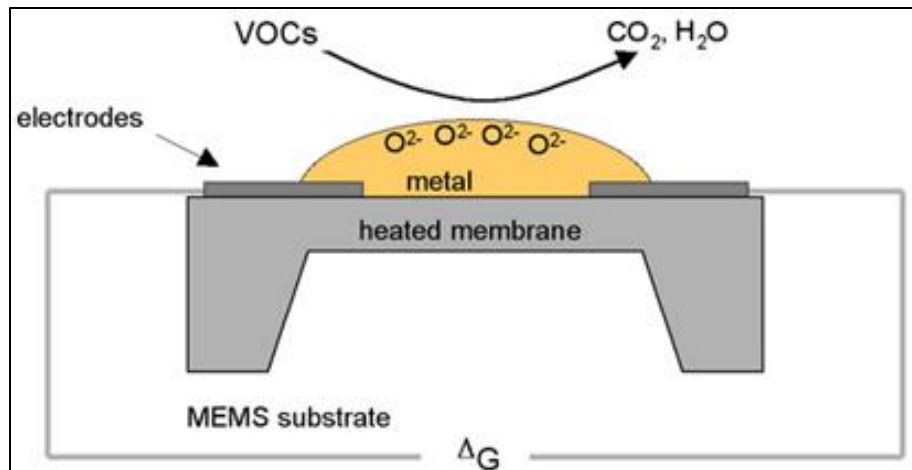


Figure A.17 Metal oxide substrate.

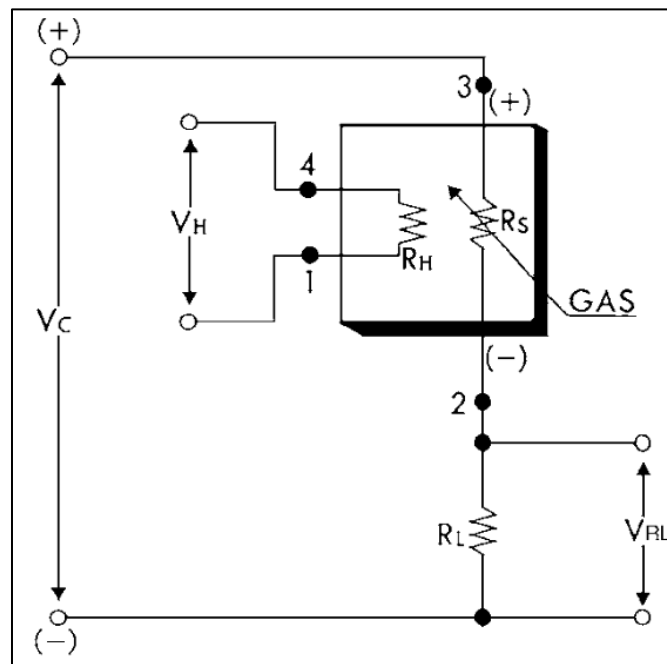


Figure A.18 TGS 2602 sensor circuit

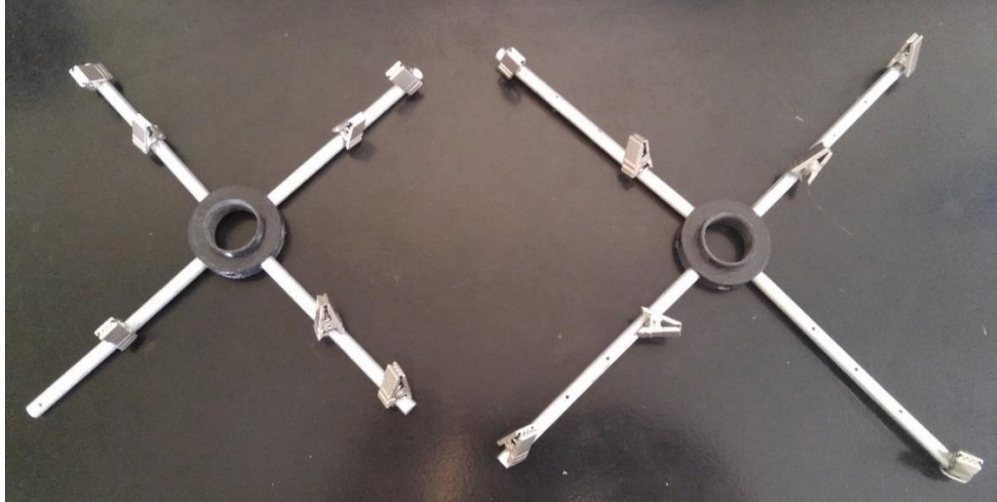


Figure A.19 First iteration sensor tree arms

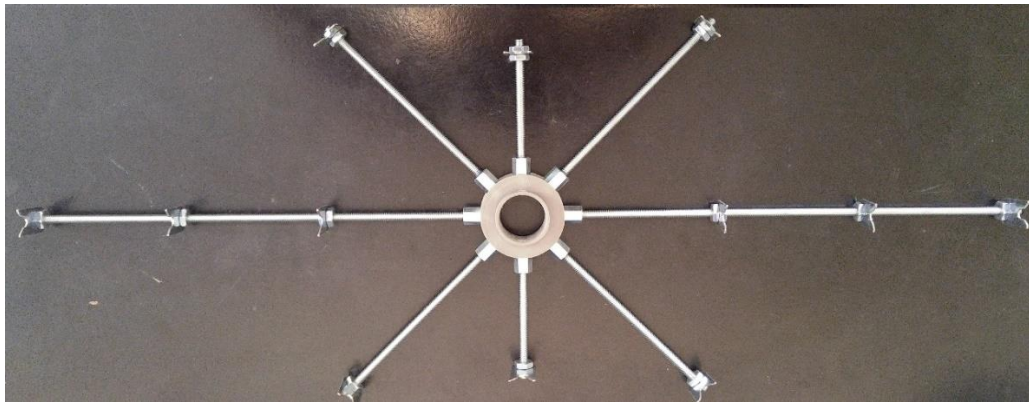


Figure A.20 Second iteration sensor tree arms

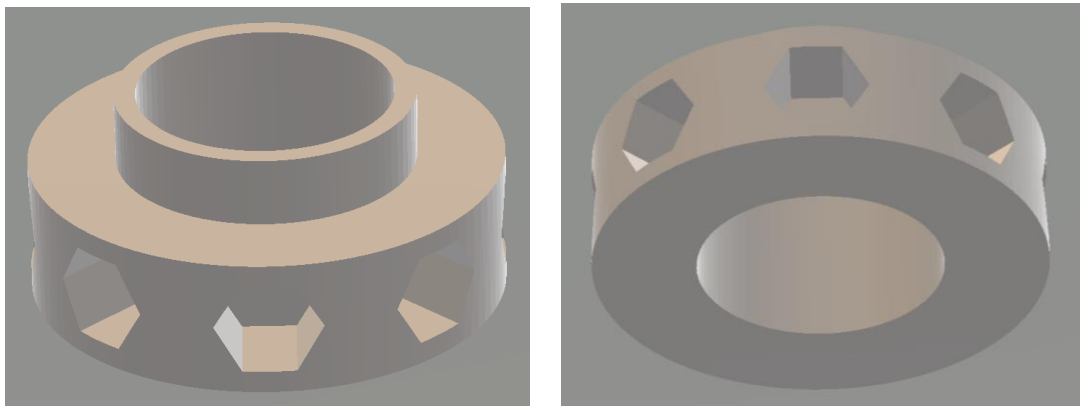


Figure A.21 3d printed center rings

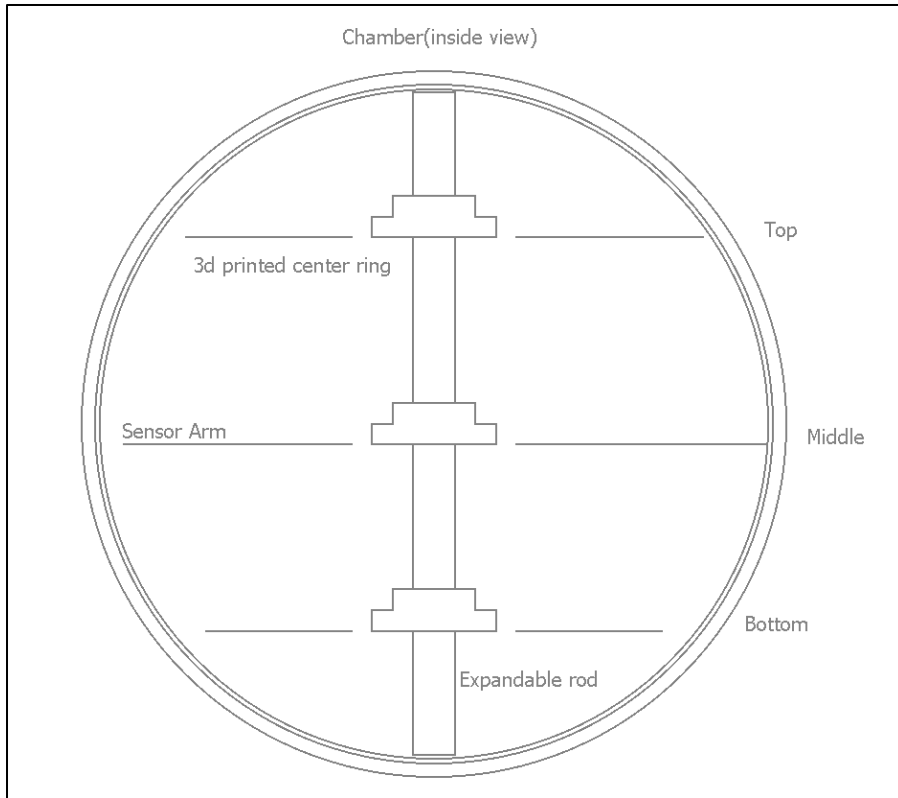


Figure A.22 3d Printed ring locations

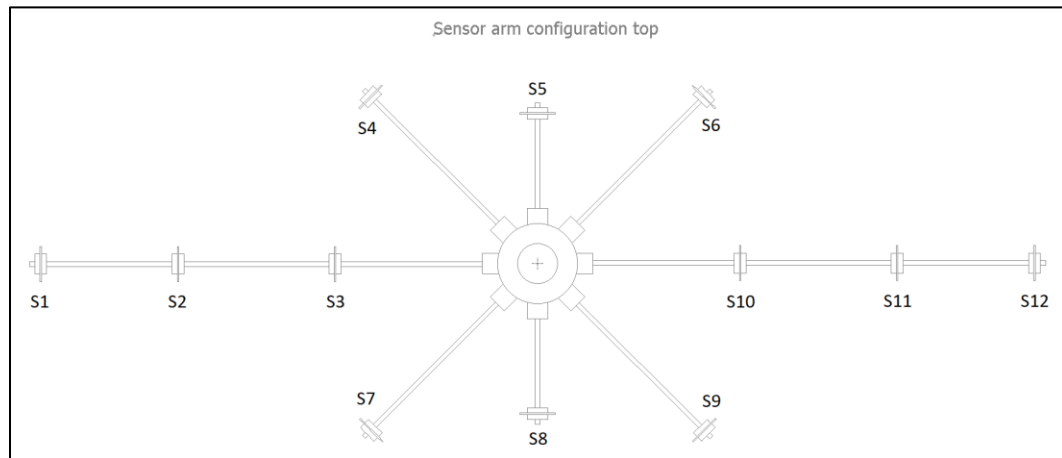


Figure A.23 Sensor locations on top tier of sensor tree

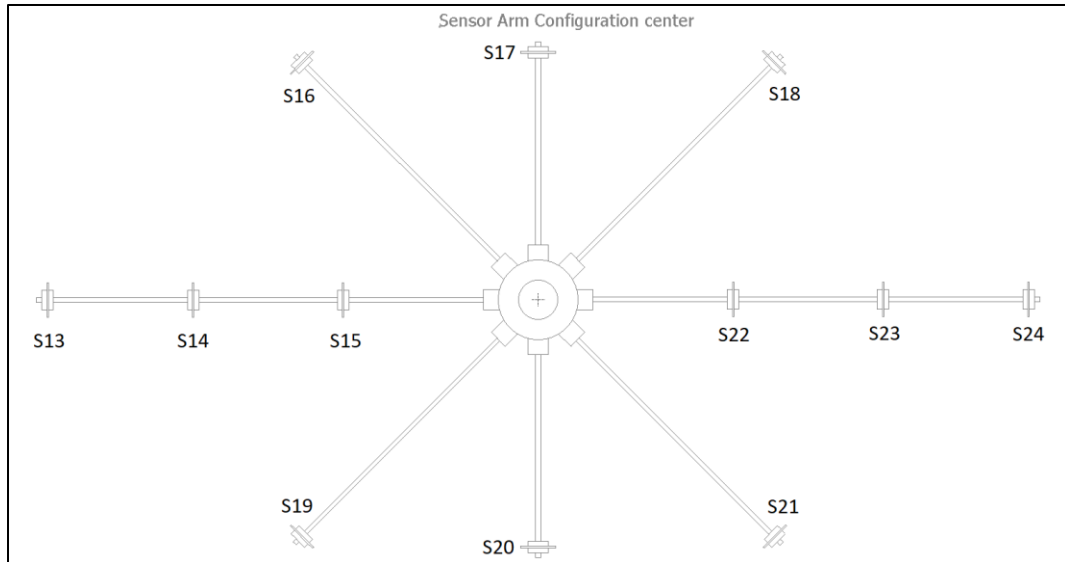


Figure A.24 Sensor locations on center tier of sensor tree

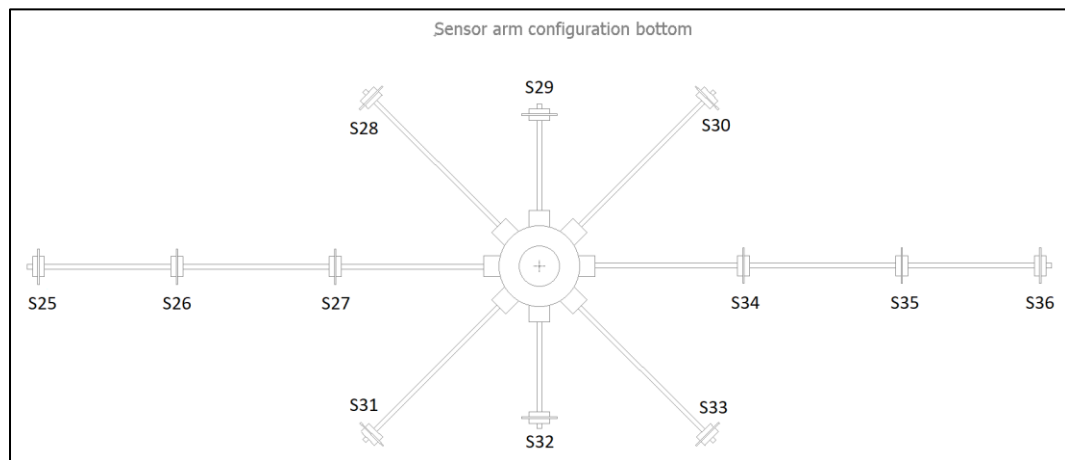


Figure A.25 Sensor locations on bottom tier of sensor tree

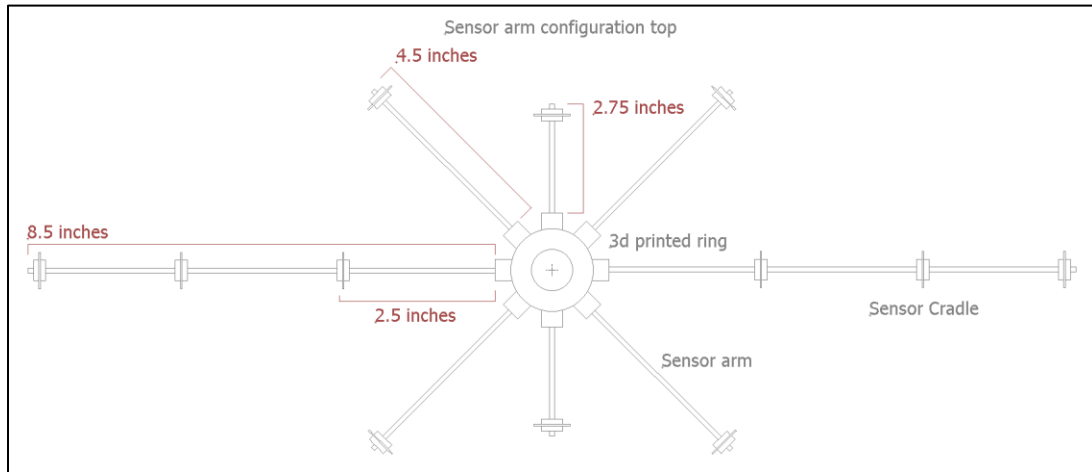


Figure A.26 Top sensor arm configuration with sensor arm measurements

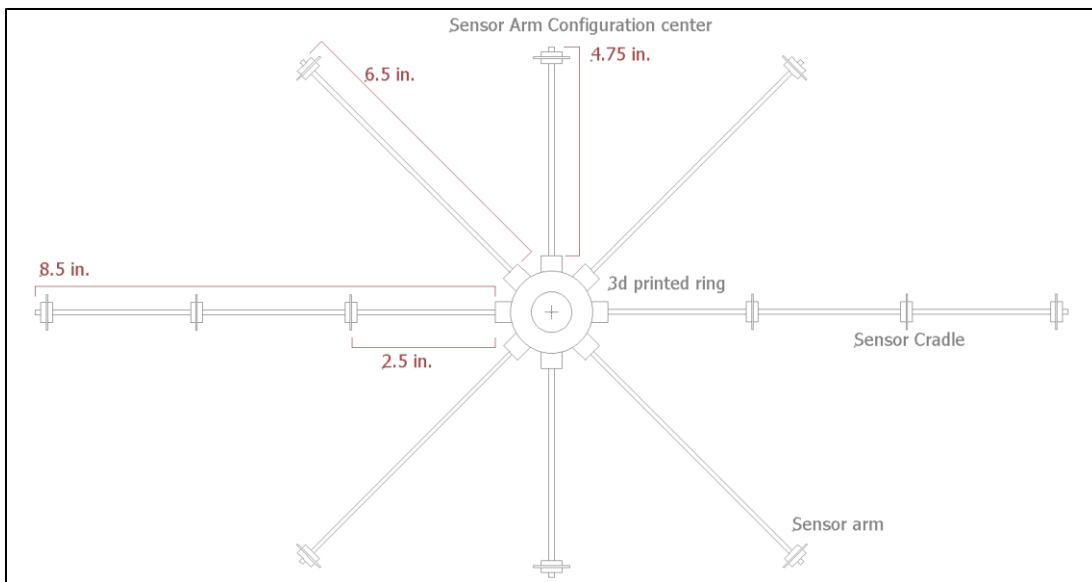


Figure A.27 Center sensor arm configuration with sensor arm measurements

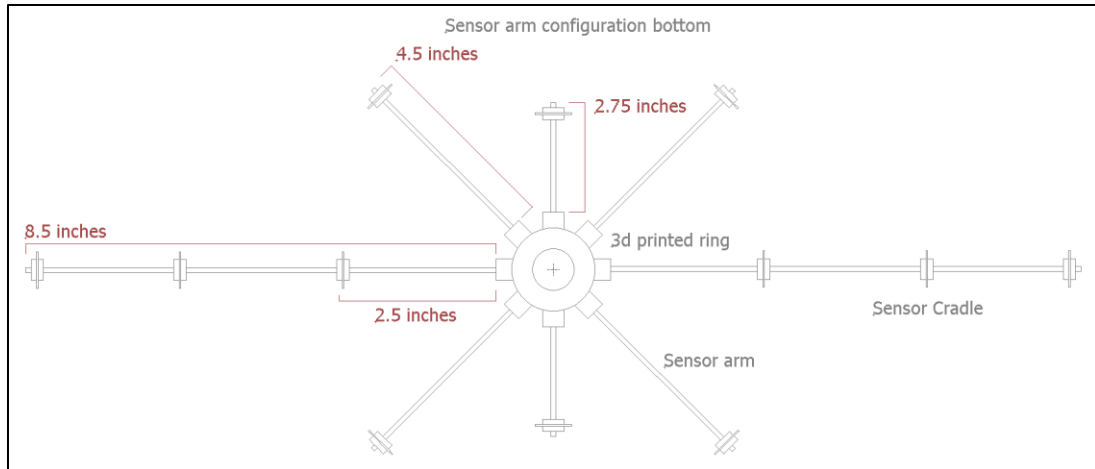


Figure A.28 Bottom sensor arm configuration with sensor arm measurements

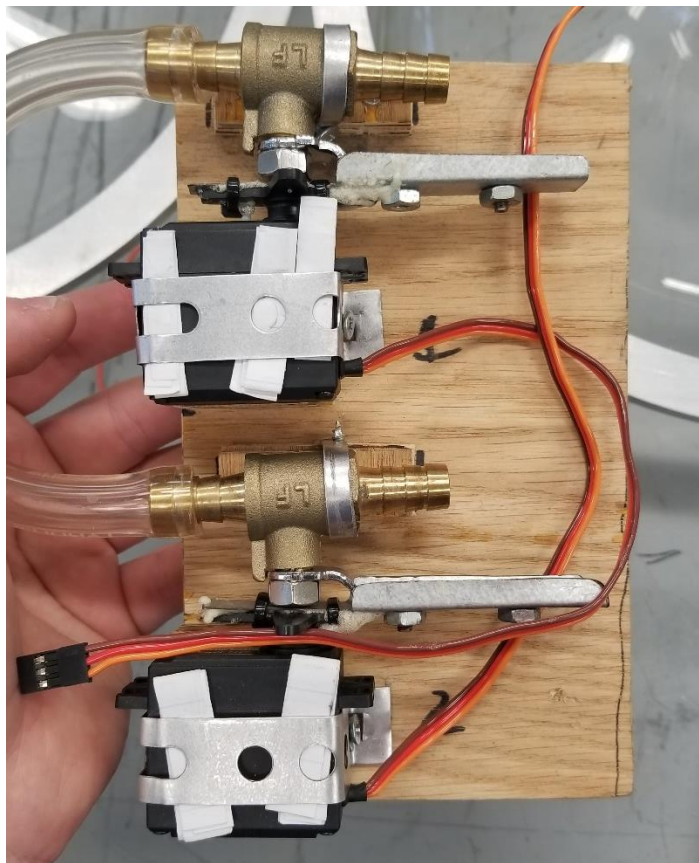


Figure A.29 Servo-controlled valves

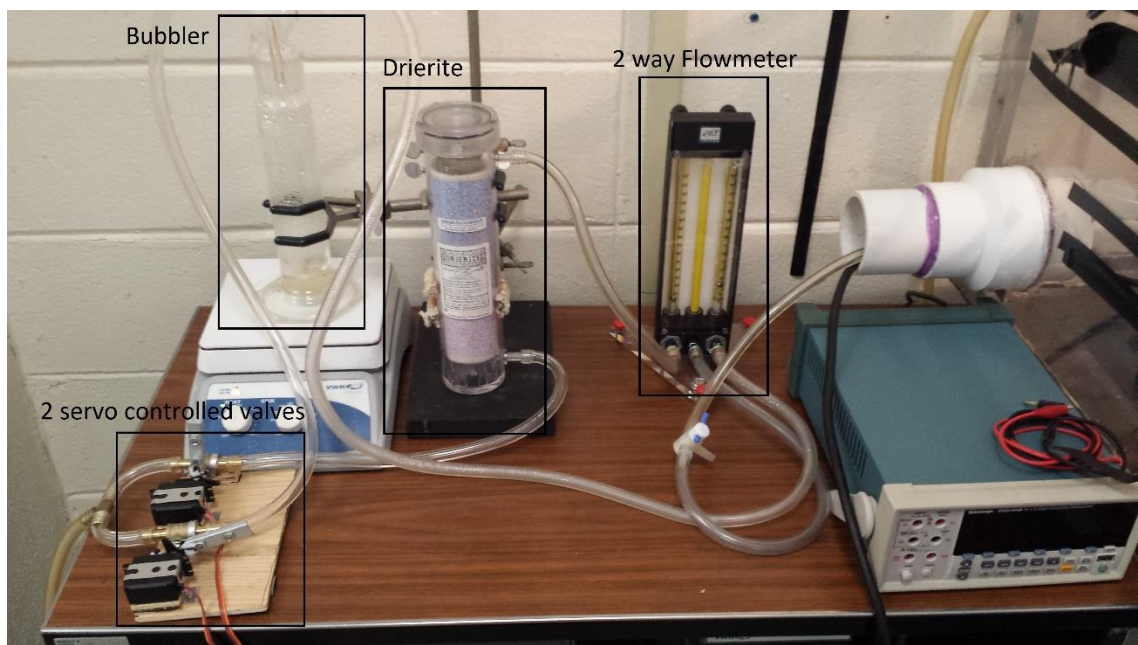


Figure A.30 Environment control setup



Figure A.31 LXG-120M camera

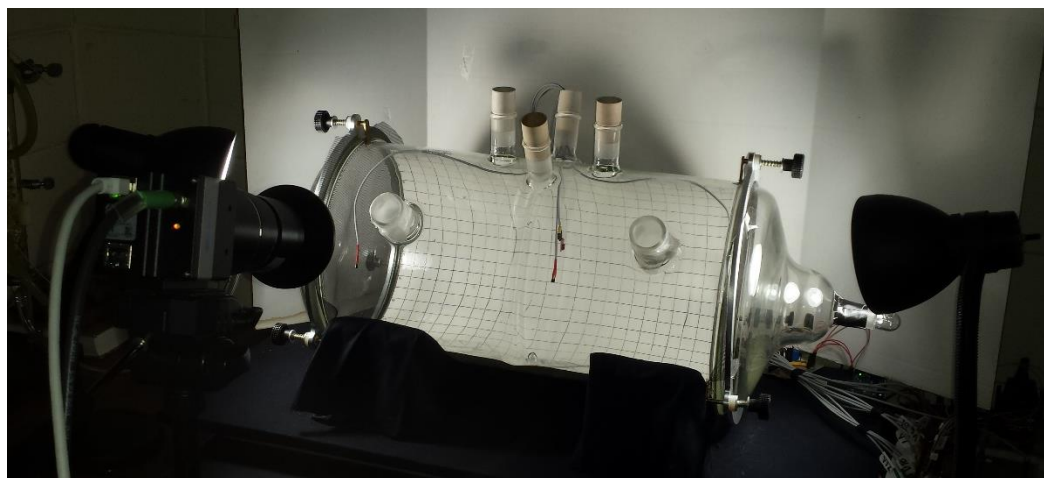


Figure A.32 Mosquito image recording setup

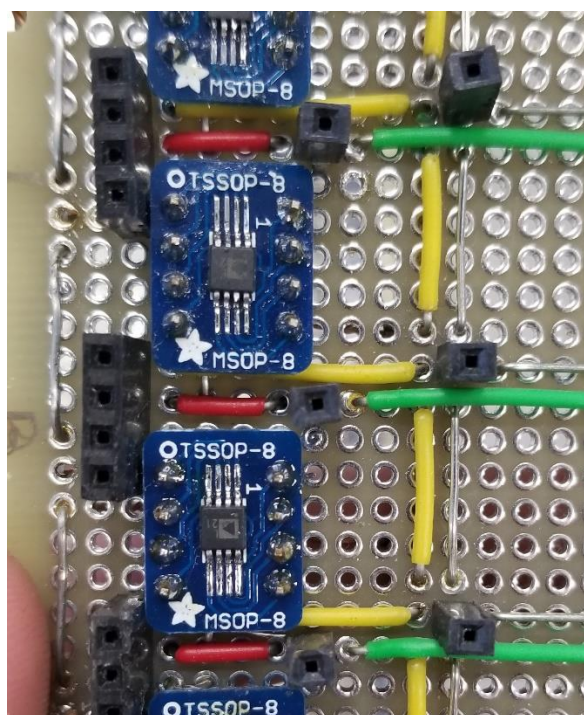


Figure A.33 MOS sensor board connection

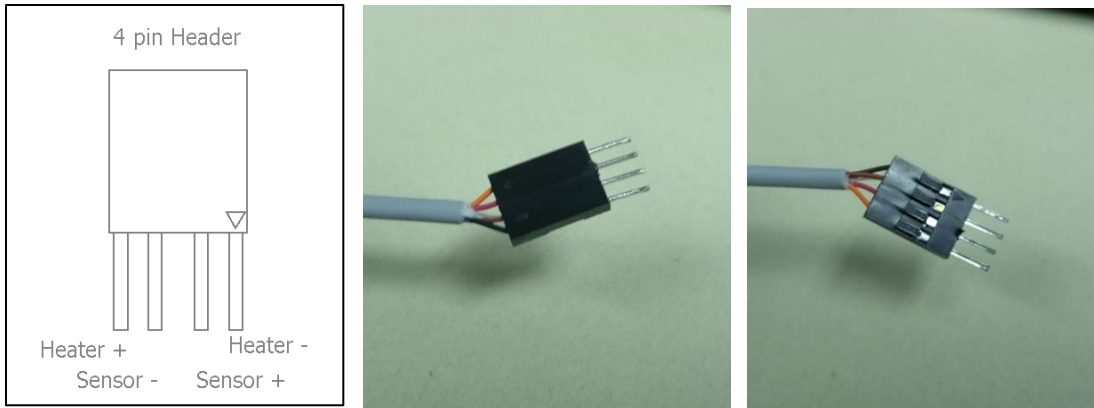


Figure A.34 MOS sensor wire four pin connector

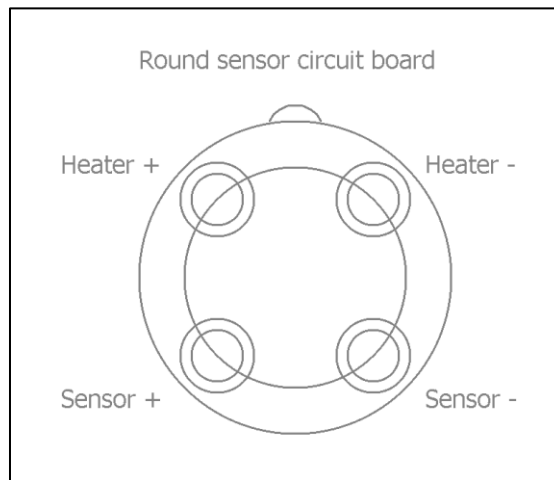


Figure A.35 MOS sensor chamber socket diagram

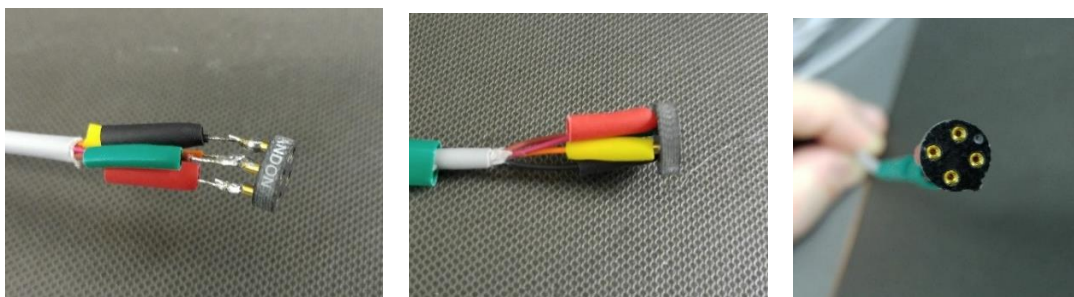


Figure A.36 MOS sensor circuit chamber socket wire

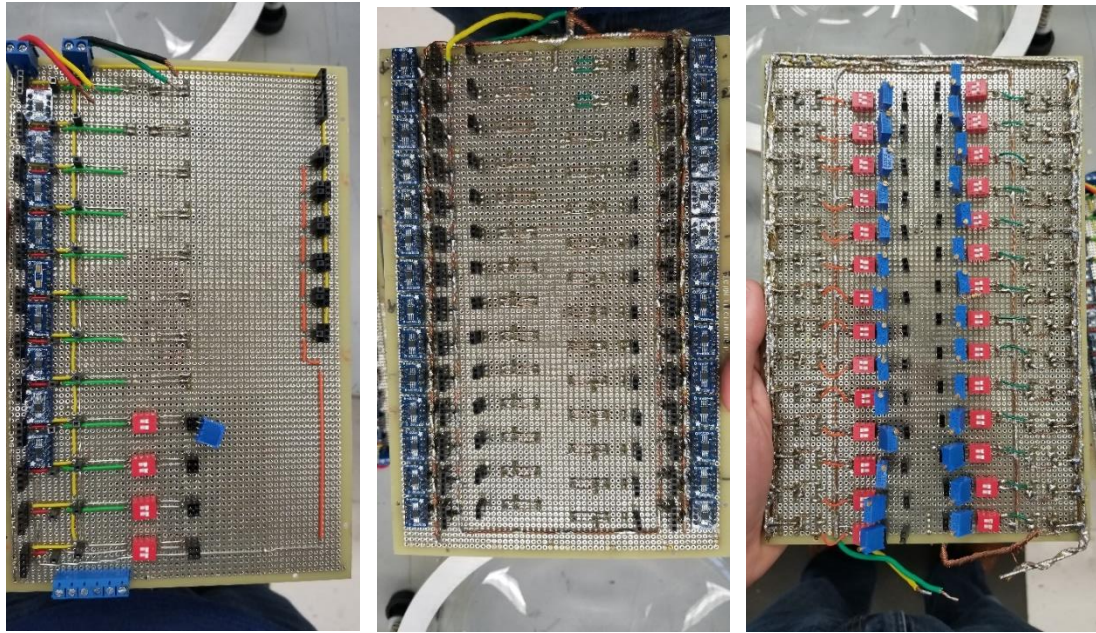


Figure A.37 Sensor board A and B front and back side.

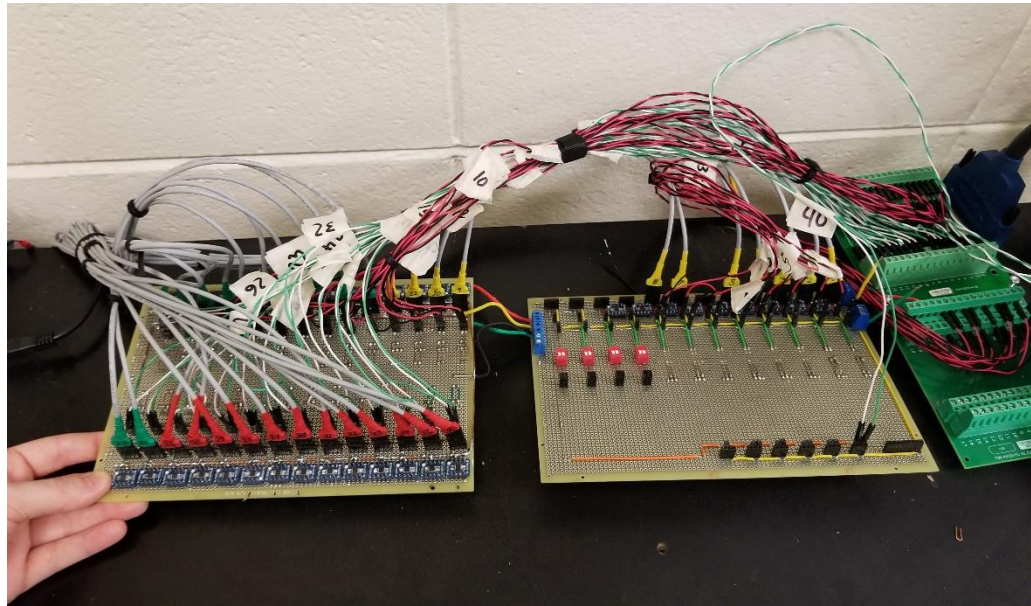


Figure A.38 Sensor board bottom view with sensor connections made

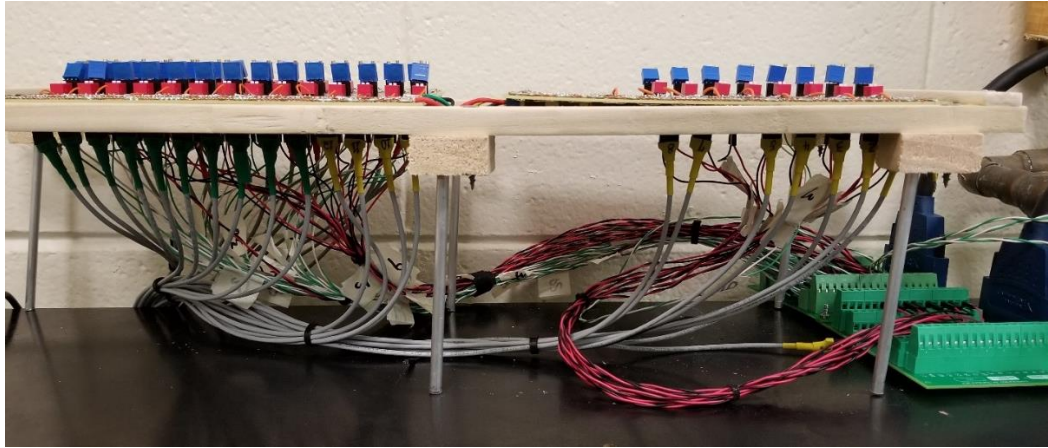


Figure A.39 Sensor board with sensor connections made

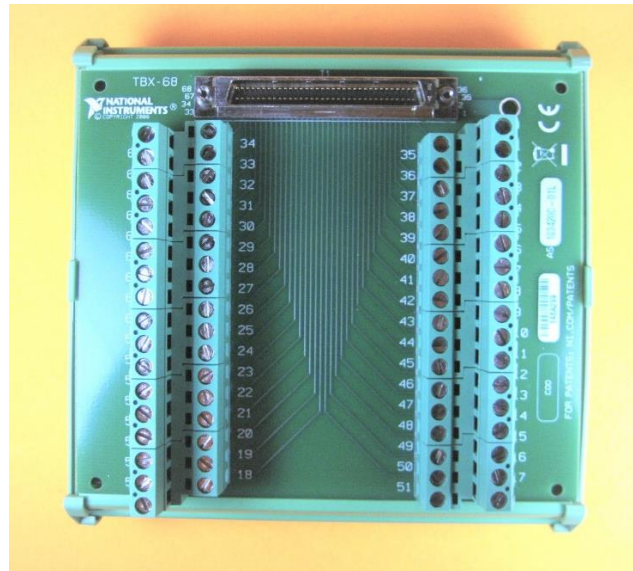


Figure A.40 TBX-68 DAQ connection terminal block



Figure A.41 National Instruments USB-6255 DAQ



Figure A.42 SH68-68-EPM shielded data cable

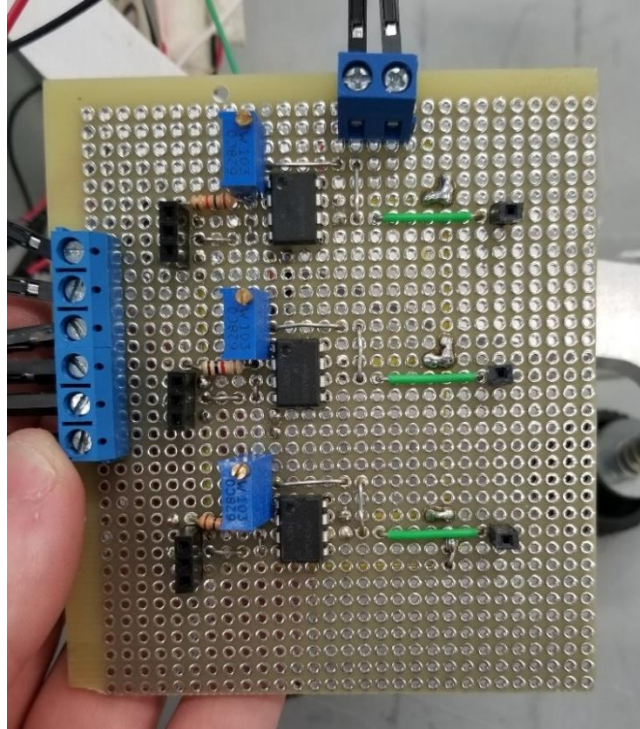


Figure A.43 Temperature amplifying board

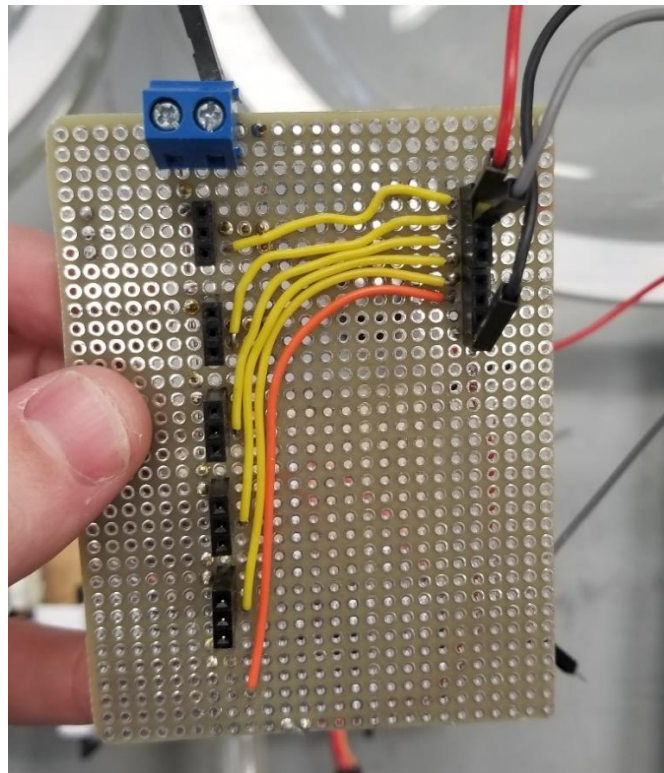


Figure A.44 Servo and relay control board

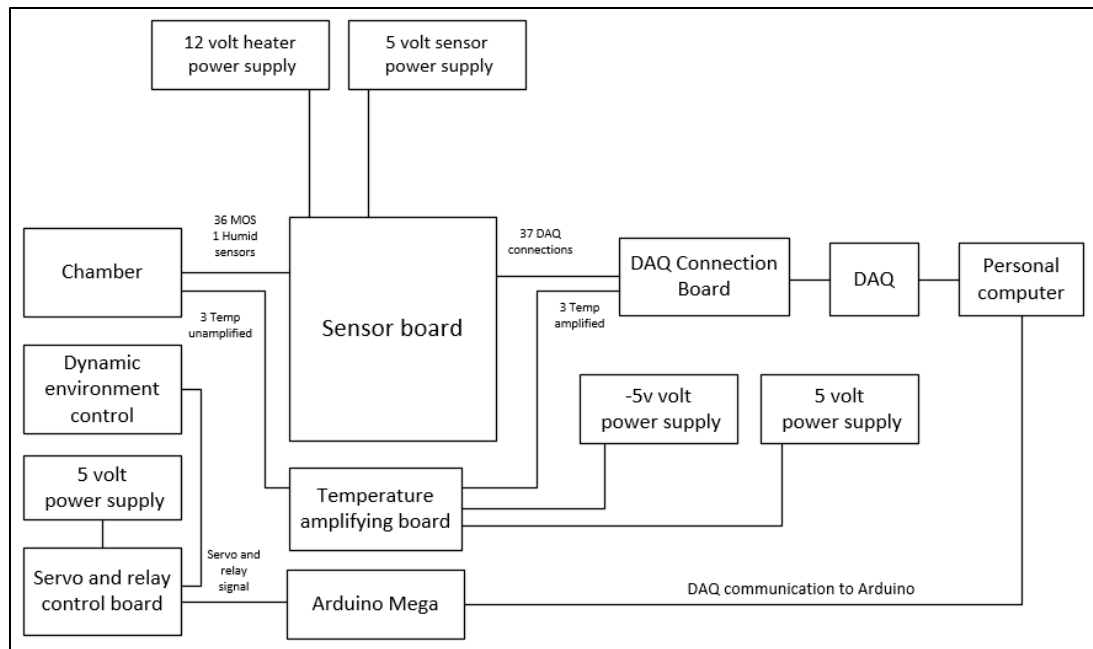


Figure A.45 Complete system circuitry diagram

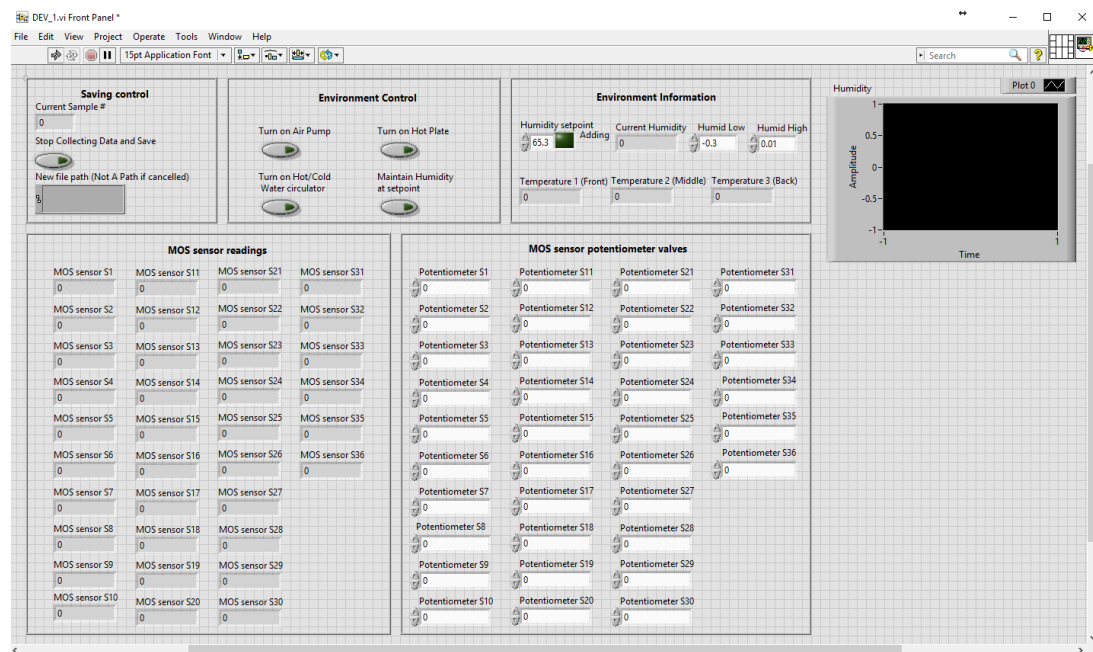


Figure A.46 LabVIEW program GUI interface

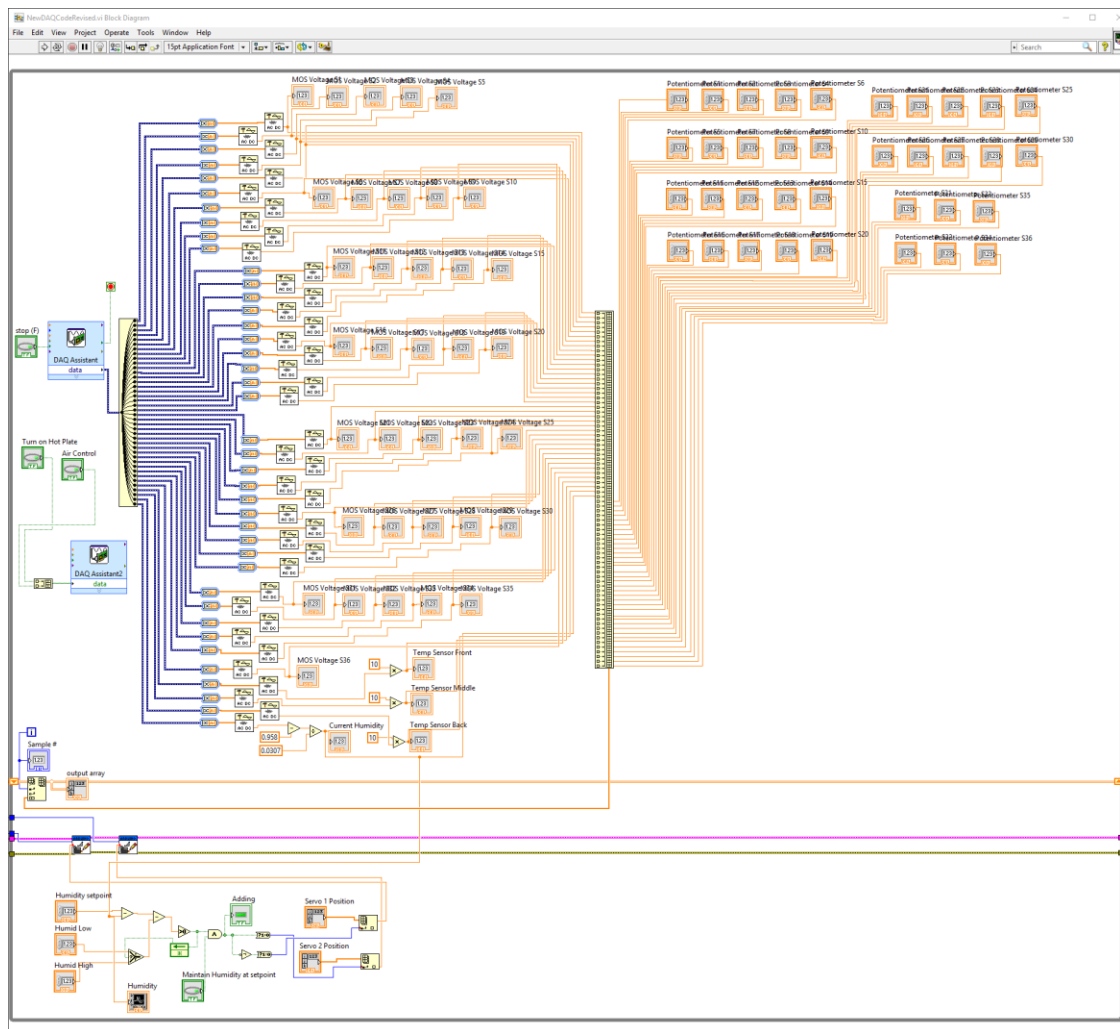


Figure A.47 LabVIEW program back end

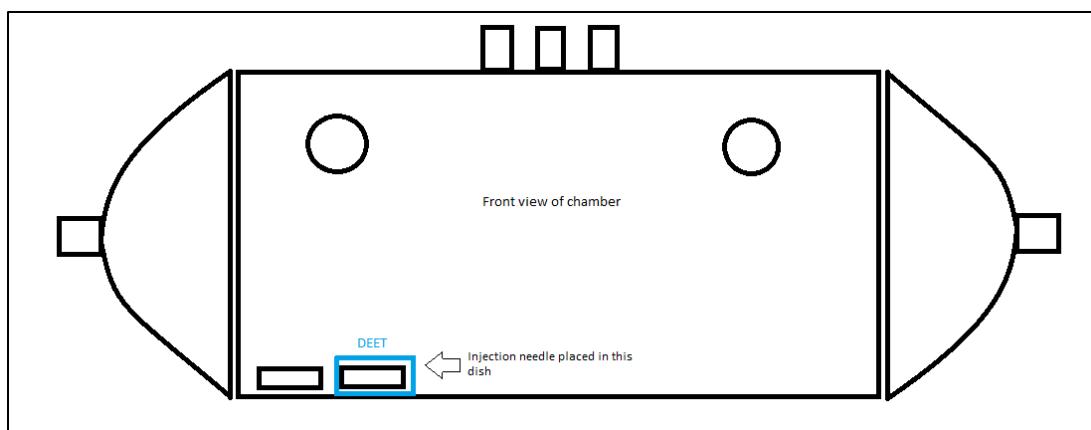


Figure A.48 MOS sensor testing injection setup



Figure A.49 Mosquito bait

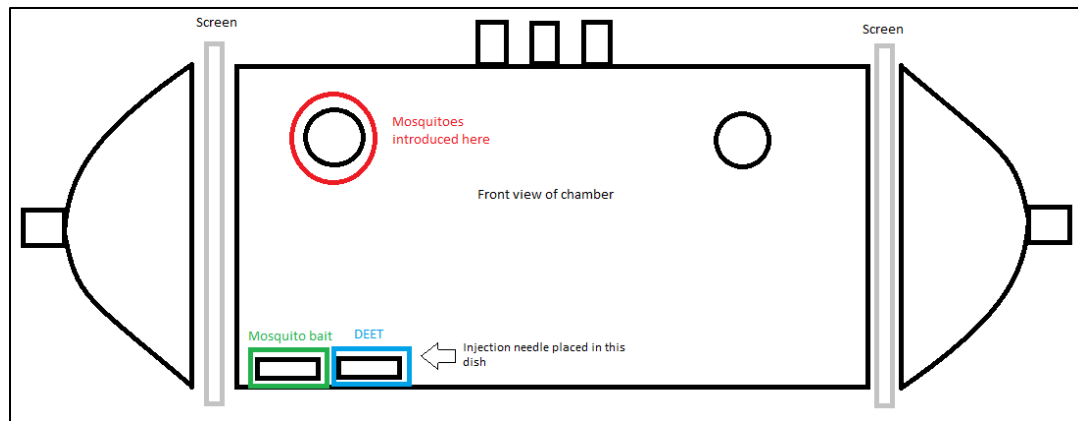


Figure A.50 Mosquito testing injection setup

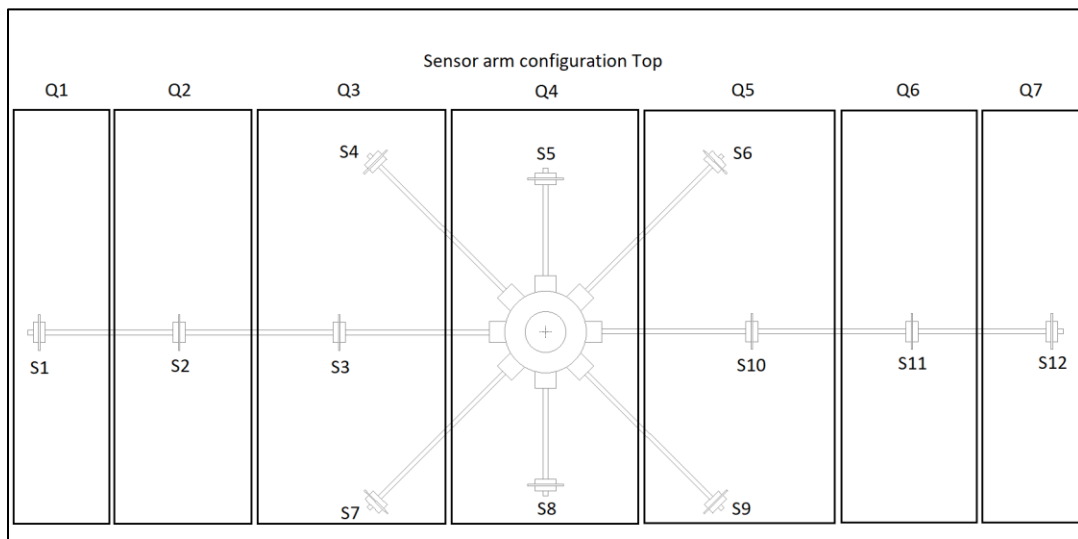


Figure A.51 Sensor arm top configuration with quadrants and sensor locations

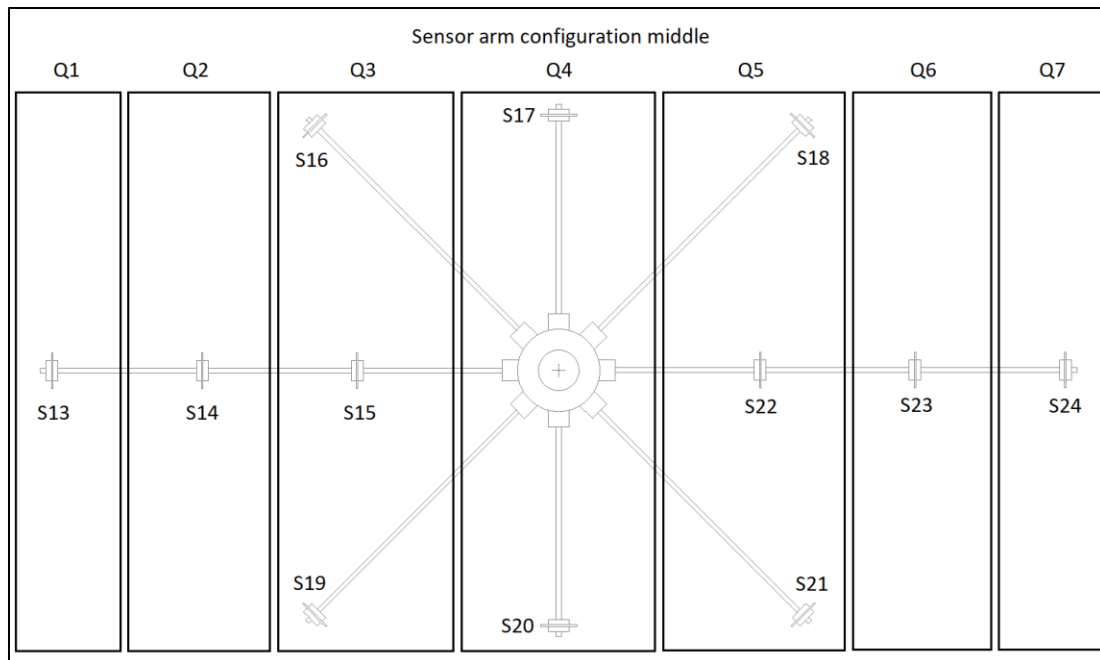


Figure A.52 Sensor arm middle configuration with quadrants and sensor locations

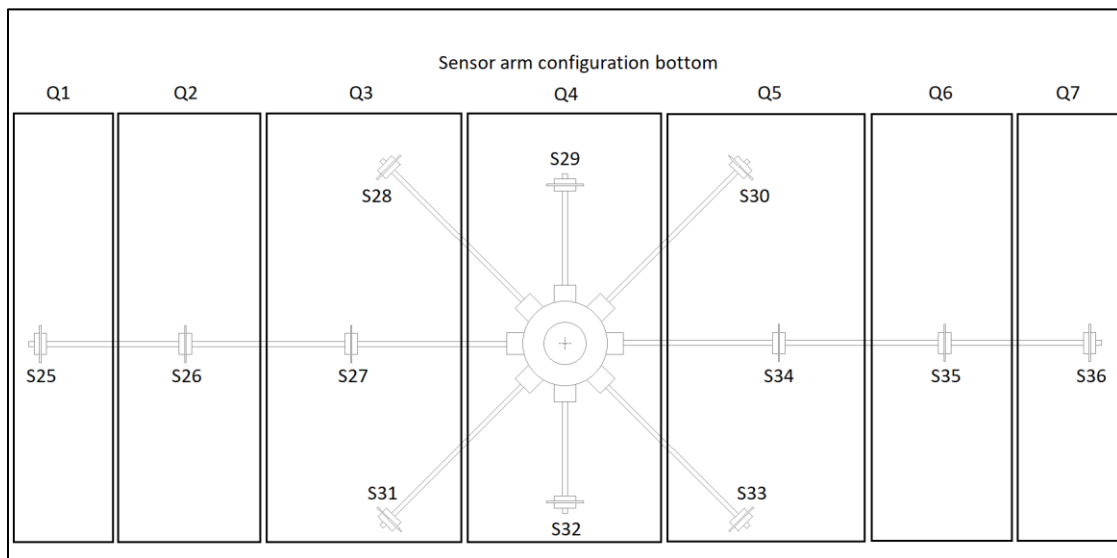


Figure A.53 Sensor arm bottom configuration with quadrants and sensor locations

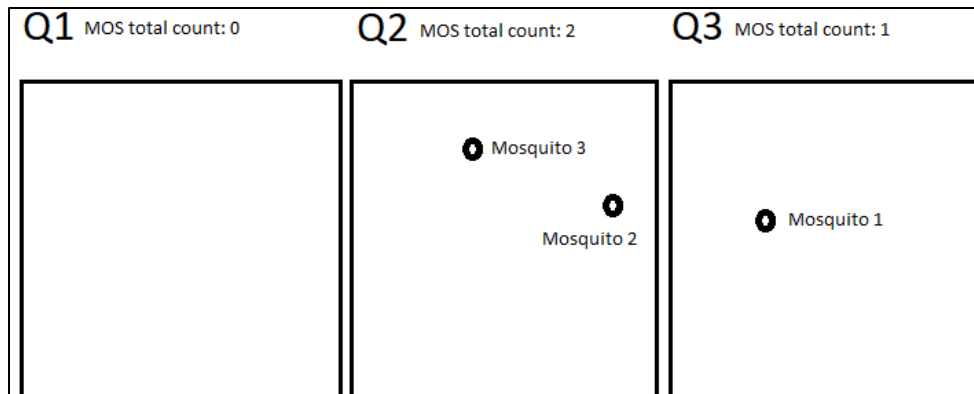


Figure A.54 Mosquito tracking software quadrant count diagram

MOS Voltage Sensor Testing SOP

Precheck before starting test

- Ensure drierite is able to remove humidity
- Ensure bubbler has water to add humidity
- Ensure power connections are not loose
- Observe sensor connections to the board, Daq connections from the board to Daq terminal block
- Ensure both Teflon dishes are located in the same place near the left side of the chamber
- Ensure airflow meter has proper airflow settings for both drierite and humidity
- Ensure airflow connections are not loose
- Ensure septa placed into the 4 joints are sealed.
- Ensure Mosquito introduction holes are sealed.

Data capture procedure

- Turn on computer
- Turn on power supplies for Heater voltage rail, sensing voltage rail, and servo valves
 - o This begins heating the MOS sensors
 - o This turns on the humidity and temperature sensors
- Start LabVIEW voltage capture software
 - o This begins capturing voltages of the MOS, humidity and temperature sensors.
 - o Options to turn on air supply, humidity control and hot plate are available

- Ensure settings for humidity and servo valves are set properly in the LabVIEW program
- Turn on hot plate using the button on the LabVIEW program
 - This ensures the system can put higher levels of humidity into the chamber quickly
 - Its good to turn it on 15 minutes prior to establishing controlled environment
- Allow approximately 20 minutes for MOS sensors to reach near baseline in open air (chamber with both ends removed)
- Once MOS sensors have reached near baseline voltages place two 25ml Teflon dishes in the left side of chamber.
 - The Teflon dish to the left is a placeholder for bait for mosquitoes
 - The Teflon dish to the right is for DEET sample
- Place 18-inch needle fed through a 29/42 septa into the center 29/42 joint. Align the needle into the second Teflon dish
- Place left chamber end on the left end of the main chamber and using the end bracket to secure the chamber end to the main chamber.
- Place right chamber end in the same manner.
- Place the 29/42 to barbed connection into the right chamber end.
- Place the 29/42 to barbed connection into the left chamber end. This barbed connection is connected to the output of the airflow meter and will supply air to the chamber.
- In the LabVIEW program turn on maintain humidity at setpoint
 - This will use the servo valves to switch between drierite and bubbler pushing humidity up and down.
- Turn on air supply to the chamber using turn on air button on LabVIEW
- Allow approximately 15 minutes for MOS sensors to reach baseline (approximately 1.00 volt) in the environment air.
- Check current humidity and temperature. Ensure they are within operating parameters
 - Relative Humidity at 65% and Temperature at 25°C
- Adjustments can be made to potentiometers to align sensors that are not with +/- .05 volts of 1.00 volt.
 - This should only be done if absolute necessary
- Using a 5ml syringe pull 1ml of DEET into the syringe. Reduce the number of air bubbles within the syringe if possible.
- Restart LabVIEW program to reset the sample count (once per second)
- Place syringe at the end of the 18-inch needle fed through septa.
- Inject DEET sample into the Teflon dish when sample count is at 30 samples

- Start a 10-minute timer
- Remove syringe from end of 18-inch needle
- Using a 5ml syringe pull another 1ml of DEET into the syringe. Reduce the number of air bubbles within the syringe if possible.
- Place the syringe at the end of the 18-inch needle fed through septa.
- Inject second DEET sample into the Teflon dish when timer expires or at approximately 630 samples
- Start a second 10-minute timer
- Remove syringe from end of 18-inch needle
- Using a 5ml syringe pull a final 1ml of DEET into the syringe. Reduce the number of air bubbles within the syringe if possible
- Place the syringe at the end of the 18-inch needle fed through septa.
- Inject final DEET sample into the Teflon dish when timer expires or at approximately 1230 samples
- Start a final 10-minute timer.
- Remove syringe from end of 18-inch needle and set it aside
- Allow for timer to end.
- In the LabVIEW program click the “Stop capturing and export to CSV”
 - o This will export voltage data to a CSV file.

Clean up procedure

- Before turning off the environment control remove the right chamber end by removing the bracket and set the chamber end aside.
 - o This prevent the MOS sensors from being exposed to a static DEET environment.
 - o This can cause baselines to be difficult to achieve.
- Turn of hotplate, air supply, and maintain humidity using controls in the LabVIEW program
- Remove the left chamber end by removing the bracket and set the chamber end aside.
- Remove air supply from 29/42 to barbed in the 29/42 joint.
- Remove 29/42 septa with the 18-inch needle fed through it from the center 29/42 joint. Ensure needle does not contact any part of the chamber
 - o This may leave residual DEET within the chamber
 - o This can cause baselines to be difficult to achieve.
- Remove the Teflon DEET dish from the chamber being careful not to spill it.
- Remove DEET from Teflon dish in a safe manner.
- Using acetone clean syringe, 18-inch needle, and Teflon dish

- Place 18-inch needle and Teflon dish into low Temp oven to remove residual acetone.

Powering down system

- Exit LabVIEW program
- Shut down computer
- Turn off power supplies

Mosquito Movement Testing SOP

Precheck before starting test

- Ensure drierite is able to remove humidity
- Ensure bubbler has water to add humidity
- Remove all MOS sensors from within the chamber
- Disassemble sensor arm and remove from inside chamber
- Ensure both Teflon dishes are located in the same place near the left side of the chamber
- Ensure airflow meter has proper airflow settings for both drierite and humidity
- Ensure airflow connections are not loose
- Ensure septa placed into the 4 joints are sealed
- If grid paper is not already placed on the inside of the chamber add grid paper
- Place only a single temperature and humidity sensor into the chamber via front 29/42 joint.
- Leave mosquito introduction hole to be used open
- Set up hot water circulator and connect water connections to hot water coil.
- Set up connections from flowmeter to the hot water coil and from hot water coil to chamber input.

Data capture procedure

- Turn on computer
- Turn on power supplies for Sensing voltage rail and servo valves
 - o This turns on the humidity and temperature sensors
- Start LabVIEW voltage capture software
 - o This begins capturing voltages of humidity and temperature sensors.
 - o Options to turn on air supply, humidity control and hot plate are available

- Ensure settings for humidity and servo valves are set properly in the LabVIEW program
- Turn on hot water circulator and Adjust the temperature of the hot water circulator to 85°C
- Turn on hot plate using the button on the LabVIEW program
 - o This ensures the system can put higher levels of humidity into the chamber quickly
- Place two 25ml Teflon dishes in the left side of chamber. place the Teflon dish near the left edge of the chamber.
 - o The Teflon dish to the left is for a bait sample
 - o The Teflon dish to the right is for DEET sample
- Place small amount of bait at the center of the first Teflon dish.
- Place 18-inch needle fed through a 29/42 septa into the center 29/42 joint. Align the needle into the second Teflon dish
- Place left chamber end on the left end of the main chamber and using the end bracket to secure the chamber end to the main chamber.
- Place right chamber end in the same manner.
- Place the 29/42 to barbed connection into the right chamber end.
- Place the 29/42 to barbed connection into the left chamber end. This barbed connection is connected to the output of the airflow meter and will supply air to the chamber.
- Attach LXG-120M to a tripod
- Connect LXG-120M camera to the computer via 2 Ethernet cables.
- Place the camera in front of chamber.
- Place both adjustable lamps on each side of the chamber, with light directed into the chamber end.
- Ensure the lamps provide a consistent light throughout the chamber.
- Turn off any overhead lights to remove any glare.
- Using the Baumer camera viewer align the camera so that the chamber ends align with image ends. Ensure the camera is focused on the chamber.
- In the Baumer camera viewer adjust the exposure time to further tweak the lighting within the chamber.
- Mark the tripod location.
- In the LabVIEW program turn on maintain humidity at setpoint
 - o This will use the servo valves to switch between drierite and bubbler pushing humidity up and down.
- Turn on air supply to the chamber using turn on air button on LabVIEW
- Check current humidity and temperature. Ensure they are within operating parameters

- Relative Humidity at 65% and Temperature at 25°C
- Gather 20 female mosquitoes placed within a holding tube
- Place the Mosquitoes within the chamber using a mosquito introduction hole.
- Start Image capture program
- Enter a directory to store image specifically on an SSD drive.
- Enter the number of frames to capture.
 - 11400 will capture frames for 10 minutes
- Enter an exposure time. Press enter to start image capture.
 - Typically 10000us
- Start a 10-minute timer
- Before the first 10-minute timer expires a DEET sample must be prepared.
- Using a 5ml syringe pull 1ml of DEET into the syringe. Reduce the number of air bubbles within the syringe if possible.
- Place syringe at the end of the 18-inch needle fed through septa.
- Inject DEET sample into the Teflon dish at the end of the image capture and 10-minute timer.
- Restart image capture program using the same settings as before.
- Start a 10-minute timer
- Before the first 10-minute timer expires a DEET sample must be prepared.
- Using a 5ml syringe pull 1ml of DEET into the syringe. Reduce the number of air bubbles within the syringe if possible.
- Place syringe at the end of the 18-inch needle fed through septa.
- Inject DEET sample into the Teflon dish at the end of the image capture and 10-minute timer.
- Restart image capture program using the same settings as before.
- Start a 10-minute timer
- Before the first 10-minute timer expires a DEET sample must be prepared.
- Using a 5ml syringe pull 1ml of DEET into the syringe. Reduce the number of air bubbles within the syringe if possible.
- Place syringe at the end of the 18-inch needle fed through septa.
- Inject DEET sample into the Teflon dish at the end of the image capture and 15-minute timer.
- Restart image capture program using the same settings as before.
- Start a final 10-minute timer
- Remove syringe from end of 18-inch needle and set it aside
- Allow for timer to end and finish image capture.

Clean up procedure

- Turn of hotplate, air supply, and maintain humidity using controls in the LabVIEW program
- Remove the left chamber end by removing the bracket and set the chamber end aside.
- Ensure Mosquitoes do not escape the chamber
- Remove Mosquitoes from chamber and dispose of them.
- Remove air supply from 29/42 to barbed in the 29/42 joint.
- Remove 29/42 septa with the 18-inch needle fed through it from the center 29/42 joint. Ensure needle does not contact any part of the chamber
 - This may leave residual DEET within the chamber
 - This can cause baselines to be difficult to achieve.
- Remove the Teflon Bait Dish from the chamber.
- Remove Bait from Teflon dish in a safe manner
- Remove the Teflon DEET dish from the chamber being careful not to spill it.
- Remove DEET from Teflon dish in a safe manner.
- Using acetone clean syringe, 18-inch needle, and Teflon dish
- Place 18-inch needle and Teflon dish into low Temp oven to remove residual acetone.

Powering down system

- Exit LabVIEW program
- Shut down computer
- Turn off power supplies

REFERENCES

Katz, Tracy M., Jason H. Miller, and Adelaide A. Hebert. "Insect Repellents: Historical Perspectives and New Developments." *Journal of the American Academy of Dermatology*, 10 May 2007.

Xiao Liu, Sitian Cheng, Hong Liu, Sha Hu, Daqiang Zhang, and Huansheng Ning. A survey on gas sensing technology. *Sensors*, 12(7):9635–9665, 2012.

World Health Organization. "Guidelines for Efficacy Testing of Mosquito Repellents for Human Skin." (2009): WHO. Web.

Ronca, Debra "Which animals kill the most people in the wild?" 15 December 2008. *HowStuffWorks.com*. 23 July 2016

Rentokill "Mosquito Borne Diseases." *DeBugged.*, 16 Nov. 2015. Web. 23 July 2016.

Zika "Zika Virus." World Health Organization. Web. 23 July 2016.
<<http://www.who.int/topics/zika/en/>>.

Mal "Fact Sheet about Malaria." World Health Organization. Web. 23 July 2016.
<<http://www.who.int/mediacentre/factsheets/fs094/en/>>.

AMCA. "Vector Control Methods." *American Mosquito Control Association*. Web. 23 July 2016. <<https://amca.memberclicks.net/control>>.

Impoinvil, Daniel E., Sajjad Ahmad, Adriana Troyo "Comparison of Mosquito Control Programs in Seven Urban Sites in Africa, the Middle East, and the Americas." *Health Policy (Amsterdam, Netherlands)*. U.S. National Library of Medicine, Oct. 2007. Web. 23 July 2016.

Core "Core Vector Control Methods." *World Health Organization*. Web. 23 July 2016.
<http://www.who.int/malaria/areas/vector_control/core_methods/en/>.

Supp "Supplementary Vector Control Methods." *World Health Organization*. N.p., n.d. Web. 23 July 2016.
<http://www.who.int/malaria/areas/vector_control/complementary_methods/en/>.

Resist "Insecticide Resistance." *World Health Organization*. Web. 23 July 2016.
<http://www.who.int/malaria/areas/vector_control/insecticide_resistance/en/>.

EPA "DEET." *EPA*. Environmental Protection Agency, n.d. Web. 23 July 2016.
<<https://www.epa.gov/insect-repellents/deet>>.

Ditzen, Mathias. "Insect Odorant Receptors Are Molecular Targets of the Insect Repellent DEET." *How Does DEET Work? Study Says It Confuses Insects (Update)*. Science Magazine, 2008. Web. 24 July 2016. <<http://phys.org/news/2011-09-deet-insects.html>>.

World Health Organization. "WHO Guidelines for Efficacy Testing of Spatial Repellents." Web. 24 July 2016.

Fradin, Mark S., and John F. Day. "Comparative Efficacy of Insect Repellents Against Mosquito Bites." *Http://www.nejm.org*. 4 July 2002. Web. 24 July 2016. <<http://www.nejm.org/doi/pdf/10.1056/nejmoa011699>>.

Beever, Richard. "Mosquito Repellent Effectiveness: A Placebo Controlled Trial Comparing 95% DEET, Avon Skin So Soft, and a "special Mixture"." *Www.bcmj.org*. , 5 June 2006. Web. 24 July 2016.

Yoon, Jong Kwang, Kang-Chang Kim, and Yeondong Cho. "Comparison of Repellency Effect of Mosquito Repellents for DEET, Citronella, and Fennel Oil." *Journal of Parasitology Research*, Apr. 2015. Web. 24 July 2016. .

Abiy, Ephrem, Teshome Gebre-Micheal, Meshesha Balkew, and Girmay Medhin. "Malaria Journal." *Repellent Efficacy of DEET, MyggA, Neem (Azadirachta Indica) Oil and Chinaberry (Melia Azedarach) Oil against Anopheles Arabiensis, the Principal Malaria Vector in Ethiopia*. Malaria Journal, 19 Dec. 2014. Web. 24 July 2016.

Rodrigues, Stacy D., Lisa L. Drake, David P. Price, John L. Hammond, and Immo A. Hansen. "Journal of Insect Science." *The Efficacy of Some Commercially Available Insect Repellents for Aedes Aegypti (Diptera: Culicidae) and Aedes Albopictus (Diptera: Culicidae)*. N.p., 5 Oct. 2015. Web. 24 July 2016.

New Mexico State University (NMSU). "Some Surprising Results Found Testing Mosquito Repellents." *ScienceDaily*. ScienceDaily, 10 Nov. 2015. Web. 24 July 2016.

Coleman, Ryan D., "Automated Data Acquisition of DEET Time-dependent Concentration Profiles" (2016). *Honors Theses*. 417. https://aquila.usm.edu/honors_theses/417